2014

Health monitoring of pavement systems using smart sensing technologies

Shuo Yang
Iowa State University

Health monitoring of pavement systems using smart sensing technologies

by

Shuo Yang

A thesis submitted to the graduate faculty

in partial fulfillment of the requirements for the degree of

MASTER OF SCIENCE

Major: Civil Engineering (Civil Engineering Materials)

Program of Study Committee:
Halil Ceylan, Major Professor
Kasthurirangan Gopalakrishnan
Sunghwan Kim
Peter C. Taylor
Liang Dong
Paul G. Spry

Iowa State University

Ames, Iowa

2014

TABLE OF CONTENTS

Page

LIST OF FIGURES

Page

LIST OF TABLES

Page

ACKNOWLEDGEMENTS

I would like to thank my major professor and committee chair, Dr. Halil Ceylan for his support in this study. His valuable guidance is the key for me to complete my master degree. His knowledge and work ethics inspire me for my future career plans. His patient, inspiration, and encouragement are precious for me and it has been a great pleasure and good fortune for me to work with him.

Furthermore, I would like to thank my committee members, Dr. Kasthurirangan Gopalakrishnan, Dr. Sunghwan Kim, Dr. Liang Dong, Dr. Peter C Taylor, and Dr. Paul G Spry, for their guidance and constructive comment for this research. It's great pleasure for me that they can review my thesis and serve on my exam committee. Special thanks are extended to Dr. Kasthurirangan Gopalakrishnan and Dr. Sunghwan Kim for their extra invaluable assistance to my research.

In addition, I would also like to thank my friends, colleagues, the department faculty and staff for giving me a wonderful experience at Iowa State University. I want to also offer ‘’’my appreciation to my friends and co-workers Keyan Shen, the graduate student in Electrical and Computer Engineering, Dr. Daji Qiao, the associate professor in Electrical and Computer Engineering, and Mr. Robert Frank Steffes, the lab manager in the Portland Cement Concrete Research Laboratory. This study could not have been completed without their help.

Finally, I would like to thank to my wonderful family, including my parents and brother. Their love, encouragement, understanding, support and patience always inspire me throughout my whole life.

ABSTRACT

Pavement undergoes a process of deterioration resulting from repeated traffic and/or environmental loading. By detecting pavement distress and damage early enough, it is possible for transportation agencies to develop more effective pavement maintenance and rehabilitation programs and thereby produce significant cost and time saving. Structural Health Monitoring (SHM) has been conceived as a systematic method for assessing the structural state of pavement infrastructure systems and documenting their condition. Over the past several years, this process has traditionally been accomplished through the use of wired sensors embedded in bridge and highway pavement. However, the use of wired sensors has limitations for long-term SHM and presents other associated cost and safety concerns. Recently, Micro-Electromechanical Systems (MEMS) and Nano-Electromechanical Systems (NEMS) have emerged as advanced/smart-sensing technologies with potential for cost-effective and long-term SHM.

To this effect, a study has thus been initiated to evaluate the off-the-shelf MEMS sensors and wireless sensors, identify their limitations, and demonstrate how the acquired sensor data can be utilized to monitor and assess concrete pavement behavior. The feasibility of implementing a wireless communication system into a MEMS sensor was also investigated.

Off-the-shelf MEMS sensors and wireless sensors were deployed in a newly constructed concrete highway pavement. During the monitoring period, the temperature, moisture, and strain profiles were obtained and analyzed. The monitored data captured the effects of daily and seasonal weather changes on concrete pavement, especially, early-age curling and warping behavior of concrete pavement. These sensors, however, presented

issues for long-term operation, so to improve performance, a ZigBee protocol-based wireless communication system was implemented for the MEMS sensors.

By synthesizing knowledge and experience gained from literature review, field demonstrations, and implementation of wireless systems, issues associated with sensor selection, sensor installation, sensor packaging to prevent damage from road construction, and monitoring for concrete pavement SHM are summarized. The requirements for achieving Smart Pavement SHM are then explored to develop a conceptual design of smart health monitoring of both highway and airport pavement systems for next-generation pavement SHM. A cost evaluation was also performed for traditional as well as MEMS sensors and other potential smart technologies for SHM.

CHAPTER 1

INTRODUCTION

Background

Pavement is a fundamental transportation infrastructure system to sustain both moving vehicles and people. Common pavement system construction materials include soil, aggregates, concrete, and asphalt. Pavement material types for pavement surface layer can be divided into Portland Cement Concrete (PCC) and Hot Mix Asphalt (HMA), also known as rigid (PCC) pavement and flexible (HMA) pavement, respectively.

Portland Cement Concrete (PCC) is a mixture of cement, aggregates, and water that gains strength in its initial stage through a reaction called hydration. The first use of PCC for pavement in the United States was a local street construction project in Ohio in 1893; from the 1970s to now PCC is widely used in highway pavement construction (Pasko, 1998). Currently, there are more than 64,000 miles of paved concrete roads in the United States (FHWA, 2012a). Asphalt concrete is a mixture of mineral aggregates and asphalt which will be compacted in the field for pavement construction. Similar to PCC pavement, HMA pavement is also widely used in pavement construction in the United States.

Like any other man-made structural system, pavement can fail due to environmental load, traffic load, or a combination of both. Environmental load such as temperature (curling stress) and moisture (warping stress) can cause volumetric distortion at an early stage of PCC pavement. Such environmental and mechanical loads combined with PCC aging will greatly influence long-term pavement performance and pavement distress (Ruiz et al., 2005).

According to the ASCE 2013 Report Card, the current national pavement system is assessed a "D" grade, reflecting poor pavement condition. The Federal Highway Administration estimates that it needs approximately $170 billion to effectively improve pavement condition and performance. Structural Health Monitoring (SHM) is considered to be a systematic approach that could be employed to monitor and preserve rapidly-deteriorating pavement assets. Traditional SHM approaches utilizing wired sensors have been used to track pavement response under environmental and traffic loads, including temperature, moisture, strain, stress, deflection, etc. However, over the past twenty years, fewer pavement instrumentation projects have been initiated and almost all of them were associated with negative issues such as high array density, wire damage, high installation cost and time, low survivability of wired sensors for long term operation, etc. Recent achievements in Micro-Electromechanical Systems (MEMS) or Nano-Electromechanical Systems (NEMS) technology make it possible to manufacture sensors using microfabrication techniques. This kind of advanced/smart-sensing technology, including wireless sensors, shows vast potential for improving the traditional SHM approach. However, MEMS-based and wireless-based smart-sensing technologies have up to now been little used for monitoring pavement response in the field, and the requirements for using those kinds of smart sensing technologies have not yet been thoroughly discussed.

Research Objectives

The overall objective of this study was to review both existing and emerging sensing technologies for pavement health monitoring through a detailed literature review supplemented by a full-scale pavement instrumentation project on a real highway. However,

due to limited pavement construction in the field, this thesis will more focus on the smart sensing technologies used for PCC pavement. The MEMS-technology-based sensing method represents an innovative solution to pavement infrastructure health monitoring, and wireless sensors generally exhibit lower installation cost and time compared with traditional wired sensors. However, the system requirements of Smart Pavement SHM under actual traffic load and weather conditions have not yet been investigated and discussed, so the specific objectives of this study include:

- To evaluate the field performance of commercial off-the-shelf MEMS sensors and wireless sensors
- To identify the system requirements of MEMS sensors and wireless communication systems for Smart Pavement SHM
- To investigate packaging methods for wireless communication system implemented to MEMS sensors

Thesis Organization

This thesis consists of six chapters. Chapter 1 will introduce the background and objectives of this study. Chapter 2 is a comprehensive literature review of Structural Health Monitoring (SHM), including recent successes in applying Micro-Electromechanical Systems (MEMS) and wireless-system technology to SHM. In Chapter 3, the performance of off-the-shelf MEMS sensors for monitoring US Highway 30 pavement is discussed, and a concrete maturity curve based on laboratory test and field temperature data is developed. Chapter 4 describes field experience using a wireless system for a MEMS multifunction sensor in a US Highway30 highway project. Chapter 5 summarizes issues of SHM and the

requirements of Smart Pavement SHM and provides cost evaluation and architecture of Smart Pavement SHM systems for both highway and airfield pavement. Chapter 6 summarizes the conclusions and recommendations from this study. Figure 1-1 is a flow chart representing the thesis structure.

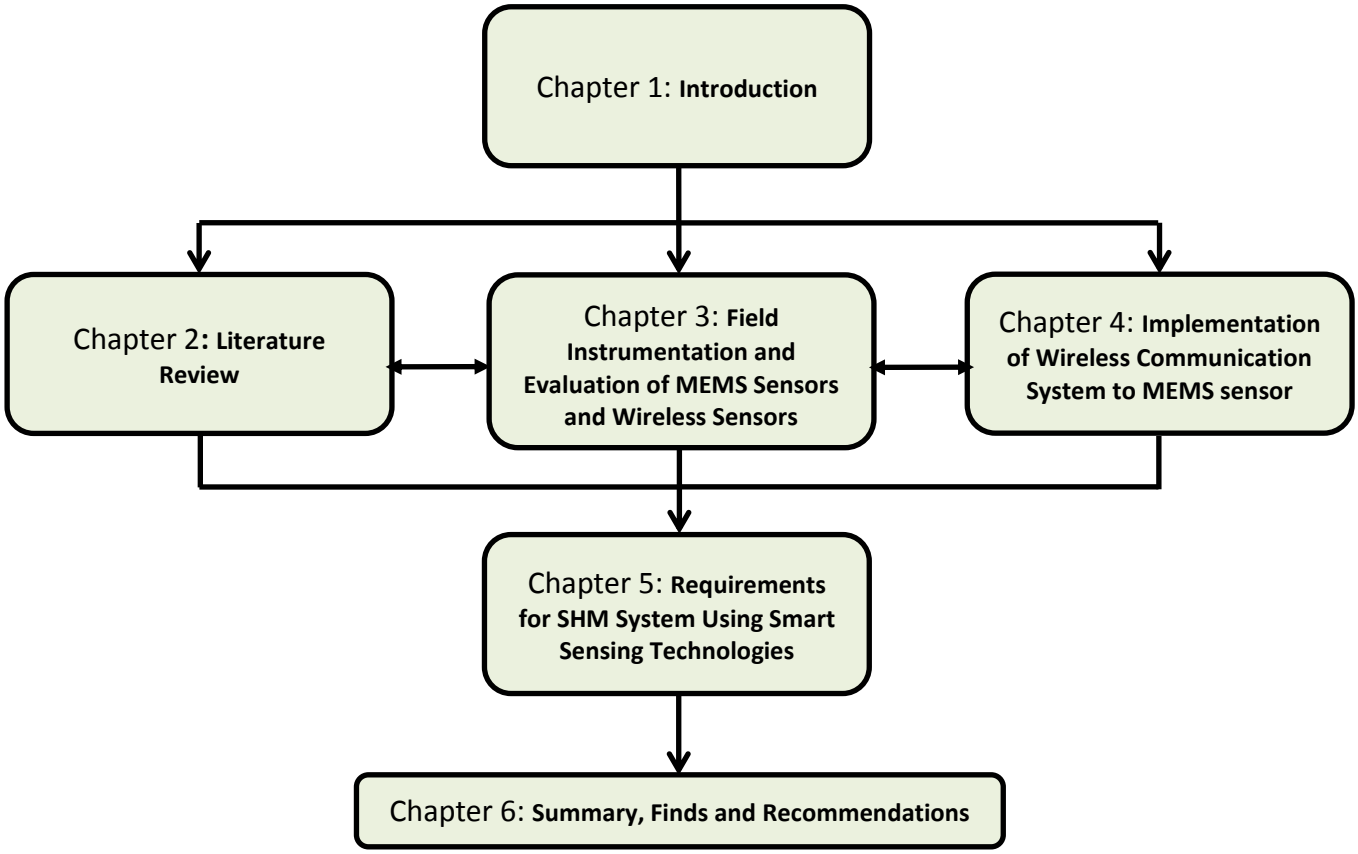

Figure 1-1. Thesis organization flow chart.

CHAPTER 2

LITERATURE REVIEW

Structural Health Monitoring

History of SHM in Civil Infrastructure

Structural Health Monitoring (SHM) is the process of implementing structural damage detection strategy and evaluating structural state to learn load and response mechanisms (Farrar and Worden, 2007; Brownjohn, 2007). In recent years it has become a rapidly-growing priority for transportation infrastructures to identify and monitor structural deterioration. An ideal SHM application can monitor the integrity of in-service structures on a continuous real-time basis, and data processing and analysis can be subsequently used to assess the symptoms of operational anomalies that may cause service or safety issues (Wong, 2004).

Early development of health-monitoring techniques focusing on vibration-based damage identification methods can be traced to the 1970s in the oil industry and the aerospace community in conjunction with offshore platforms and space shuttles. Investigating modal properties and related quantities of civil infrastructures like bridges and buildings using vibration- based damage-identification methods has been done since the 1980s. However, difficulties in using vibration-based damage-identification methods for large-scale structures during that time sometimes occurred, often due to variable environmental and operation conditions; this frequently resulted in an expensive and time-consuming process of damage assessment (Phares et al., 2005; Qi et al., 2005; Farrar and Worden, 2007).

SHM can be widely used as an approach to in-service structural integrity assessment in bridges, buildings, towers, dams, offshore installations, pavements, etc. Traditional SHMs for such civil infrastructures have utilized wired sensors strategically deployed in the structures to monitor and record external conditions and associated structural response. Among these structures, bridges and buildings have represented the most common SHM applications in civil infrastructures. SHM implemented in bridges is used to characterize their dynamic behavior under unpredictable mechanical and environmental loads that may result in unanticipated behavior (Modares and Waksmanski, 2012). The most common techniques include eddy current, ultrasonic, acoustic-based sensing, strain monitoring, corrosion monitoring, etc. SHM in building structures has been deployed to monitor structural performance under natural disaster conditions such as earthquakes, storms and harsh winds (Brownjohn, 2007). Furthermore, as a common practice, SHM implemented in concrete structure can also monitor concrete temperature and moisture. The producing data can be used to determine frame removal time during construction through monitoring of concrete maturity and curing processing.

Unlike bridges and buildings structures, the application of SHM in pavement systems has been used to document structural responses from a combination of vehicle and environment loads. Monitoring sensors embedded in pavement structure has been investigated since the 1960s to improve pavement design methods (Potter et al., 1969; Rollings and Pittman, 1992). However, survivability of embedded sensors in pavement structure is not always high because they can be easily damaged by asphalt/concrete medium and harsh climate conditions.

Global and Local Health Monitoring

According to Plankis and Heyliger (2013), there are four levels of damage identification. From the first level to the fourth level they are, in sequence: determination of damage presence, identification of damage location, evaluation of damage, and prediction of remaining structure service life. To address the first three levels, health-monitoring methods can be divided into global and local health monitoring. Global health monitoring is the concept of using technology to detect changes in properties such as stiffness and mass change and other dynamic global properties caused by significant structural damage. For global health monitoring, there is no need to know the location or potential location of damage. The important modal properties for global health monitoring are resonant frequencies, mode-shape vectors, mode-shape curvatures, a dynamic flexibility matrix, updating of modal parameters, and acoustic properties (Plankis and Heyliger, 2013). Local health monitoring refers to tracking damage progress and evaluation of damage level at known or predicted damage locations. In summary, global techniques are used for damage detection that may affect the integrity of a whole structure, while local techniques focus on small defects (Haque et al., 2012). Technically, traditional wired-sensors-based SHM represent a type of local health-monitoring technology.

Smart Structural Health Monitoring

Lynch (2002) defined the term "smart structure" as "*sensing and/or actuation technologies embedded within the system to provide insight to the structure's response and an opportunity to limit responses*". Then Spencer et al. (2004) stated that a sensor must have features like an on-board Central-Processing-Unit (CPU), small size, wireless capability, and promise of low cost to be considered a smart sensor. Similarly, Nagayama and Spencer

(2007) stated that a sensor can be considered "smart" if it includes an on-board microprocessor, a wireless communication system, and sensing capability. It also should be battery powered and has low cost. However, Phares et al. (2005) gave a more detailed definition of the term "smart". The term "smart" technology they defined is a "*system systematically reports on the condition of the structure by automatically making engineering-based judgments, recording a history of past patterns and intensities, and providing early warning for excessive conditions or for impending failure without requiring human intervention*. These features make the system capable of providing and facilitating *self-diagnostic, real-time continuous sensing, advanced remote sensing, self-organizing, self-identification, or self-adaptation (decision making and alarm triggering) function*". In short, smart SHM should enable structures to be capable of real-time continuous sensing of both external and internal condition changes and responding to these changes to improve performance without human intervention. To apply this concept to pavement, a Smart Pavement SHM should be long-term and cost-effective as well. However, a truly "smart" system or structure meeting all these requirements has never existed if this definition is rigorously followed. It is clear, however that a practical smart SHM could be achieved by employing a "smart sensor" system having features of small size, wireless function, low cost, and an on-board Central-Processing- Unit (CPU).

Traditional SHM Approach to Pavement Infrastructure System

Highway Pavement

In the US, traditional SHM approaches for highway pavement infrastructure system have utilized full-scale test tracks instrumented by large number of sensors such as strain

gages, pressure cells, displacement gauges, subgrade moisture sensors, etc. The motivation underlying constructing and operating a full-scale pavement test track is to understand pavement response and behavior under realistic but controlled conditions (Hugo and Epps, 2004). Figure 2-1 from Hugo and Epps (2004) summarizes the common sensors used in various test tracks. Detailed descriptions of full-scale test tracks, including MnROAD, the Virginia Smart Road, and the National Center for Asphalt Technology (NCAT) Test Track are summarized in Table 2-1.

Strain gages	Pressure cells	Load cells	Displacement gauges	Subgrade moisture sensors	Other*
RIOH–ALF			RIOH–ALF		
WesTrack			HVS–A	RIOH–ALF	
HVS–A			TxMLS	WesTrack	
TxMLS			RRT–Rom	HVS–A	
PRF–La			MnROAD	TxMLS	
MnROAD			LCPC–Fr	RRT–Rom	
LINTRACK			K–ATL	NCAT	
LCPC–Fr	RIOH–ALF		In–APLF	MnROAD	
K–ATL	HVS–A		HVS–SA	LCPC–Fr	
ISETH	TxMLS		HVS–Nordic	K–ATL	
In–APLF	PRF–La		NAPTF	HVS–SA	MnROAD
HVS–SA	MnROAD		HVS–CRREL	NAPTF	LINTRACK
HVS–Nordic	LCPC–Fr		CEDEX	DRTM	FHWA–PTF
FHWA–PTF	K–ATL		CAPTIF–NZ	HVS–CRREL	DRTM
NAPTF	HVS–Nordic		CAL/APT	CEDEX	CAPTIF–NZ
DRTM	NAPTF		ARRB–ALF	CAL/APT	CAL/APT
HVS–CRREL	DRTM	RIOH–ALF	Oh–APLF	ARRB–ALF	Oh–APLF
CEDEX	HVS–CRREL	HVS–A			
CAL/APT	CEDEX	TxMLS			
ARRB–ALF	CAPTIF–NZ	PRF–La			
Oh–APLF	ARRB–ALF	MnROAD			

*Other instruments cited by respondents:

Temperature sensors—Oh–APLF; CAL/APT Temperature gauge—DRTM Emu & Bison strain coils—CAPTIF–NZ
LVDT—FHWA–PTF
Several attempts for measurement of asphalt sublayers: LINTRACK–NL
MnROAD—see website (http://mnroad.dot.state.mn.us/researc/Mnresearc.asp) and beyond the surface handout.

Figure 2-1. Sensors used in traditional pavement health monitoring (Hugo and Epps, 2004).

Table 2-1. Test tracks instrumentation.

Projects	Monitoring System	Year
MnROAD	Over 9,500 sensors included LVDT, strain gages, dynamic soil pressure cells, moisture gauges, thermocouples, resistivity probes et al. were installed	1991
Virginia Smart Road	Over 400 sensors included moisture, temperature, strain, vibration, weigh-in-motion sensors were installed	1997
NCAT Test Track in Auburn University	Copper-based strain gages, temperature sensors, soil pressures, soil moisture sensors were installed	2000

MnROAD

In 1991, the MnROAD test track (See Figure 2-2) was constructed to enable civil engineers to conduct research on making roads longer, safer, and cheaper. The project funding, approximately $25,000,000, was used to build a 2.5-mile low-volume road and a 3.5-mile main line in the I-94 roadway. Since the 1990s, more than 9,500 sensors have been installed in the test track to document effects produced by test vehicles. These sensors were linked by fiber optic or copper wires to a Data Acquisition System (DAS) connected to the MnROAD main building. The data collected from MnROAD were used to improve pavement performance and life with cost benefits related to maintenance, repairs, user delays, and congestion (MnROAD Brochure, 2014). Table 2-2 lists a summary of estimated overall cost saving from Phase 1 research (1994-2006). It is claimed that a total of $33 million was saved for Minnesota and a potential cost of $749 million was saved for the nation overall.

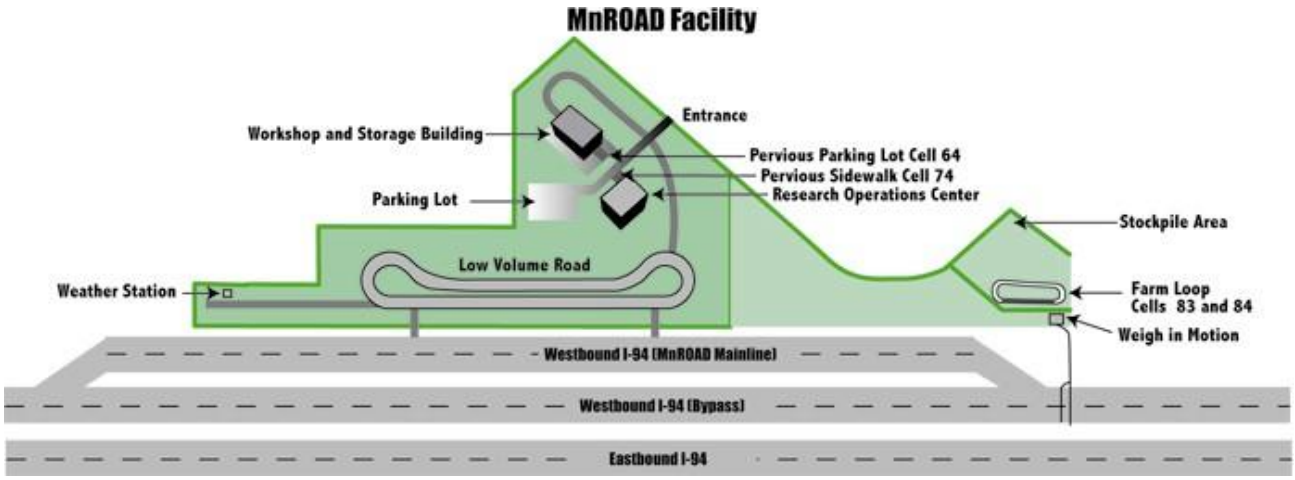

Figure 2-2. MnROAD (photo courtesy of Minnesota DOT).

Table 2-2. MnROAD cost benefits (MnROAD Brochure, 2014).

Phase I (MN) Implemented Research	Annual Savings
Spring Load Restriction Policy	$14 Million
Winter Load Increase Policy	$7 Million
Low Temperature Cracking Reduction	$5.7 Million
ME Flexible Design Method	$4 Million
ME Rigid Design Method	$1.2 Million
Sealing Pavement/ Shoulder Joints	$1.2 Million
Total	**$ 33.1 Million**

In MnROAD, the DAS were distributed as data acquisition nodes near the test cells. Each data acquisition node consisted of a series of cabinets containing sensors, data collection devices, and AC power sources as well as communication systems. The insulated cabinets were heated during winter and cooled during summer by installed fans. In order to cost-effectively install so many sensors, the construction manager of MnROAD paid considerable attention to sensor life span and sensor installation plan. However, there still were many sensor failures reported, requiring their replacement after road construction. In doing so, it was found that the in-situ sensor positions differed a great deal from the instrumentation plan, so they had to install sensors into new holes using full-depth coring.

After installation, they assumed the data from the new sensors was accurate (Tompkins and Khazanovich, 2007).

Virginia Smart Road

The Virginia Smart Road was a 5.7 mile-long limited-access highway constructed at the end of the 1990s. This road, as shown in Figure 2-3, links highway I-81 and Blacksburg, Virginia. It has all-weather test towers, variable-lighting sections, and experimental sections, as well as a control room for data analysis. The Virginia Smart Road contains more than 400 installed sensors, including thermocouples, strain gages, pressure cells, time-domain reflectometry (TDR) probes, resistivity probes, etc. However, approximately 70% of the sensors failed after two years (Al-Qadi et al., 2004).

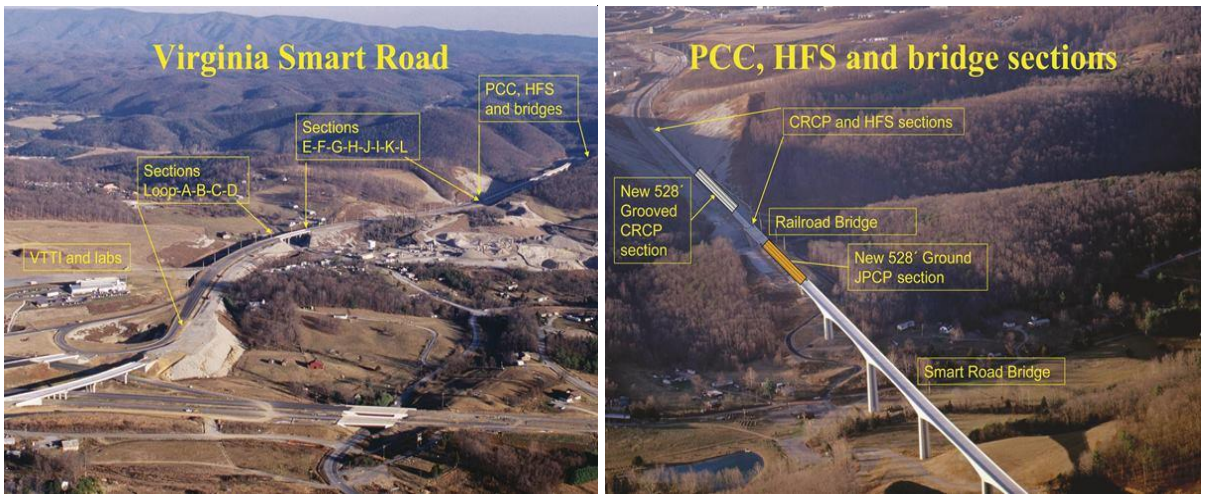

Figure 2-3. Virginia Smart Road (photo courtesy of Dr. Edgar de Leon Izeppi, Virginia Transportation Institute).

Auburn University National Center for Asphalt Technology (NCAT) Test Track

The NCAT test track, shown in Figure 2-4, was designed and built to evaluate and improve current pavement design in 2000. This 1.7-mile long test track contains more than 46 experimental sections. The test period of NCAT test track can be divided into a first and a

second round of tests. The first round of tests was initiated in 2000 and finished in 2002. After the first round, the second round started in 2003 after several sections were replaced. While many sensors, including strain gages, temperature sensors, soil pressure sensors, and soil moisture sensors, were embedded in subgrade and asphalt pavement, almost 35% of them failed before 2003 (Timm et al., 2004).

Figure 2-4. NCAT test track (photo courtesy of National Center for Asphalt Technology).

Airfield Pavement

Pavement deterioration caused by aircraft loading, temperature, and moisture variation can be a major concern in airport safety. Compared to highway pavement, airfield pavement typically deals with higher load magnitudes and higher tire pressures but fewer load repetitions from airplanes. Additionally, although both airfield and highway pavements are prone to deterioration from traffic and environment loads, airfield pavement usually predominately exhibits environmental-load-related rather than traffic-load-related stresses (FAA Advisory Circular, 2011).

In summer 2011, the Ankeny Regional Airport in Ankeny, Iowa reported a serious PCC pavement distress blowup in its runway which was caused by excessive hot weather and an associated heat wave. In this particular case, a Raytheon Premier One jet hit the blowup spot during take-off and damaged its landing gear, as shown in Figure 2-5. Blowup in an airport runway is of course very dangerous for aircraft operation, so it's significant to install sensors in airfield pavement enabling SHM to monitor pavement properties and provide a warning of pavement overheating before actual pavement distress occurs so that the appropriate maintenance process can be launched. Table 2-3 lists traditional SHM applications in the US for airport pavement systems.

Figure 2-5. Pavement blowup and damaged aircraft in Ankeny Regional Airport runway (photo courtesy of Snyder & Associates, Inc./Polk County Aviation Authority).

Table 2-3. Airfield pavement instrumentation.

Projects	Monitoring System	Year
Denver International Airport	Over 460sensors included strain gages, Thermocouples, and Time Domain Reflectometers (TDR) were installed	1990
FAA National Airport Pavement Test Facility (NAPTF)	Over 1,000 sensors including temperature, moisture and strain gages were installed	1997

Runway Instrumentation at Denver International Airport

In the 1990s, the Denver International Airport (DIA) began construction of a runway with comprehensive instrumentation of strain gages, thermocouples, and time-domain reflectometers (TDR). A total of 460 sensors were embedded in sixteen slabs of the runway to monitor the pavement response generated by aircraft wheel and environmental loading. Among the installed sensors were dynamic sensors that could measure strain, vertical displacement, airplane speed, and acceleration whenever a passing airplane triggered them. A data acquisition system (DAS) was placed in-situ for data collection and downloading to the database managed by the FAA technical center (Lee et al., 1997; Dong and Hayhoe, 2000; Rufino et al., 2004).

Federal Aviation Administration (FAA) National Airport Pavement Test Facility (NAPTF)

In 1997, the FAA began to build a full-scale pavement test facility dedicated to pavement research, as shown in Figure 2-6. NAPTF was built to provide traffic data for improving pavement thickness design procedures, investigating pavement response and failure mechanisms related to airplane landing, and examining the California bearing ratio (CBR) method for asphalt pavement design. Sensors embedded in NAPTF can be divided into two groups, static sensors and dynamic sensors. Static sensors were used to monitor temperature, moisture, and crack status every hour, while dynamic sensors were used to measure strain and deflection under vehicle or aircraft load. However, many sensors were damaged and pavement containing the sensors was scheduled for replacement on an 18-month cycle (Hayhoe, 2004).

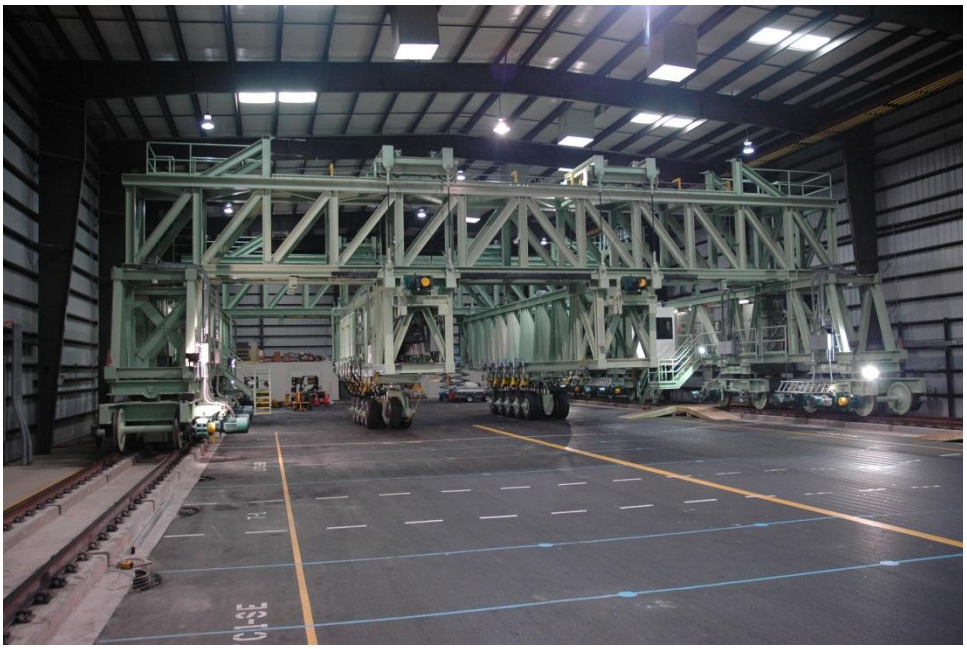

Figure 2-6. National Airport Pavement Test Facility (photo courtesy of Federal Aviation Administration).

Limitations of Current SHM Practices for Pavement System

Current SHM practice utilized in pavement systems has mainly used wired sensing technologies, resulting in low survivability of sensors with respect to both pavement construction and long-term operation. It is difficult to provide either continuously long-term monitoring for pavement structural behavior changes or real-time warning for in-service pavement failure. Furthermore, wired sensors always require high installation cost and time. If many sensors are used the cost of the DAS may also increase due to a limit in the number of data-logger connection ports. Current SHM practice also may not directly integrate actual Pavement Management Information System (PMIS) to establish Maintenance and Rehabilitation (M&R) strategies for in-service pavement systems. Other limitations such as lack of easy installation of the SHM system and optimization of the field's data collection

and storage mechanisms may also hamper the implementation of pavement SHM (FHWA, 2012b).

Hence, implementation of smart sensors should be investigated as a means for overcoming current limitations. Micro-Electromechanical Systems (MEMS) and wireless sensor systems are reviewed in the following subsection to evaluate their potential for employment in “smart sensor" development.

Micro-Electromechanical Systems

Overview

The emergence of Micro-Electromechanical Systems (MEMS) and their recent achievements represent an alternative solution to achieving long-term, continuous, real-time, and cost-effective SHM for pavement systems. Micro-Electromechanical Systems (MEMS) is a term referring to miniaturized systems consisting of microsensors and actuators fabricated by using microfabrication techniques; their critical physical dimensions could range from just one micron up to one millimeter (MEMSnet, 2014). This allows use of integrated circuits and on-board central processing units to make the system intelligent. As a result, microsensors and actuators with active perception and microcircuit control can effectively sense their environments and be able to react to changes in those environments (Varadan and Varadan, 2000; AllAboutMEMS, 2002; Phares et al., 2005).

The early motivation of “small size” sensing devices can be traced back to the first point-contact transistor developed in the 1940s by Shockley et al. at Bell Laboratories; it was about one-half inch high (SCME, 2013). Since the 1970s, the manufacturing processes of electronic devices have undergone remarkable progress associated with the use of silicon as

the dominant material. MEMS devices were first developed and widely commercialized in the 1990s. Nowadays, MEMS technologies are used in many applications (AllAboutMEMS 2002; Lee, 2004; SCME, 2013).

MEMS-based sensors are generally comprised of miniaturized mechanical-sensing elements fabricated on silicon chips. Contemporary microfabrication techniques enable a variety of complex electromechanical systems to be integrated into such miniaturized sensing elements (MEMSnet, 2014). The most distinguishing features of a typical MEMS sensor are incredibly small size and an on-board microprocessor, or CPU. Such a sensor has a much lower price due to material used and integrated interconnection. The microprocessor supports digital processing, analog-digital conversion, and basic computation. Compared to MEMS sensors, traditional sensors have both relatively larger size and higher price and they must always be equipped with data management system, so the instrumentation of traditional sensors may require a large array density in the structure if many sensors are used, which itself may result in pavement distress (e.g. cracking). MEMS sensors, on the other hand, could potentially be used to improve current SHM of pavement system performance with relatively little concern for inherent compromising properties.

MEMS Sensors for Civil Infrastructure SHM

Current researches related to SHM primarily focus on development of MEMS sensors and wireless-sensor systems. Norris et al., (2008) developed a MEMS sensor capable of measuring temperature and moisture inside concrete using the microcantilever principle, as shown in Figure 2-7. The cantilever beam used in this sensor can generate stresses related to concrete moisture. Beam curvature will be produced and the deflection can be measured as resistance by an embedded nano-strain gage (resistor) so that the stress can be calculated.

Then, based on the established relationship between stress and water concentration, the moisture content can be determined. Temperature was measured using an on-chip temperature sensor. The fabrication of the MEMS sensor was conducted in accordance using a combination of standard and customized semiconductor processing steps. Standard complementary metal-oxide-semiconductor (CMOS) procedures, i.e., photolithography and chemical wet etching, were used to form the silicon platform. After patterning and activating the moisture-sensing element, the cantilever beam was released through plasma etch. The sensor die was then surrounded by a polymeric coating and the entire chip embedded in a stainless steel jacket to protect it from the enclosing concrete.

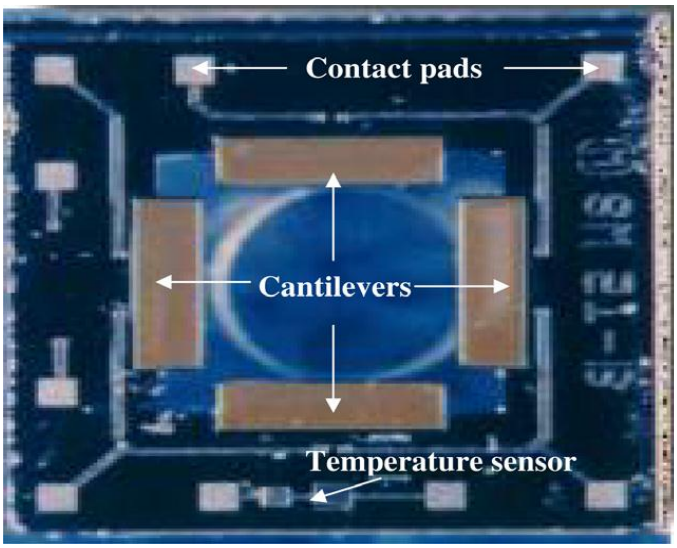

Figure 2-7. Manufactured MEMS sensor chip from Norris et al. (2008).

Other previous studies on MEMS sensors for concrete monitoring include "Smart Aggregate" by Sackin, et al. (2000), "Smart Pebbles" by Watters (2003), "Smart Dust" by Pei et al. (2007, 2009), and "Self-sustaining damage detection sensor" (Kuang, 2014). Table 2-4 lists MEMS sensors developed through previous research efforts but not all of them can be used for concrete pavement.

Table 2-4. Research related to MEMS temperature, moisture and strain sensors.

Sensor Type	Applications	Reference
Temperature	Early age concrete property monitoring	Saafi & Romine (2005)
	Monitoring pavement condition using "Smart Dust"	Pei et al. (2007)
	Cascaded "Triple-Bent-Beam" MEMS sensor for contactless temperature measurements in non-accessible environments	Andò et al. (2011)
	Wireless temperature microsensors integrated on bearings	Scott et al. (2011)
	Highly reliable MEMS temperature sensors for 275 ˚c applications	Scott et al. (2012)
	Multisensor MEMS for temperature, relative humidity, and high-g shock monitoring	Smith (2012)
	MEMS-based Pt film temperature sensor	Han et al. (2014)
	Rapid temperature measurement of meteorological detection system based on MEMS	Lu et al. (2014)
Moisture	Early age concrete property monitoring	Saafi & Romine (2005)
	Monitoring pavement condition using "Smart Dust"	Pei et al. (2007)
	A wireless, passive embedded sensor for real-time monitoring of water content in civil engineering materials	Ong et al. (2008)
	Multisensor MEMS for temperature, relative humidity, and high-g shock monitoring	Smith (2012)
	A highly sensitive humidity sensor with a novel hole array structure using a polyimide sensing layer	Choi et al. (2014)
	A CMOS humidity sensor for passive RFID sensing applications	Deng et al. (2014)
	Digital hygrometer for trace moisture measurement	Islam et al. (2014)
	MEMS-based humidity sensor based on thiol-coated gold nanoparticles	Lin et al. (2014)
Strain	Early age concrete property monitoring	Saafi & Romine (2005)
	A carbon nanotube strain sensor for SHM	Kang et al. (2006)
	Microwave Weigh-In-Motion (WIM) sensor	Liu et al. (2007)
	Smart pavement monitoring system	Lajnef et al. (2011)
	High-performance piezoresistive MEMS strain sensor with low thermal sensitivity	Mohammed et al. (2011)
	Novel MEMS strain sensor	Saboonchi & Ozevin (2012)
	Surface-Bonded MEMS strain sensors	Moradi &Sivoththaman (2013)

Although there has been considerable research focusing on MEMS sensors, the majority of studies are still at the proof-of concept level. For MEMS sensors used in

pavement SHM, one must consider short-term effects such as high temperature, moisture, and alkali environment in fresh concrete, as well as the effect of fine particles from concrete compounds. Long-term effects such as freezing-thawing cycles in actual pavement must also be considered.

Wireless Sensor Network (WSN)

Traditional wired sensors generally require high installation costs and time as well as avoidance of wire-damage problems. For example, Cho et al. (2008) reported that a contractor spent over $5,000 on each wired sensing channel in a high-rise building practicing SHM. Furthermore, Hong Kong government spent more than $8 million to install a total of 350 wired sensing channels in the Tsing Ma Suspension Bridge (Farrar, 2001). In view of such examples, economic motivation facilitates the adoption of wireless sensors to replace traditional wired sensors. In general, wireless sensor network can utilize Radio Frequency (RF), acoustics, infrared transmission, and lasers as transmission media. In terms of SHM, RF has mainly been used, and it follows specific topologies and protocols associated with signal transmission.

Wireless Network Topologies

A WSN can be represented as a cluster in an SHM system, so the whole system can be structured using three common topologies for civil infrastructures: start, peer-to-peer, and multi-tier, as shown in Figure 2-8 (Lynch and Loh, 2006). Star topology is designed to allow each node (wireless sensor) to communicate only with a designated center server. The connection between node and the center server is usually coaxial or fiber optical cable; the center server should be capable of data storage and high rate transmission. Peer-to-peer

topology is designed so that each node can communicate with any other with no center server in the system. This topology leaves sensors free to join or disconnect from the network. In other words, it can provide resiliency if a sensor fails or is added. Multi-tier network is a topology in which there is more than one central server in the wireless system. In this topology, central servers can communicate with one another and each of them can communicate with several designated wireless sensors as well (Lynch, 2002; Lewis, 2004; Lynch and Loh, 2006; Aygun and Gungor, 2011).

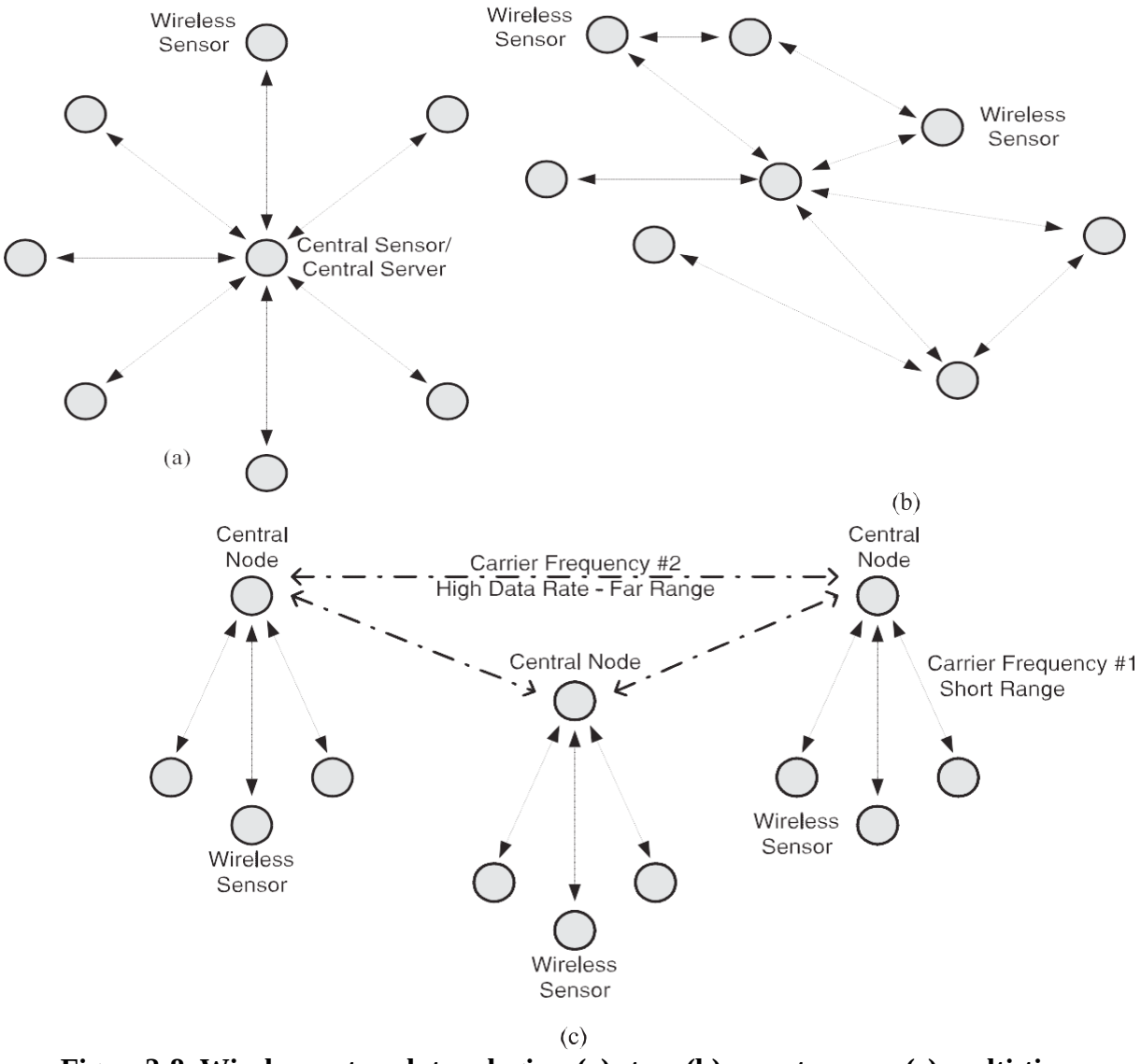

Figure2-8. Wireless network topologies: (a) star; (b) peer-to-peer; (c) multi-tier network topologies (Lynch and Loh, 2006).

Wireless Network Protocols

Wireless network protocols are defined to standardize rules, conventions, and data structure for networked communication using various wireless devices (Lloret, 2009). Such protocols govern how data is packaged, sent, and received in the entire wireless system. In general, wireless protocols are mainly based on two Institute of Electrical and Electronics Engineers (IEEE) communication standards, IEEE 802.11 and IEEE 802.15.4. These two standards for wireless systems generally have been associated with low power consumption, high throughput, and reasonable communication range. However, compared to an IEEE 802.11 device, an IEEE 802.15.4-based wireless system typically has longer battery life and greater range. ZigBee is a typical IEEE 802.15.4-based protocol; it will be further discussed in Chapter 4 (Al-Khatib et al., 2009; Aygun and Gungor, 2011).

Passive and Active Sensors: Case of Radio Frequency Identification (RFID) System

Radio Frequency Identification (RFID) is a wireless identification technology using radio waves to identify an object (tag), acquire data, and write data to the tag (Ruan, et al., 2011). Typically, an RFID system is composed of an RFID tag and an RFID reader. In general, RFID can be divided into passive and active sensor systems. Passive RFID needs no battery. Instead, its power comes from a wireless signal received and converted by an antenna. Conversely, active RFID requires a battery to provide its energy for functioning; active RFID is usually more expensive (Bouhouche et al., 2014). Inclusion of the battery will lead to larger size and limited lifetime. Active RFID also uses a larger-capacity memory module than passive RFID. Additionally, active RIFD usually employs read/write devices while passive RIFD uses read tags only. Passive RFID generally has a shorter read range (< 5 m) and a higher-power reader is therefore required (Roberts, 2006). Moreover, RFID

performance could be adversely affected by electromagnetically ‘‘noisy’’ environments (Lynch and Loh, 2006; Roberts, 2006). However, even though the term “passive” or “active” is mainly used for RFID tags, sensor systems may generally be defined as passive or active depending on whether or not they are self-powered.

Wireless Sensor System Application in SHM of Pavement

As promising sensing paradigms providing Smart Pavement SHM, wireless sensors and sensor networks have been extensively investigated during the 21st century in both academic and commercial fields; they represent improvements in installation processes, data aggregation, signal analysis, sensor clustering, event localization, time synchronization, measurement progress, discrete monitoring, and event-based monitoring as well as in cost saving (Krüger et al., 2005). They also reduce the threat of wire damage in concrete.

Wireless sensor technologies were initially developed and deployed only for military and heavy industrial purposes (SILICON LABS, 2014a). Early applications of wireless-sensor-based SHM in civil infrastructure began with bridges and buildings. Maser et al. (1996) built a two-level wireless telemetry system to measure strain and dynamic load-changing in a highway bridge. The first level of this system contained small transducers powered by self-contained batteries that were used to detect rotation, acceleration, and strain of the bridge structure. The measured data were first transmitted through a wireless transceiver to an on-site data repository and then transmitted via cellular link to a second-level wireless system at the agency office (Maser et al., 1996). For pavement applications, Bennett et al. (1999) in the UK carried out a study assessing performance of wireless sensors developed for monitoring strain and temperature in asphalt pavements; this might be the earliest wireless-sensor-based pavement-monitoring system. In their study, two strain gages

and two thermometers were placed in an instrumented cylindrical core embedded in pavement. Data collected from sensors was transmitted to a roadside laptop via a radio frequency (RF) wireless link located approximately 4 m from the core. A success rate test conducted before opening to traffic proved that the wireless system had good reliability. However, after traffic opening, a decrease in transmission reliability was observed.

In the latter part of 1990, many researchers began working on wireless-sensor platforms for civil infrastructures in which mobile computing and wireless transmission components converged with the sensing transducers (Lynch and Loh, 2006). Table 2-5 provides a summary table of development of wireless sensor platforms and their corresponding technical parameters for both commercial and academic fields from 1998 to 2009, based on the work by Lynch and Loh (2006), Cho et al. (2008), and Aygun and Gungor (2011). Among the studies shown in the table, the focus was mainly on developing new wireless sensing units, and detailed descriptions of the underlying processes were summarized by Lynch and Loh (2006). Through standardization and establishment of the IEEE 802.15.4 standard in 2007, researchers began adapting IEEE 802.15.4 standards-based devices to traditional sensors to make them "wireless" (Salman et al., 2010). Because of these standards, it was unnecessary to develop scratch from all layers of the Open Systems Interconnection (OSI) reference model for new systems, and these standards-based independently-developed wireless systems could easily communicate with one another as well (Nagayama and Spencer, 2007).

Table 2-5. Summary table of development of wireless sensor platforms from 1998 to 2009 (Lynch and Loh, 2006; Cho et al. 2008; Aygun and Gungor, 2011).

Developer and Year	Processor	Radio	Frequency	Availability
Straser and Kiremidjian (1998)	Motorola 68HC11	Proxim/ProxLink	900 MHz	Research
Bennett and Hayes-Gill (1999)	Hitachi H8/329	Radiometrix	418 MHz	Research
Lynch et al. (2002)	Atmel AVR8515	Proxim RangeLan2	2.4 GHz	Research
Mitchell et al. (2002)	Cygnal 8051	Ericsson Bluetooth	2.4 GHz	Research
Kottapalli et al. (2003)	Microchip PIC16F73	BlueChip RBF915	900 MHz	Research
Lynch et al. (2003)	AV90S8515	Proxim RangeLan2	2.4 GHz	Research
Aoki et al. (2003)	Renesas H8/4069F	RealtekRTL-8019AS	–	Research
Basheer et al. (2003)	ARM7TDMI	Philips Blueberry	2.4 GHz	Research
Casciati et al. (2004)	–	Aurel XTR-915	914.5 MHz	Research
Wang et al. (2004)	Analog ADuC832	Linx Technologies	916 MHZ	Research
Mastroleon et al. (2004)	Microchip PIC-micro	BlueChip RFB915B	900 MHz	Research
Ou et al. (2004)	Atmega 8L	Chipcon CC1000	433 MHz	Research
Sazonov et al. (2004)	MSP 430F1611	Chipcon CC2420	2.4 GHz	Research
Farrar et al. (2005)	Intel Pentium	MotorolaneuRFon	2.4 GHz	Research
Pei et al. (2005)	Motorola 68HC11	Max-stream Xstream	2.4 GHz	Research
Musiani et al. (2007)	ATMega128L	ChipconCC1100	1 MHz	Research
Wang et al. (2007)	ATMega128	9XCite	900 MHz	Research
Bocca et al. (2009)	MSP430	ChipconCC2420	2.4 GHz	Research
Zhou et al. (2009)	MSP430	ChipconCC2500	2.4 GHz	Research
Zhu et al. (2009)	Atmega128	XStream	2.4 GHz	Research
Rockwell, Agre et al. (1999)	Intel Stron	Conexant RDSS9M	916 MHz	Commerce
US Berkeley- Crossbow (2003)	Atmega128L	Chipcon CC1000	916 MHz	Commerce
Intel-iMote2 (2003)	ARM7TDMI	Wireless BT Zeevo	2.4 GHz	Commerce
Microstrain, Galbreath et al. (2003)	PIC16F877	RF Monolithics	916 MHz	Commerce

As a common wireless technology, RFID was used a great deal in wireless sensor systems as well. Lajnef et al. (2013) conducted a study to develop a passive RFID strain-sensing system for asphalt pavement health monitoring and fatigue damage detection. The wireless-sensor system developed in this study was a passive radio-frequency system containing a low-power-consumption wireless integrated circuit sensor interfaced with a piezoelectric transducer. This piezoelectric ceramic transducer was designed with an array of

ultra-low power floating gate (FG) computational circuits and could generate enough power to supply an FG analog processor for the sensor under stress. Each sensor node distributed in the pavement could store the data and then periodically transmit it to a vehicle-mounted Radio frequency (RF) reader.

A wireless-sensor network can also be built by connecting traditional sensors to a commercial wireless-transmission node. Xue et al. (2014) designed a sensing network with various commercial sensors for pavement-health monitoring. In that 2011 study on Virginia State Route 114, the sensors included horizontal and vertical strain gages, load cells, thermocouples, and moisture sensors embedded at the bottom of a reconstruction pavement section. All embedded sensors were connected to V-Link wireless voltage nodes near the pavement through wires of different diameters connected to a wireless data logger to collect sensor data and transmit it to a base station via RF. In this system, V-Link nodes had to be first interfaced with the sensors using wires. Once data was collected, numerical simulation was conducted using the monitored strain-response data through finite-element analysis (FEA) based software to compare it with the measured field data. Back-calculation of pavement dynamic modulus was also demonstrated in this study using data collected from a test vehicle. A Mechanistic-Empirical Pavement Design Guide (MEPDG) based on a fatigue-cracking and rutting-prediction model was used to estimate the accumulated damage from distress; this was intended for use in initiating an early warning of pavement deterioration. However, according to their paper, all vertical strain gages failed after five months, probably due to harsh environment and excessive load (Xue et al., 2014).

Wireless sensor networks offer huge benefits for SHM application. There are several different ways to build such networks, but using wireless systems for SHM in pavement is

still in the study phase and there are still several challenges to be resolved. These challenges include noisy wireless environment, limited bandwidth, low signal strength, hardware architecture, embedded software, energy consumption, battery life, weather effects on data collection, data aggregation, communication hops for large scale structure, etc.

CHAPTER 3

FIELD INSTRUMENTATION AND EVALUATION OF COMMERCIAL OFF-THE-SHELF MICRO-ELECTROMECHANICAL SYSTEMS (MEMS) SENSORS AND WIRELESS SENSORS

This chapter describes a field demonstration of off-the-shelf MEMS sensors and wireless sensor system applications in actual in-service concrete applications. The specific objectives of the field demonstration are to

- Evaluate the performance of commercially available off-the-shelf MEMS sensors and wireless sensors
- Identify current limitations of these MEMS sensors for SHM of pavement infrastructure
- Demonstrate how sensing data can be utilized to monitor concrete pavement behavior

Description of Site

In summer 2013, new jointed plain concrete pavement (JPCP) construction projects were carried out in US Highway 30 under the supervision of the Iowa Department of Transportation (Iowa DOT). The project site was located near the southeast area of Ames, IA, as shown in Figure 3-1. To evaluate the performance of the off-the shelf MEMS sensors used for concrete pavement health monitoring, one section from this newly constructed highway pavement was selected for instrumentation to identify requirements for a smart sensing system to advance SHM application for concrete pavement systems.

Figure 3-1. US-30 highway project location. (Source from Map data @2013 Google).

Figure 3-2 illustrates the concrete pavement construction plan of this project. The newly-constructed pavement section was approximately 10 inches in thickness and constructed above a granular subbase with thickness ranging from 6 to 10.3 in. The PCC pavement was crowned with a 2.0% transverse slope and had widths of 12 ft. and 14 ft. for passing lane and travel lane, respectively. The transverse-joint spacing was set at 20 ft., reflecting general practice in Iowa. Dowel bars with baskets were placed on the subbase before concrete paving.

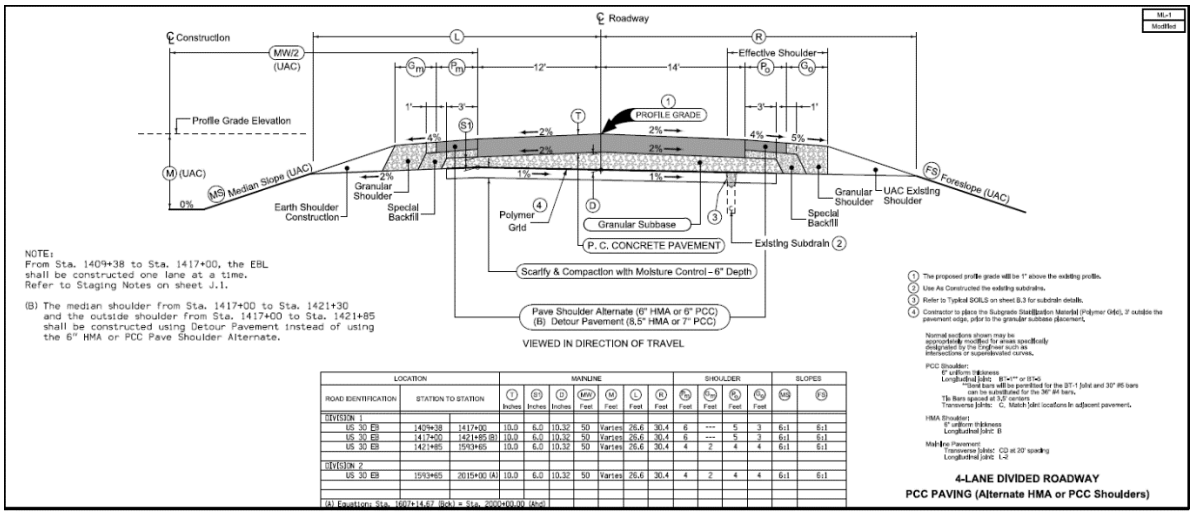

Figure 3-2. US-30 highway construction plan.

Installation of sensors was conducted on May 23, 2013, one day before concrete paving in US Highway 30 at 8:00 am on May 24, 2013. A slipform paver moved from west to east to pour fresh concrete on the subbase. A viborator followed the paver to consolidate the fresh concrete using viboration tubes. Surface smoothing was performed manually. A slipform paver dragging a piece of burlap was used to create texture for the pavement surface and a chemical curing compound sprayed on the paving surface. Shoulder backfilling was conducted approximately 14 days after concrete paving; a 6-in thick Hot-Mix Asphalt (HMA) shoulder was then placed on June 10, 3 days after shoulder backfilling. One day later, granular shoulder was added to the pavement. The constructed pavement was opened to traffic on June 14, 2013. Table 3-1 lists details of the construction timeline.

Table 3-1. US-30 highway construction timeline.

Timeline	
Date	Activities
May 23, 2013	Sensor installation
May 24, 2013	Concrete paving
June 7, 2013	Backfilling for shoulder
June 10, 2013	HMA shoulder paving
June 11, 2013	Granular shoulder paving
June 14, 2013	Opened to traffic

Description of Sensors

Temperature and moisture are vital factors contributing to concrete properties such as strength and durability. Low temperature and rapid loss of moisture can result in insufficient development of strength, and different temperature and moisture gradients in concrete can

contribute to curling and warping behaviors that may result in cracks if the induced stress exceeds the concrete strength. A total of 30 sensors, including off-the-shelf MEMS based temperature and moisture sensors and strain gages, were evaluated in this study. The sensors used were Radio-Frequency Identification (RFID) temperature tags, Sensirion digital humidity sensors SHT71, Thermochron iButtons, and Geokon model 4200 strain gages. A detailed description of each type of sensor is presented in the following sections.

Radio-Frequency Identification (RFID) Temperature Tag

The wireless RFID tags from the HardTrack Concrete Monitoring System, WAKE, Inc. were selected for temperature monitoring due to their low cost, extensive communication range, durability in concrete and low power consumption. This active wireless RFID tag is a MEMS-based temperature sensor with advanced UHF RF technology that can provide real-time data collection and storage. This RFID system consists of a RFID transponder called "i-Q32T" and a portable handheld transceiver called "Pro", which are shown in Figures 3-3 and 3-4 (IDENTEC SOLUTIONS, 2008; WAKE, Inc., 2010). Figure 3-3 shows that the tag contains an internal temperature logger to capture the temperature of concrete at definable intervals, and a battery for power (IDENTEC SOLUTIONS, 2008). The antenna inside this tag enables the Pro to identify the tag to read/extract data or to change the time interval. In this study, temperature readings were taken every 30 minutes. By communicating with the portable Pro, the collected temperature data could be imported into this handheld transceiver for data-saving and concrete-maturity calculation using a PCC maturity concept. Consequently, this RFID tag was applicable to concrete-temperature monitoring, and its excellent accuracy exceeded that of the ASTM C1074-93 requirement. This tag had a claimed capability of transmitting and receiving data within distances of up to 100 feet (30

meters) from the handheld device or up to 300 feet (100 meters) from a fixed interrogator; its operational life could be greater than 6 years due to its low power consumption (IDENTEC SOLUTIONS, 2008).

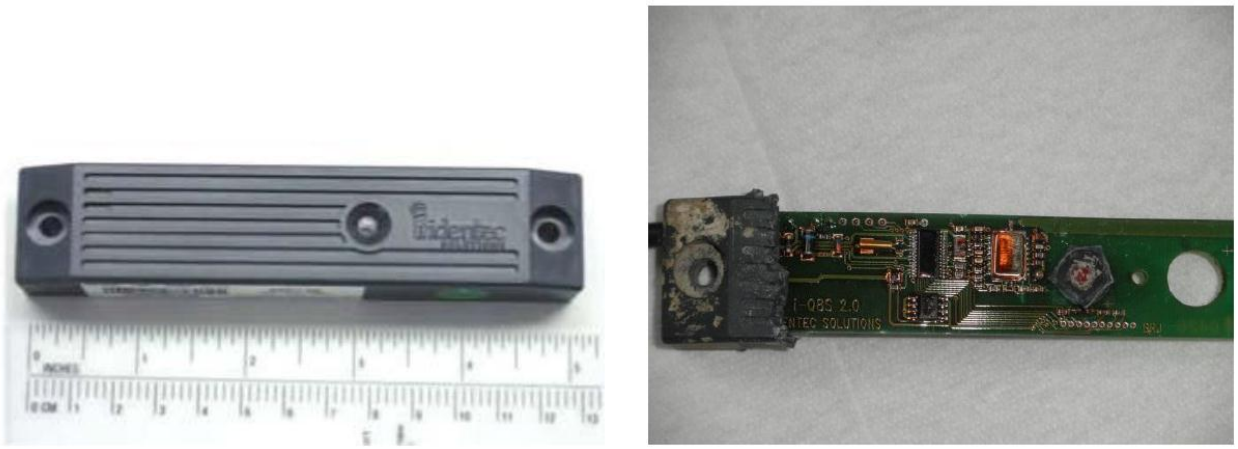

Figure 3-3. i-Q32T wireless RFID transponder (photo courtesy of WAKE, Inc.).

Figure 3-4. HardTrack portable handheld transceiver Pro (photo courtesy of WAKE, Inc.).

Figure 3-5 illustrates the whole RFID system, including the portable handheld transceiver Pro. In this system, the i-Q32T RFID tag can be divided into an "embedded

probe" and an "extended probe". The embedded probe was the tag the temperature logger installed inside of the i-Q32T tag, but when making deep pours the RFID tag could be equipped with a stainless steel temperature probe, referred to as an "extended probe" in this thesis, to enable it to penetrate deeper into large concrete structures. RFID extended probes are typically used in large-scale structures like dams to measure the temperature of concrete several feet below the concrete surface, but the i-Q32T tag with an antenna can still be placed at the surface to transmit data. The biggest advantage of the "extended probe" was that it could be removed from the tag so the tag could be recycled if there was no need to use the extended probe. Both embedded probe and extended probe are shown in Figure 3-5.

Figure 3-5. RFID tag and portable Pro.

MEMS Digital Humidity Sensor

The Sensirion digital humidity sensor SHT71 evaluated in this study was classified as a commercial multifunctional off-the-shelf MEMS sensor that could simultaneously measure Relative Humidity (RH) and temperature. Figure 3-6 (a) and (b) show pictures of the MEMS

digital humidity sensor and the evaluation kit, respectively. The commercial MEMS digital humidity sensor, developed by Sensirion, Inc., is a kind of metal pin-based sensor integrating both the sensing elements and signal processing circuitry on a silicon chip to provide a fully-calibrated digital output. In this sensor, a unique capacitive sensing element consisting of paired conductors was used to capture RH while another band-gap sensor measured temperature. The paired conductors were separated by a dielectric, a kind of polymer to absorb or release water proportionally with the relative environmental humidity. The capacitance change was measured by an electronic circuit to calculate RH (Sensirion, Inc., 2014). To simultaneously protect the sensor from interference, a "micro-machined" finger electrode system with different polymer-covered layers was used to produce the capacitance for this MEMS sensor.

The MEMS digital humidity sensors must be connected with evaluation kit EK-H4 (Figure 3-6 (b)) at all times to continuously monitor temperature and RH. Moreover, it is should also be pointed out that this evaluation kit does not have memory, so a laptop with related software must be connected at all times to store the measurements. Time intervals could be set through the laptop; in this study measurements were performed at one-minute intervals.

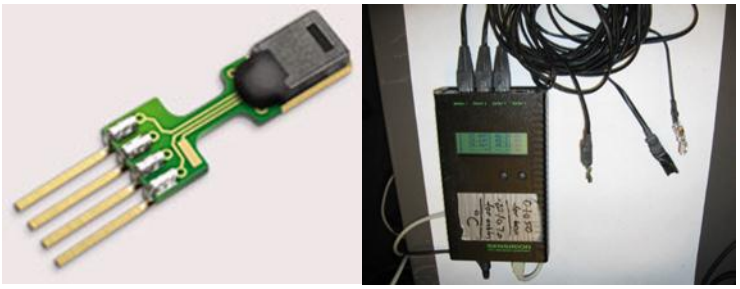

(a) (b)

Figure 3-6. Sensirion sensor system: (a) Sensirion SHT71 sensor; (b) evaluation kit.

Thermochron iButton

The Thermochron iButton from Maxim Integrated Products, Inc. is designed for temperature measurement and storage. This low-cost and reliable temperature sensor is equipped with a wide-temperature-range thermometer (14 to 185˚F) and has a protected memory section. It is able to record time and temperature at user-defined intervals of up to 255 minutes, and total of 2048 temperature readings can be stored (Maxim Integrated, 2014). Therefore, the monitoring period could be extended to 340 days based on the maximum measurement interval if the internal battery could guarantee a minimum of 2 years' working time at room temperature. Furthermore, this iButton sensor is protected by a durable stainless steel shield with plastic cover to ensure that it is working properly in the concrete environment.

The main advantages of the iButton temperature sensor are large memory, long battery life, rugged packaging, and low cost. iButtons have been used in field projects for temperature monitoring of fresh concrete during construction. For example, the Texas Department of Transportation conducted a demonstration project in 1999 using a large number of iButtons; Des Moines International Airport utilized iButtons to monitor the temperature history of fresh concrete (Tully, 2007). Figure 3-7 is a picture of an iButton. It can be seen that the iButton requires a USB cable for data downloading. Unlike the MEMS digital humidity sensor, the iButton doesn't require constant connection with the laptop because it has its own memory system. In this study, iButtons were used as reference sensors to measure internal temperature of concrete at 30-minute measuring intervals.

Figure 3-7. Thermochron iButtons and USB cable.

Strain Gage

The strain gage evaluated in this project was the Model 4200 Vibrating Wire Embedment Strain Gage manufactured by Geokon, Inc., and shown in Figure 3-8. This is a 6 in. long static strain sensor designed for direct embedment in concrete; it makes measurements based on a vibrating-wire principle (See Figure 3-9). When the gage is embedded in concrete, strain changes will cause the two metal blocks to move relative to one another, and the resulting tension generated in the steel wire can be determined by plucking the wire and measuring its resonant frequency of vibration (Geokon, Inc., 2014).

The advantages of the Model 4200 Vibrating Wire Embedment Strain Gage claimed by its manufacturer include excellent long-term stability, maximum resistance to effects of water, and a frequency output suitable for transmission over very long cables. Use of stainless steel ensures that it is waterproof and corrosion-free, but strain measurement is affected by temperature, so the model 4200 strain gage incorporates an internal thermistor for simultaneous measurement of temperature.

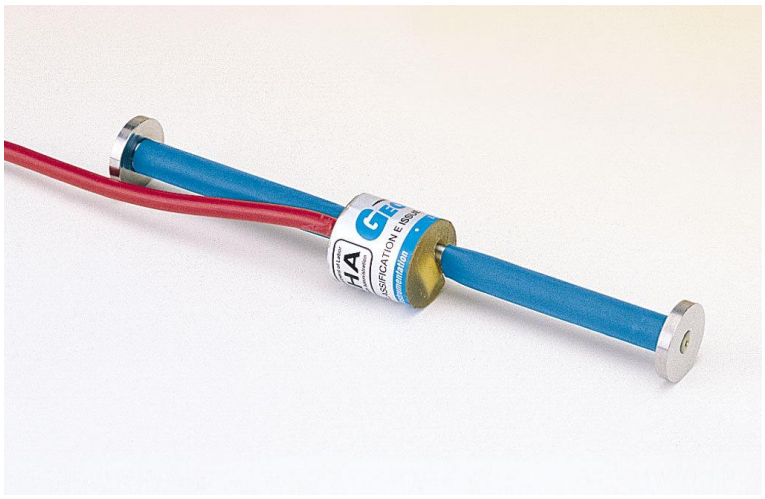

Figure 3-8. Geokon model 4200 strain gage (Geokon, Inc., 2014).

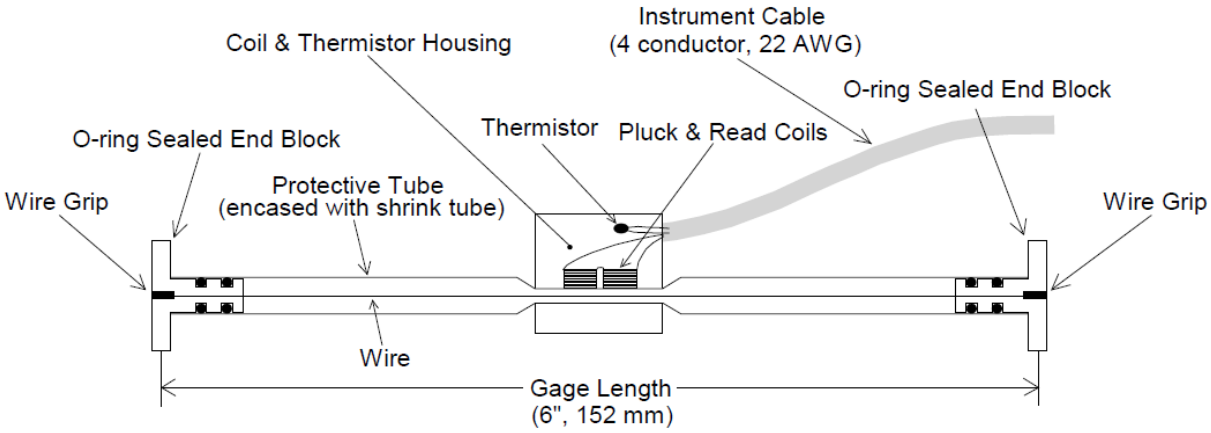

Figure 3-9. Model 4200 Vibrating Wire Strain Gage (Geoko, Inc., 2014).

Figure 3-10 shows a picture of the entire strain measurement system including the Geokon model 8002 data-logger used for data collection. This data-logger can be conveniently powered either by widely available alkaline D cells, or by an external 12 V source. It has an operating time ranging from 8 days to 2 years, depending on the scan interval. However, in this study the strain reading was recorded every minute so the estimated operational time was about two and one-half days.

Figure 3-10. Datalogger and Model 4200 strain gage.

Installation of Sensors

The instrumented pavement section was located in the driving lane of US Highway 30. A total of 30 sensors, including 14 RFID temperature tags (9 extended probes and 5 embedded probes), 4 MEMS digital humidity sensors, 5 iButtons, and 7 longitudinal strain gages were installed at different locations throughout at various concrete pavement depths and placed near to DAS for ambient temperature monitoring.

Location of Sensors

In general, concrete pavement edges and corners will suffer more from load than other positions (Darestani, 2007), so the locations selected in this project were the corners and mid-panels of the slab. Figure 3-11 (a) and (b) show the detailed instrumented plan of this slab. Referring to these two figures, there were five cross-sections (section A-A through E-E) totally instrumented with these sensors. The distances from each section to the shoulder were all different. Among these cross sections, section A-A, 44 in. away from the HMA

shoulder, was instrumented at mid-span using 4 RFID embedded probes, 4 iButtons, and 2 strain gages. The RFID tags were installed at distances of 3, 5, 6, and 7.5 inch below the pavement surface, and iButtons were installed at distances of 4, 5, 8.5, and 10 inches below the surface, respectively. Strain gages were embedded only at the top and bottom positions, 2 and 8.5 in. away from the pavement surface. Section B-B, located at the joint between two adjacent slabs, was 40 in. away from the HMA shoulder. It was instrumented using only one strain gage under a dowel bar, as shown in Figure 3-12. Section C-C was 28 in. away from the shoulder. It was instrumented using 8 RFID extended probes and 3 MEMS digital humidity sensors. Among these embedded RFID tags, 5 RFID extended probes were embedded in the corner at distances of 2, 4, 6, 8, and 10 inches below the surface and 3 RFID extended probes were embedded in the mid-span at distances of 2, 5.5, and 8.5 inches below the pavement surface. With regard to the 3 MEMS digital humidity sensors, they were embedded at the same locations where the 3 RFID extended probes were installed. Section D-D, located 20 in. away from the HMA shoulder, was instrumented by strain gages only. In this section, 2 strain gages were embedded at the top and bottom in the corner at 2 and 9 inches below the surface. Another pair of strain gages was embedded at the top and bottom in the center, 2 and 9 inches, respectively, below the surface. The last section, E-E, was 8 in. away from the shoulder and was instrumented using only one MEMS digital humidity sensor, located just 0.1 in. below the surface at the mid-span.

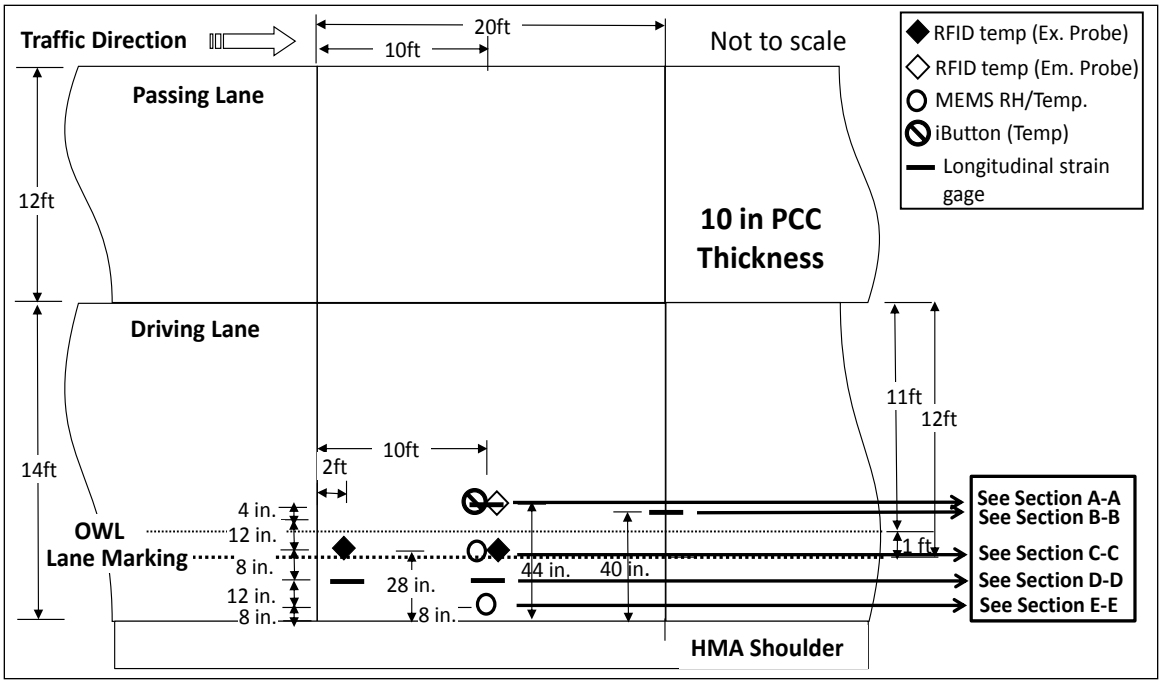

(a)

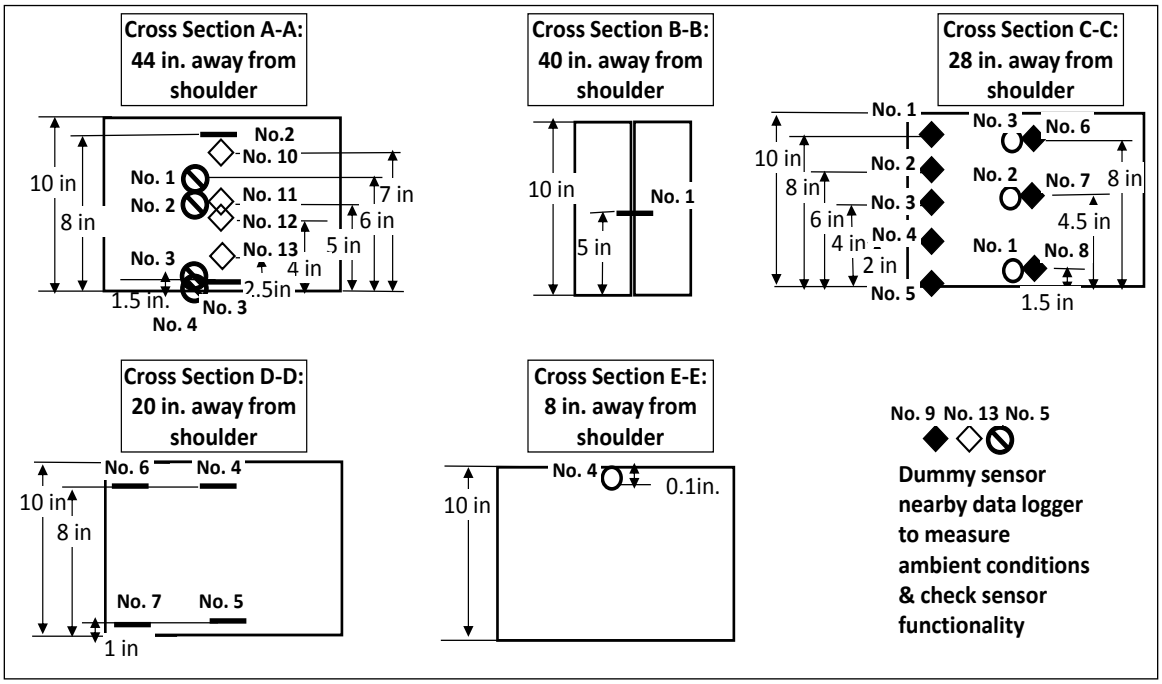

(b)

Figure 3-11. Sensor instrumentation plan: (a) top view; (b) cross-section view.

Figure 3-12. Installation of strain gage at joint.

Processes of Installation

All sensors were pre-installed one day before concrete paving, with installation of sensors beginning in the subbase on the morning of May 23, 2013. Prior to installation of sensors, wooden bars were first inserted in the subbase in accordance with the previous installation plan. The length of these wooden bars above the subbase surface was approximately 10 in., almost equalling the thickness of PCC slab. In the next step, all sensors were mounted to these wooden bars using zip-ties to fix their positions during pavement construction, as shown in Figures 3-13 (a) and (b).

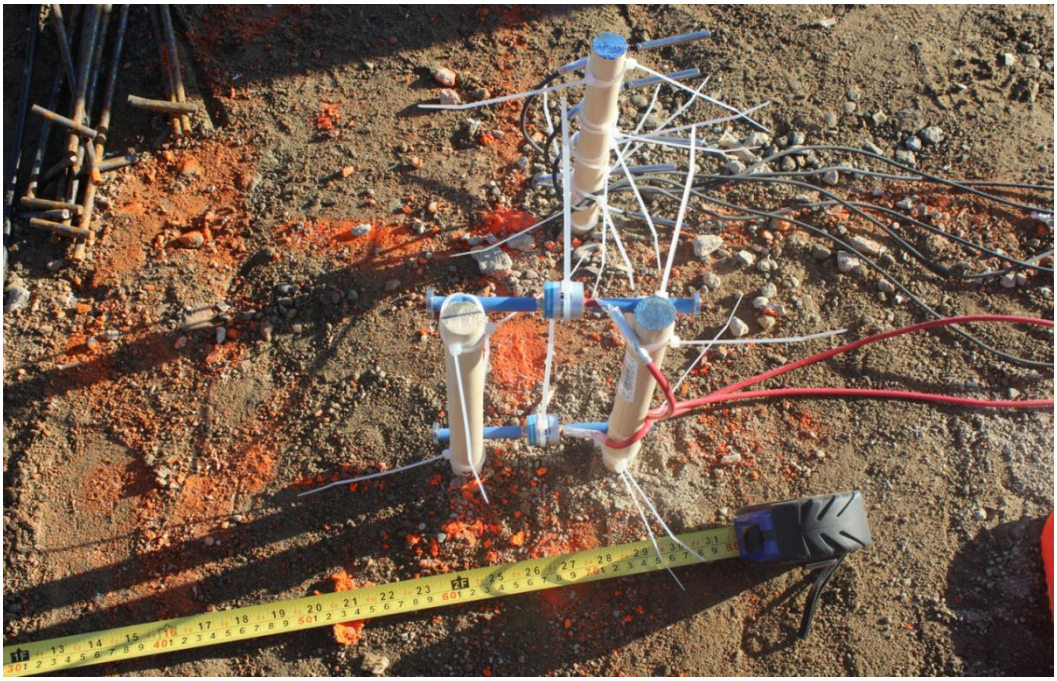

(a)

(b)

Figure 3-13. Installation of sensors: (a) near slab corner; (b) near mid-span edge.

As shown in the above two figures, two wooden bars were used to fix the location of strain gages and RFID tags. While a wooden bar would not cause any issues related to

thermal conductivity that might may affect strain and temperature measurement, it should be pointed out that the strain gages and the RFID tags were placed in alignment with traffic direction, the same as the direction of concrete paving. Additionally, iButtons and MEMS digital humidity sensors were mounted on the back of the wooden bars to reduce the direct force of concrete paving. All these strategies were applied to help sensors survive during paving construction.

It should be noted that, during installation of sensors, wires from sensors needed extra attention because there was no way to repair them once inside the concrete if they are broken or have loose connection issues. In this project, all the sensors deployed in US Highway 30 were wired sensors except for RFID tags; even the RFID extended probe had a long cable between the temperature probe and the "i-Q32T" tag. To protect these wires, all were spliced and soldered to create connections and then placed in a polyvinyl chloride (PVC) pipe, as shown in Figure 3-14. The PVC pipes were then placed in a ditch dug in advance and then wires were connected to the Data Acquisition System, as shown in Figure 3-15.

Figure 3-14. Wires in PVC pipe.

Figure 3-15. PVC pipe in ditch with wires.

Data Acquisition System (DAS)

Figure 3-16 shows the on-site DAS of the sensors used in US-30 highway. It can be seen that both the DAS and the batteries were stored in a plastic shield box. The laptop was used to collect data from MEMS digital humidity sensors, and the rechargable batteries were used to supply power to the laptop only. The box located approximately 14 ft. away from the HMA shoulder was covered by an orange protective blanket. All devices were placed on a wooden board supported by two concrete caps and a plastic bag was used to protect them from rain. These protective strategies were used to protect the DAS from animals, rain, wind, etc., because it was important to keep the DAS away from external disturbances. Additionally, ambient RFID tags (both extended probes and embeded probes) and iButtons were placed beside the shield box to capture ambient temperature conditions, as shown in Figure 3-17.

Among the sensors deployed in the US Highway30 project, only RFID tags and iButtons were quipped with internal batteries. MEMS digital humidity sensors and strain gages, as well as the DAS, required batteries to make them function during the monitoring period. However, the batteries could provide only 3 days' power for the laptop, so data acquisition and battery replacement were scheduled every two days to achieve continuous data collection during the initial stages up until June 28, 2013. However, these procedures were time and labor-consuming, so different times were scheduled for summer and winter data-acquistion times late due to traffic and environmental conditions.

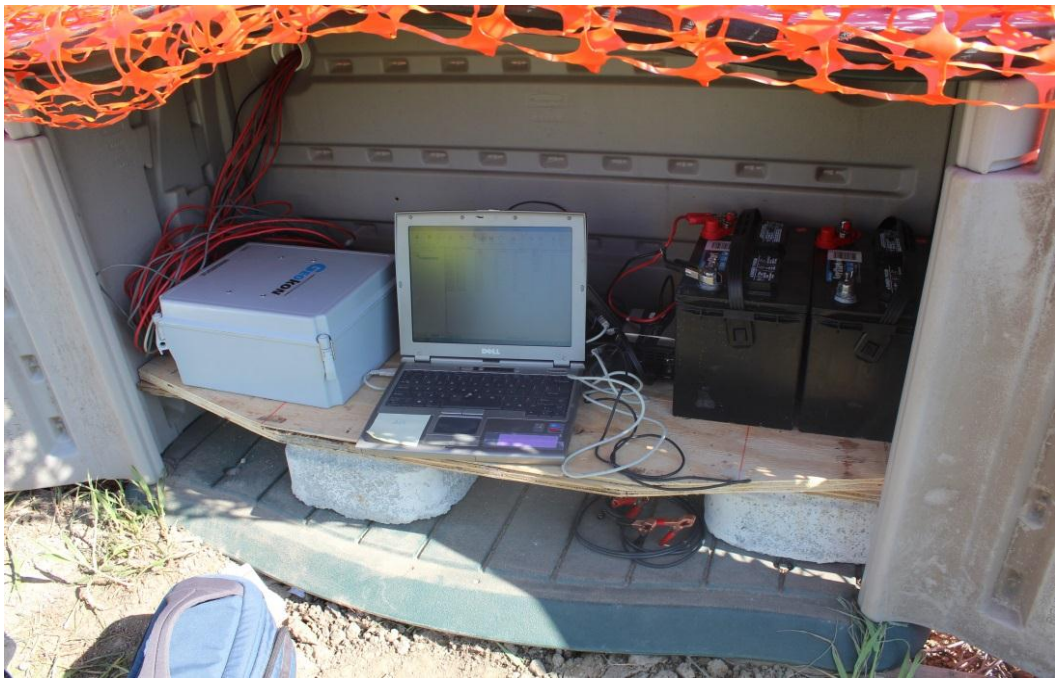

Figure 3-16. Data Acquisition System (DAS).

Figure 3-17. Ambient sensors.

Concrete Paving

Concrete paving for the instrumented pavement section started at 7:45 am on May 24, 2013. Before concrete paving, dowel bars with baskets were placed above the subbase. The average water/cement ratio for the concrete ranged from 0.4 to 0.43. The time of initial and final set were determined at 4.84 and 7.17 hours, respectively, in acordance with ASTM C 403, attached as Appendix C. During road construction, both a paver and a vibrator were used. A huge amount of fresh concrete first poured on the subbase was spread out by the passing paver, as shown in Figure 3-18. A vibrator with vibration tubes followed the paver to produce consolidated concrete. The vibrator leveled off the concrete as it passed through and the workers behind the vibrator then smoothed the surface. Finally, the surface was textured by dragging a piece of burlap in the longitudinal direction. Water was sprayed onto the

pavement surface after texturing, followed by spraying of chemical components for curing purposes.

Figure 3-18. Concrete paving.

However, both paver and vibrator were sources of potential threat of sensor damage due to their auger and vibration forces that might break either the sensors or the wires during pavement construction. Moveover, dropping a heavy mass of concrete could crush the sensors and tear up the wires. Therefore, to protect the sensors as much as possible, fresh concrete was carefully pre-poured on the top of sensors to mitigate the force from the paver, vibrator, and dropped concrete, as shown in Figures 3-19 (a) and (b). Then, after concrete paving, a MEMS digital humidity sensor was embedded 0.1 in. below the pavement surface at cross section E-E, as shown in Figure 3-20.

(a)

(b)

Figure 3-19. Sensor protection during road construction: (a) obtain fresh concrete from paver; (b) pour concrete on the sensors.

Figure 3-20. Embedment of MEMS digital humidity sensors.

The temperature probes of RFID tags (extended probes) were mounted on wooden bars, and the i-Q32T tags (transponder) were placed in a protective wooden box beside the concrete slab, as shown in Figure 3-21. This box was used to protect the tags during shoulder construction as shown in Figures 3-22 (a) and (b). As a result, data measured inside the concrete could be successfully transmitted from the transponders in the box. Figure 3-23 shows the traffic opening on June 14, 2013, and the protective wooden box for RFID tags can be seen at the bottom of the picture.

Figure 3-21. RFID extended probe in wooden box.

(a)

(b)

Figure 3-22. Shoulder construction: (a) backfilling; (b) HMA shoulder paving.

Figure 3-23. Traffic opening.

Sensor Performance Evaluation

JPCP behavior before traffic opening was mainly affected by environmental conditions. The monitored concrete properties for the test section on US Highway 30 were temperature, moisture, and strain. This section mainly provides detailed descriptions of both quantity and quality evaluation of sensor performance. Furthermore, concrete pavement behavior (curling and warping) associated with the monitored concrete properties is discussed.

Temperature and Moisture

In concrete pavement, knowledge of temperature profile is essential for stress analysis. Different temperature gradients throughout the entire concrete depth and excessively high ambient temperatures such as from heat waves can result in structural failure. In this study, temperature measurements were mainly captured by RFID tags, MEMS digital humidity sensors, and iButtons embedded throughout entire depth of the PCC pavement. The measurements from iButtons were used as reference temperatures to be compared with the other two types of temperature sensors.

Moisture content plays a significant role in cement hydration because it may not proceed properly under low-moisture conditions. Moisture-gradient changes inside concrete, just like temperature gradients, can lead to concrete deformation. Moisture-content distribution is also crucial in evaluating the severity of shrinkage during setting and hardening processes. However, moisture content measured in concrete is usually represented by humidity level. Moisture typically means amount of water present in a material, but humidity is the amount of water vapor present in air or gas and can be represented as either absolute humidity or relative humidity (Das, 2009; Ye et al., 2006). Absolute humidity is the ratio of the mass of water vapor to the volume of air or gas, while relative humidity (RH) refers to the percent of the water content in air compared to the saturated moisture level at the same temperature and pressure (Ye et al., 2006).

Monitoring Period Overview

The entire monitoring period extended from May 24, 2013 to April 1, 2014, approximately 10 months after traffic opening. However, to obtain continuous data, data acquisition had to be scheduled every two days, which was an unrealistic requirement over the entire 10 months due to the remote location of the DAS, the harsh climate, and the limited labor force. As a result, the longest continuously-monitored period actually used is described and discussed in this section.

RFID Tag (Extended Probe)

Figures 3-24 (a) and (b) illustrate the temperature profiles captured by RFID extended probes at slab corner and center, 28 in. away from HMA shoulder. Probes No. 1 through 5 were 2, 4, 6, 8, and 10 in., respectively, below the pavement surface, and probe No.9 was an ambient temperature sensor. Probes No. 6 through 8 were located 2, 5.5, and 8.5 in.,

respectively, below the surface. As seen in Figure 3-24, a maximum temperature of 111 ˚F and a minimum temperature of 0 ˚F were observed during May through April in 2014. The average temperature rose to about 80 ˚F in summer and rapidly went down to about 20 ˚F in winter. Furthermore, fewer and fewer sensors remained functional as time passed; the sensors embedded in the center were not functional after December, 2013.

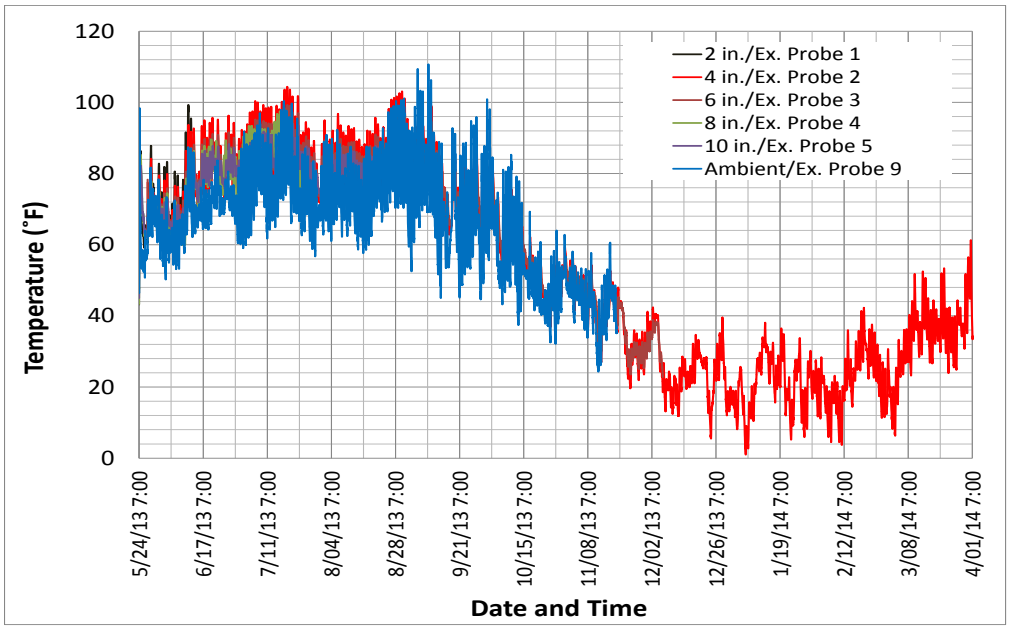

(a)

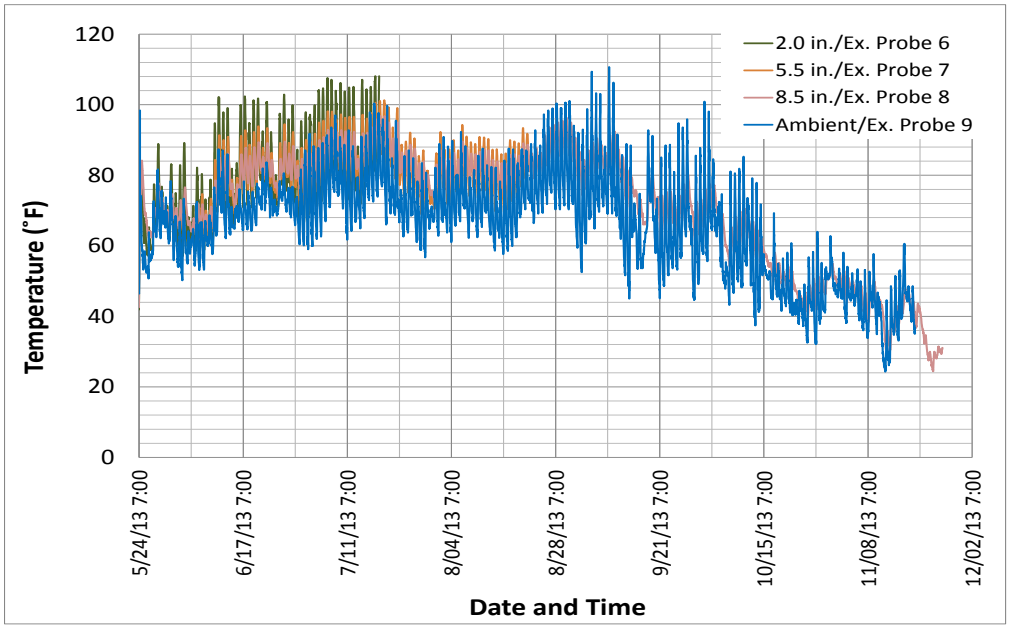

(b)

Figure 3-24. RFID extended probe measurement: (a) in the corner; (b) in the center.

RFID Tag (Embedded Probe)

Figure 3-25 illustrates the temperature profile captured by RFID embedded probes in mid-span 44 in. away from the shoulder. RIFD extended probes No.10 through 13 were embedded 3, 5, 6 and 7.5 in. below pavement surface and probe No.14 was an ambient temperature sensor. From Figure 3-25, the temperature ranged from 20 to 108 ˚F before December 6, 2013, similar to the temperature captured by RFID extended probes embedded in the center. However, fewer and fewer RFID-embedded probes remained functional as time passed and no embedded probes were functional after December 7. Note that the ambient temperature probe No. 14 was removed on July 19, 2013. Furthermore, based on observation, it was found that the temperature difference between top concrete and bottom concrete was in the range from 4 ˚F to 12 ˚F.

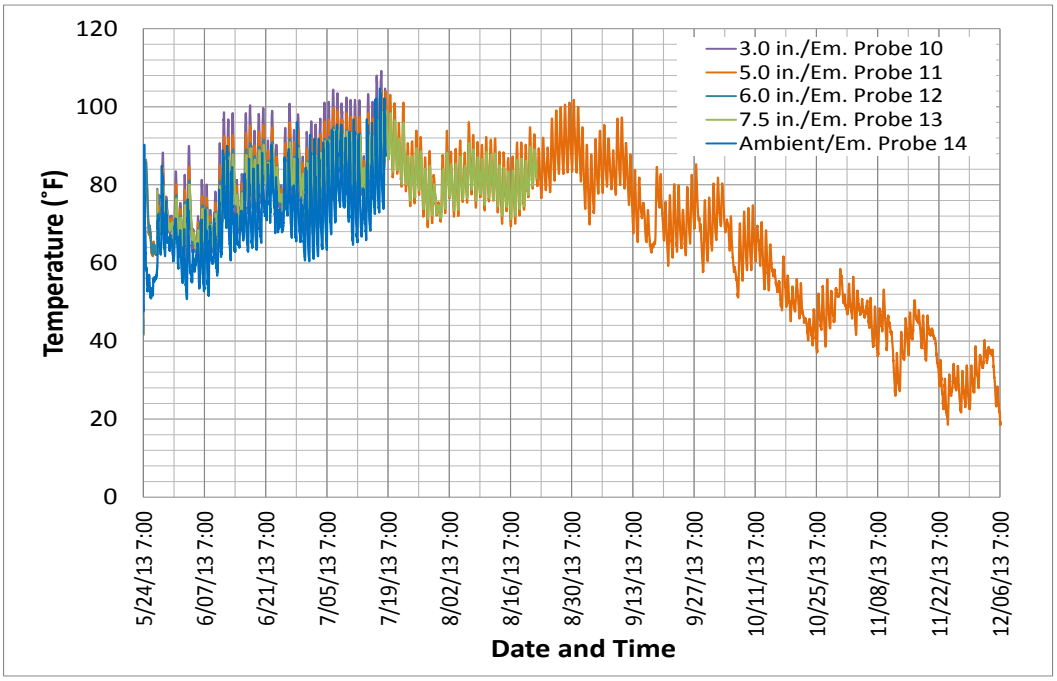

Figure 3-25. RFID embedded probe measurement in the mid-span.

MEMS Digital Humidity Sensor

Four MEMS digital humidity sensors were embedded in US Highway 30. MEMS digital humidity sensors No. 1 through 3 were embedded 8.5, 5.5, and 2 in. below the pavement surface and No. 4 was just 0.1 in. below the pavement surface. However, sensors No. 1 and 2 were unable to collect data within just a few hours after concrete paving. This could probably be attributed to wire damage or loose connections incurred by the concrete paver, the vibrator, or the high-alkali environment prevailing during concrete hydration. Note also that data could not be acquired in the period May 26 through 28, 2013 because the battery (power supply) for the DAS was not recharged. Figures 3-26 and 3-27 give the temperature and RH profiles captured by the MEMS digital humidity sensors.

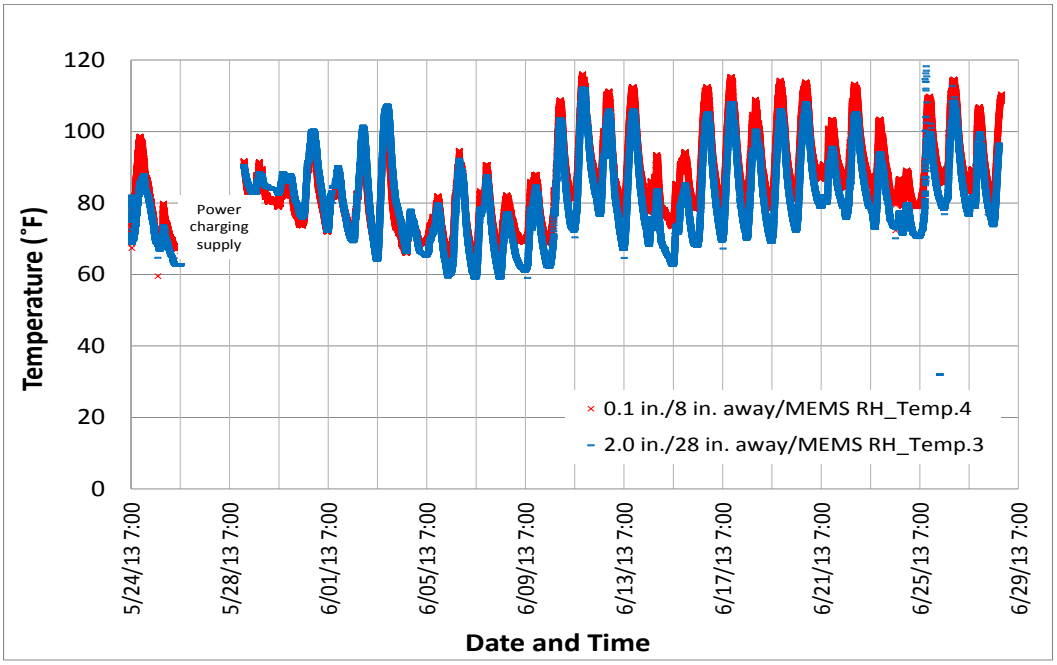

Figure 3-26. Temperature measurement of MEMS digital humidity sensors.

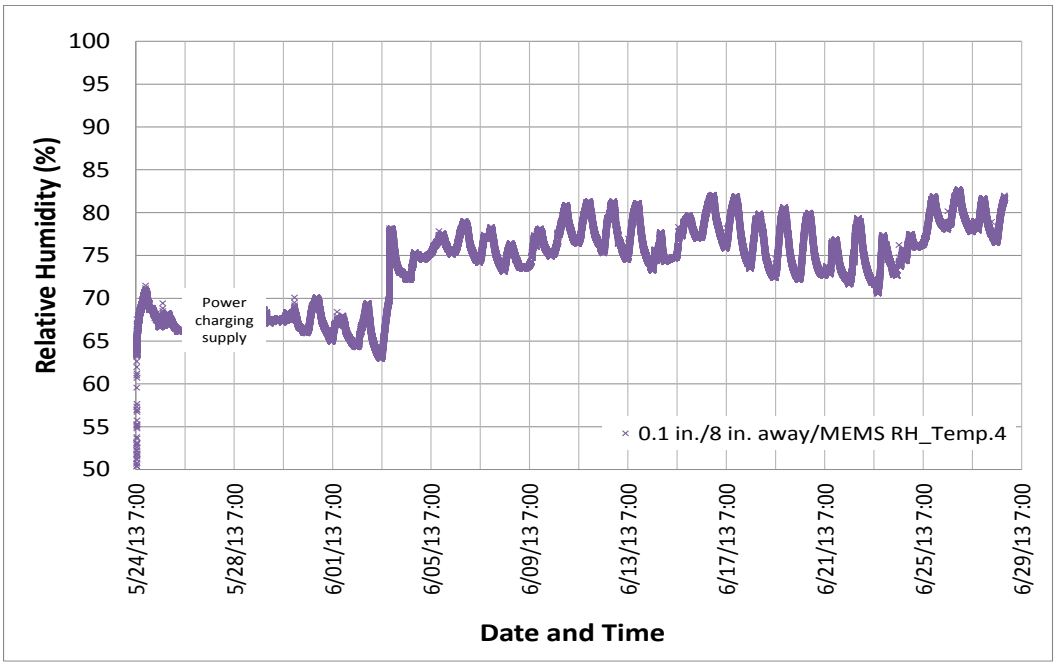

Figure 3-27. RH measurement of MEMS digital humidity sensor.

According to Figure 3-26, the temperature before June 29 ranged from 60 to 120 ˚F. It can also be seen that sensor No. 4 in its initial stage reflected higher temperature in daytime and lower temperature at night. This is because sensor No. 4 was closer to the pavement surface so it would be more easily affected by ambient environment such as solar radiation. Meanwhile, temperature at the pavement top would drop more rapidly than that at the bottom. However, in later stages, sensor No. 4 also exhibited a higher temperature at night; this was probably due to a heat wave reported in June 2013. According to Figure 3-27, the RH was about 67% in the beginning followed by a sharp increase in RH from 63% to 78% observed on June 3, 2013, and due to a serious thunderstorm occurring on June 3 and 4, 2013. Following that, the RH value fluctuated between 70% and 80% most of the time.

iButton

Figure 3-28 illustrates temperature measurements taken from the iButton between May 24 and August 22, 2013. iButtons No. 1 to 4 were embedded 4, 5, 8.4, and 10 in. below

pavement surface, and iButton No. 5 was an ambient temperature sensor. Among these sensors, only one iButton (No. 4) stopped functioning (on July 18, 2013). It can be seen that the temperature range measured by iButtons ranged from 47 to 105 ˚F, lower than the values captured by the RFID tags. This was because the highest temperature was captured by iButtons No. 1 and 2 installed at the midpoint of the pavement depth, so their readings were lower than the values captured by the RFID tags and the MEMS digital humidity sensors located near the top of pavement. However, comparing ambient temperature measurements, the ambient RFID extended probe and the embedded probe had the same reading, approximately 2 ˚F higher than the ambient iButton's measurement.

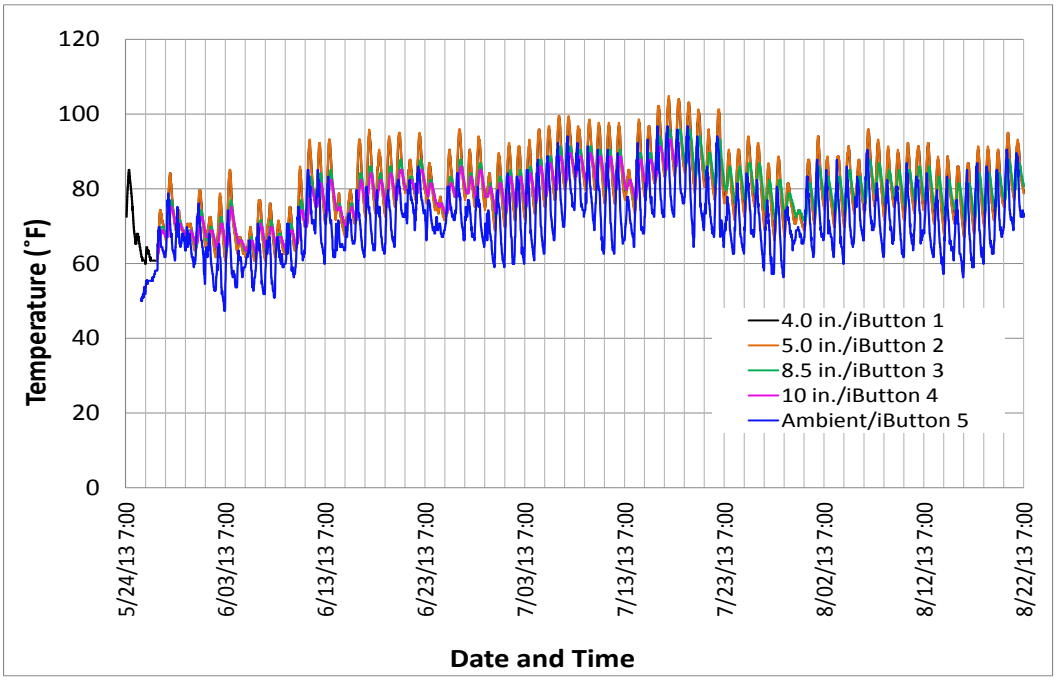

Figure 3-28. Temperature measurement from iButtons.

Strain Gage

Strain is a significant indicator of concrete structural quality. Figure 3-29 illustrates the strain change captured in the period between May 24 and June 29, 2013. Strain gages No. 3 and 5 were embedded 8.5 and 9 in. below the pavement surface at the slab corner, while

strain gages No. 6 and 7 were embedded 2 and 9 in. below the pavement surface at the mid-span edge. The other strain gages, No. 1, 2, and 4, stopped functioning immediately, probably due to wire issues. In Figure 3-29, positive and negative microstrain represented tension and compression, respectively. However, after opening to traffic, the strain readings were greatly affected by the traffic load. The strain behavior after traffic activity began was not in the research scope and therefore not discussed in this section. A detailed description of strain behavior before traffic opening is provided in the next section.

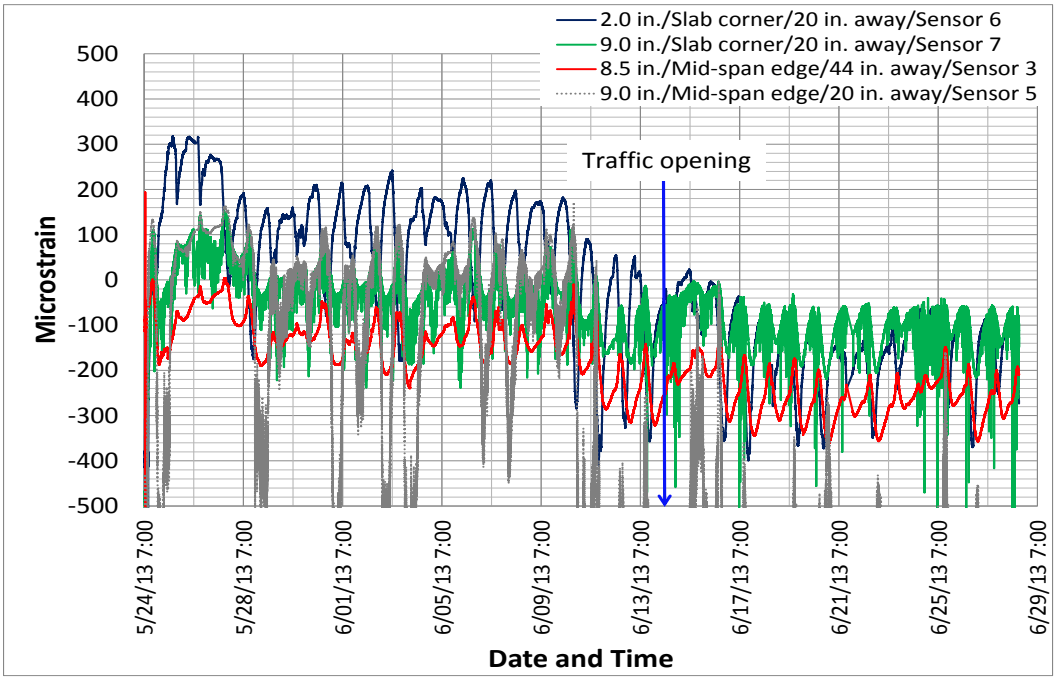

Figure 3-29. Strain measurement.

Before Traffic Opening (May 2013 to June 2013)

The overall monitoring period was divided into three periods: before traffic opening, two months after traffic opening (summer), and six months after traffic opening (winter). Traffic opening occurred on June 14, 2013, and there was therefore no vehicular effect on pavement properties before that date. The strain behavior of pavement associated with

environmental effects from temperature and moisture could be analyzed for this period. Figures 3-30 through 3-34 illustrate temperature, RH, and strain captured by the sensors.

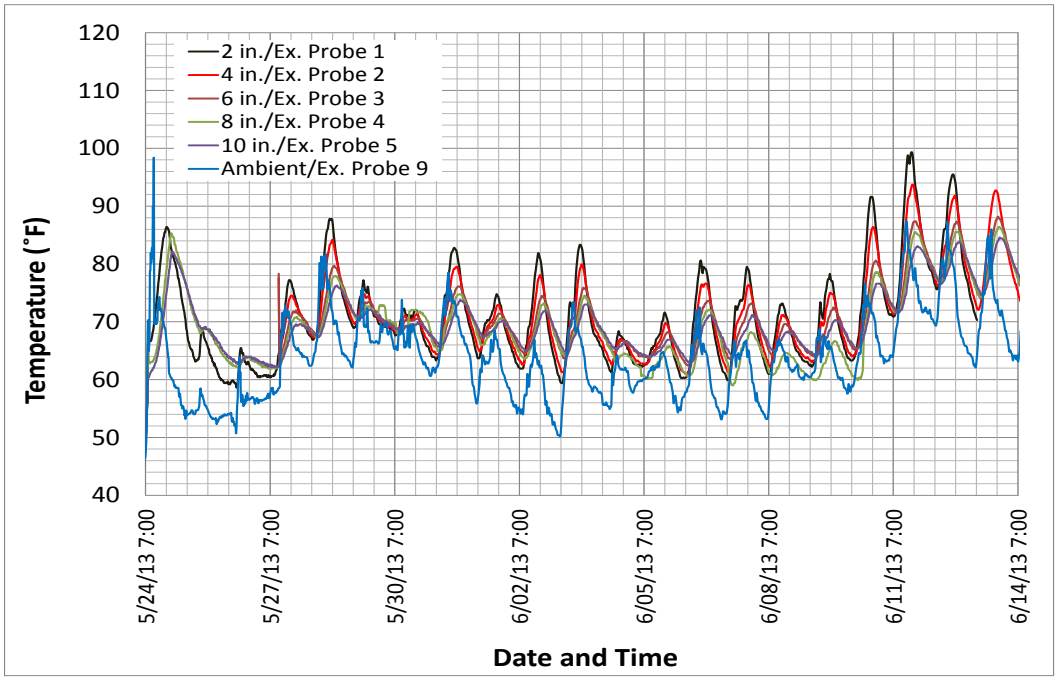

(a)

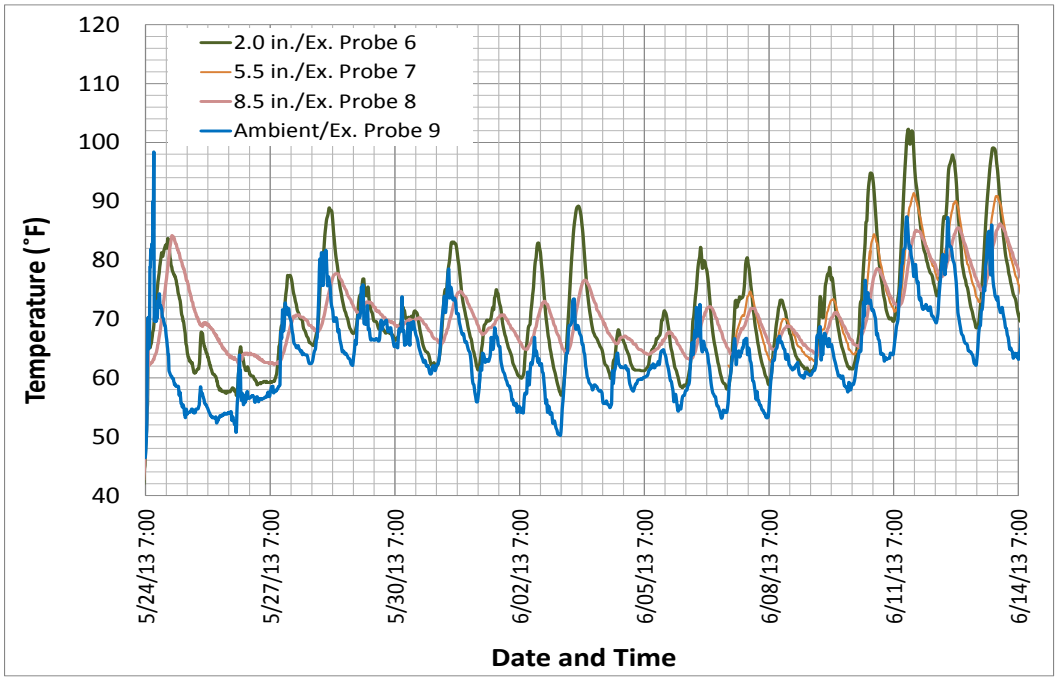

(b)

Figure 3-30. Measurement of RFID extended probes before traffic opening: (a) in the corner; (b) in the center.

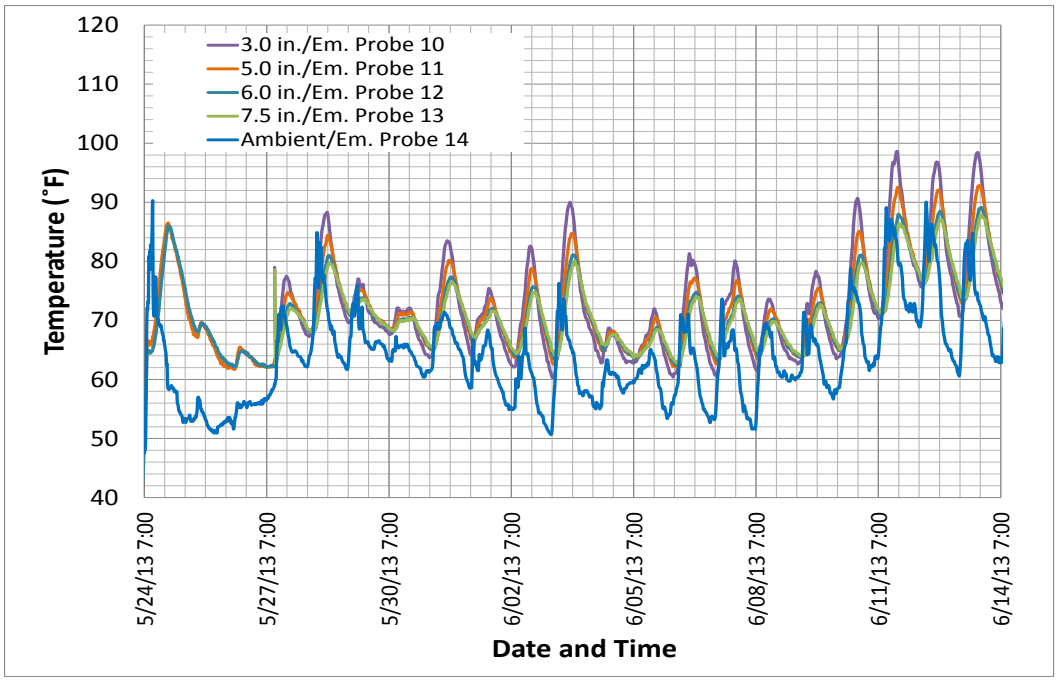

Figure 3-31. Measurement of RFID embedded probes before traffic opening.

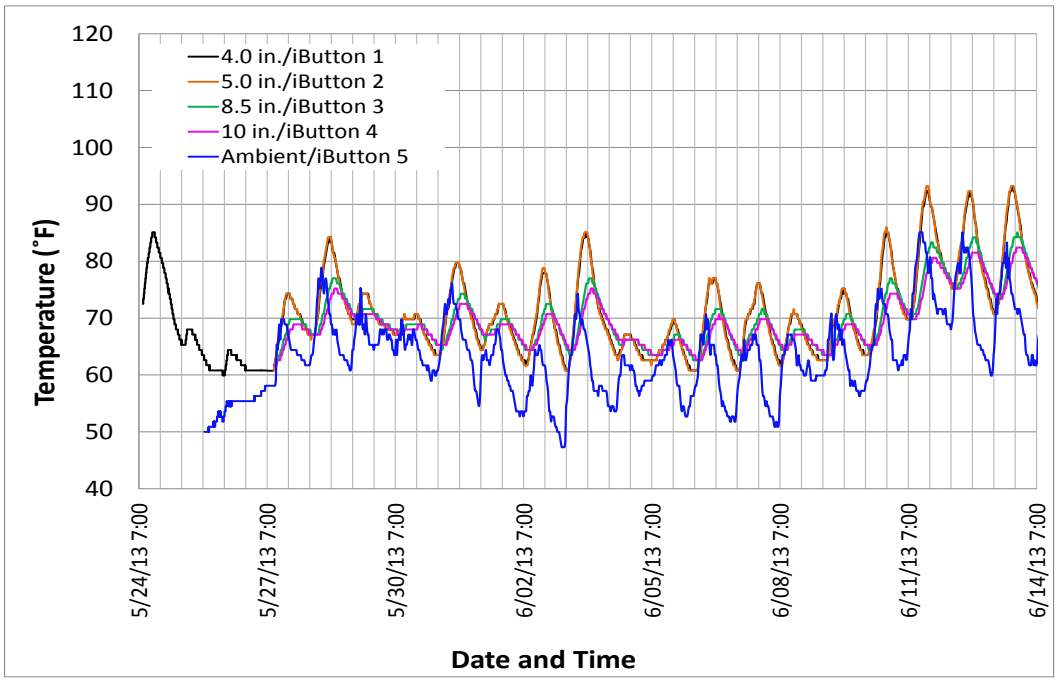

Figure 3-32. Measurement of iButtons before traffic opening.

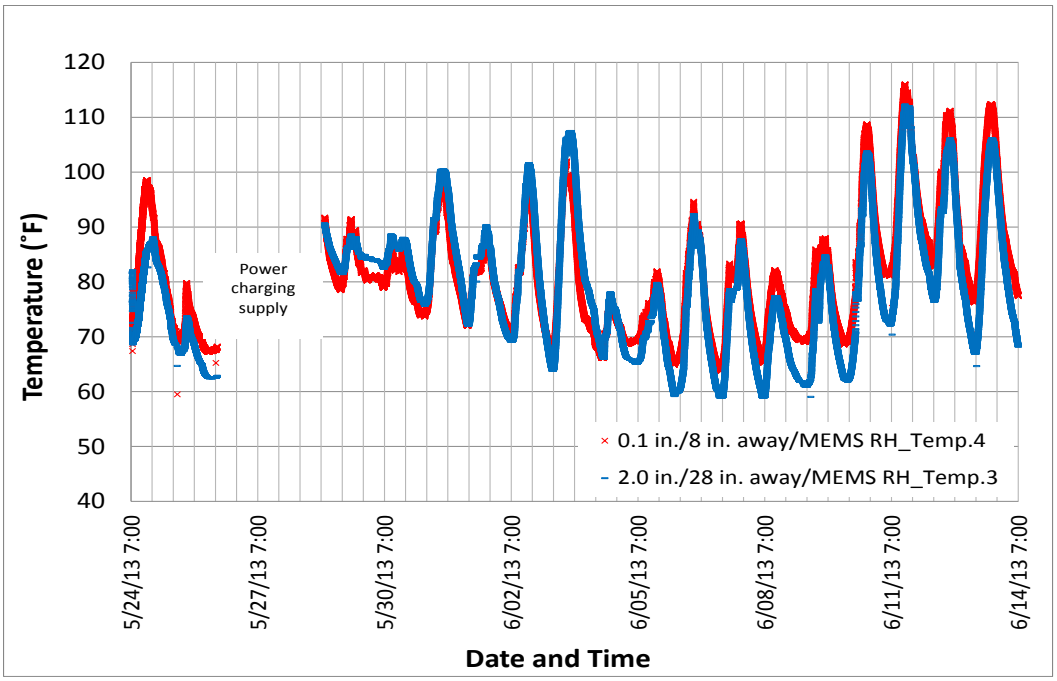

(a)

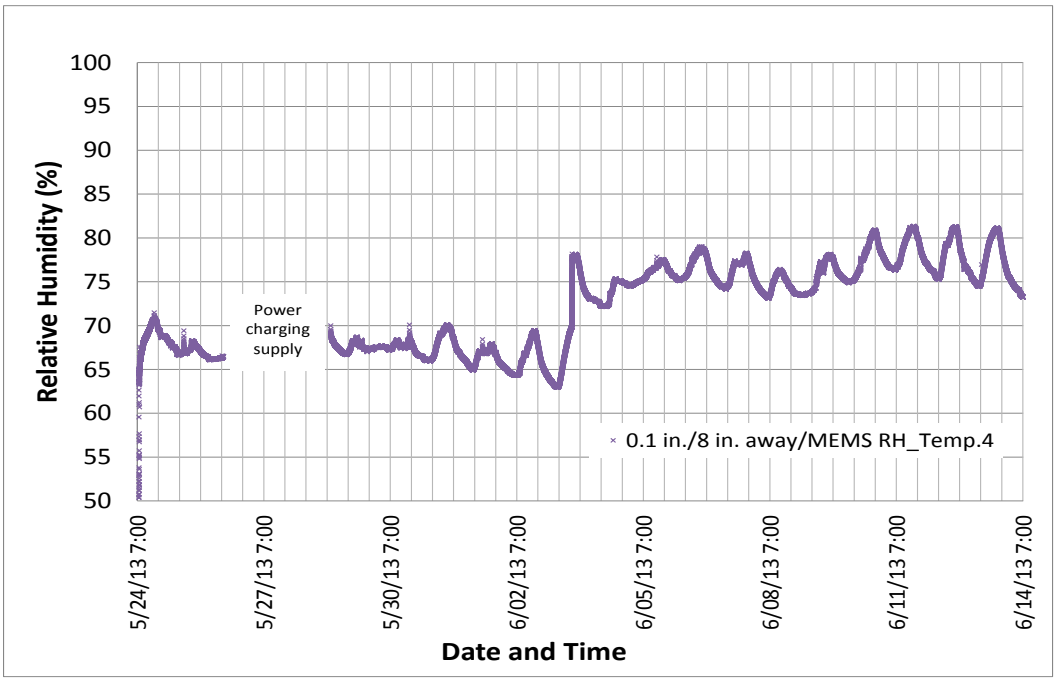

(b)

Figure 3-33. MEMS digital humidity sensor measurement before traffic opening: (a) temperature measurement; (b) RH measurement.

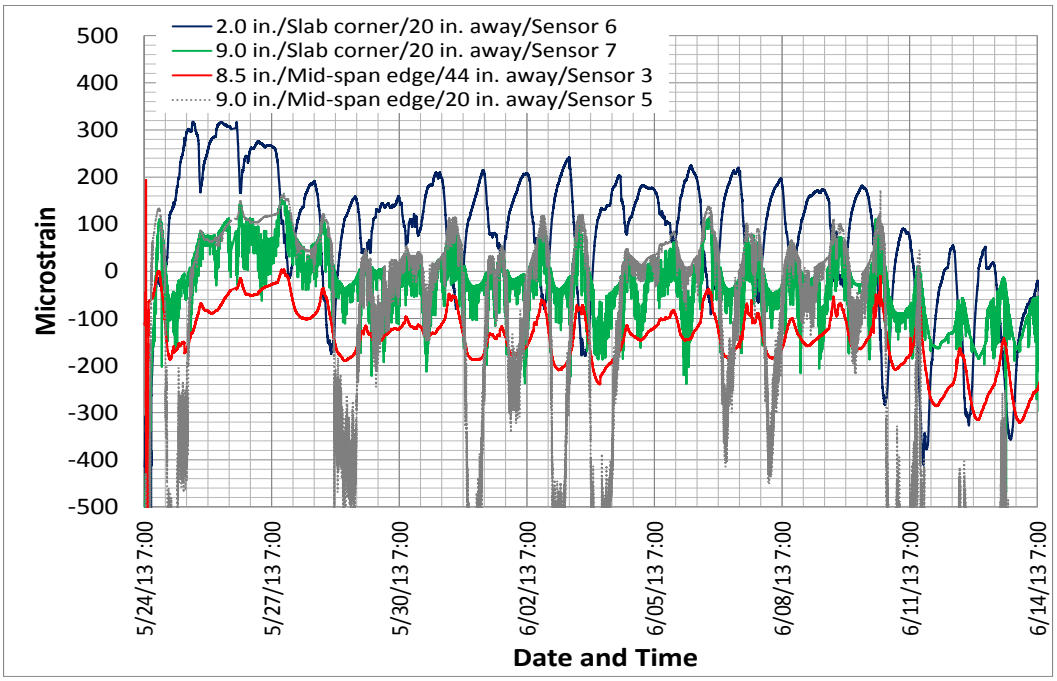

(g)

Figure 3-34. Strain profile before traffic opening.

Figures 3-30 to 3-33 illustrate temperature measurements from RFID tags (extended and embedded probes) and iButtons, as well as MEMS digital humidity sensors, show similar temperature trends. All sensors captured the sharp increase in temperature due to the cement hydration reaction at the beginning of concrete paving. Furthermore, these figures also show that the temperature at the concrete top was usually higher than the temperature at the bottom in daytime but would become lower in night. This was due to the fact that the top PCC pavement was mainly influenced by daily ambient temperature while the bottom part was mainly influenced by seasonal weather (Wells et al., 2006). During daytime, temperature at the pavement top was high because of ambient temperature and solar radiation, and it dropped quickly at night. However, bottom concrete is not as sensitive to ambient temperature, so its change was much smaller than the concrete top throughout the day. It was also observed that that peak temperature occurred later when the concrete was deeper

because it took more time for deeper concrete to reach its peak temperature caused by ambient temperature change.

RH measurement exhibited a trend similar to temperature, i.e., RH went up while temperature increased according to Figures 3-33. At the beginning of concrete paving, RH built up rapidly and then the value was maintained at between 65 to 70% until a thunderstorm on June 3, 2013 caused a sharp increase in RH. After that, RH reached 78% and then fluctuated between 75 and 80%. However, only one moisture sensor remained operational so the RH profile at various depths could not be developed. However, RH generally increased when pavement depth increased (Asbahan, 2009).

Figure 3-34 illustrates strain captured by strain gages before traffic opening. It was found that the strain value was mainly in the range of -200 to +200 microstrain except for strain gage No. 5 that may have suffered from disturbance problems. The value captured was similar to that in the research study by Wells (2005), Asbahan (2009), Qin (2011), and Nassiri (2011) who found typical strain values in response to environmental loads in a range from -150 to +150 microstrain. However, according to Figure 3-34, the curve patterns of strain gages No. 3, 5, and 7 agreed but were totally opposite to those of strain gage No. 8 because the deformation behavior of pavement was different under environmental load between the bottom and the top sections. In the instrumented section, strain gages No. 3, 5, and 7 were at the bottom and strain gage No. 6 was at the top. When tension was induced at the top (strain gage No. 6), compression was induced at the bottom. This phenomenon is referred to as curling and warping behavior of concrete and is explained in the following paragraphs. However, strain gage No. 5 exhibited a noisy signal but could still provide clear curve pattern.

Curling and Warping

Curling and warping are common concrete behaviors that have been extensively investigated. In general, conventional concrete pavement deteriorates under the influence of repeated traffic and environmental load. In terms of environmental load, two well-known factors, temperature and moisture, produce significant effects called curling and warping. Curling and warping stresses are developed as a result of temperature and moisture gradients. When non-uniform temperature or moisture gradient is induced in a PCC slab, the differential strain response throughout the slab depth will lead to curvature. Generally, when the top of the PCC slab has higher temperature or moisture content, a positive gradient will be induced and the top part of the PCC slab will expand more than the bottom, resulting in downward slab curling or warping. Conversely, if the bottom of the PCC slab has higher temperature or moisture content than the top, a negative gradient will occur and the bottom part of the slab will expand more than top, resulting in upward curling or warping of the slab.

The curling and warping behavior of a PCC slab may influence the degree of support offered by the subgrade and the stiffness along the joint. When curling and warping occurs in the PCC slab, the self-weight of the slab tends to exert tensile stresses resisting the deformation caused by the curvature, as shown in Figure 3-35. Additionally, internal tensile stresses in a PCC slab can be developed by restraints to deformation such as dowel bars and friction between the PCC slab and the base course (Wells, 2005). The induced tensile stresses will be further magnified under repetitive vehicle loading and can easily lead to transverse cracking. In addition to temperature and moisture gradients in a PCC slab, curling and warping behavior of early-age concrete is also affected by early-age curing and temperature conditions during pavement construction and by other factors like solar radiation, base-layer

type, slab geometry, degree of built-in slab curvature, concrete mixture, dry shrinkage, and creep (Ceylan, 2013). To minimize effects of slab curling and warping, the concrete placement time should be adjusted to avoid weather conditions that may lead to development of built-in temperature gradients. A good curing method, including covering the entire concrete surface, should also be used. Like curling and warping behavior of a PCC slab, contraction and expansion behavior in response to temperature and moisture is also related to cracks in the slab. However, curling and warping are more complicated phenomena than contraction and expansion because they involve variations and non-uniform volume change at different slab depths and locations. Compared to curling and warping, contraction and expansion behavior of concrete mainly involves horizontal volume change of the PCC slab and this is more related to joint spacing design.

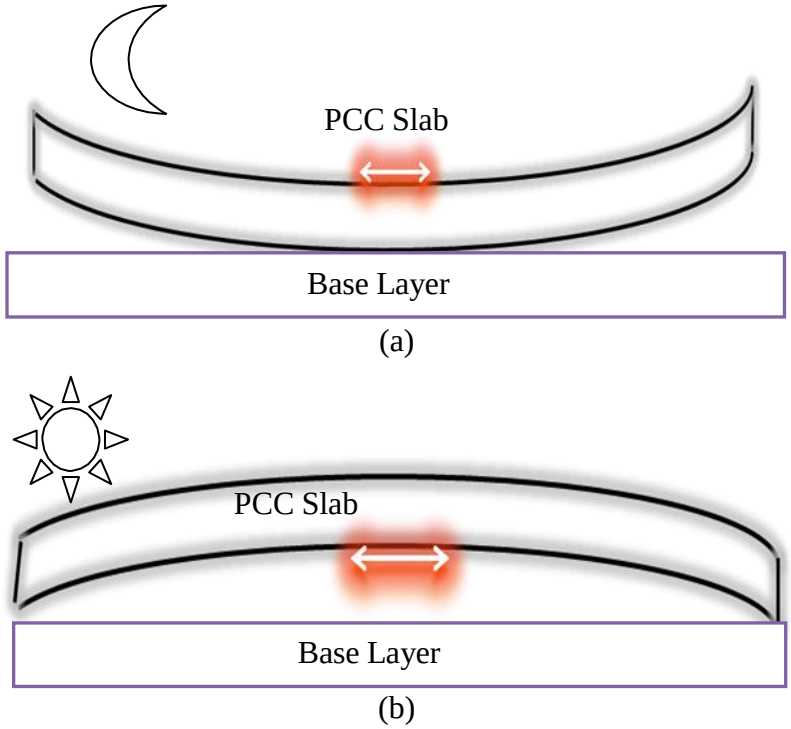

Figure 3-35. Stresses exerted due to curling and warping: (a) tensile stresses exerted at top in PCC slab with upward curvature; (b) tensile stresses exerted at bottom in PCC slab with downward curvature (Nassiri, 2011).

In summary, curling and warping are developed as a result of induced non-uniform temperature or moisture gradients that generate differential strain responses throughout the slab depth, leading to slab curvature. In this study, curling and warping are illustrated in Figure 3-36, shown below. According to Figure 3-36, when concrete curled up, the top concrete (strain gage No. 6) had a maximum of 200 tensile microstrain at 2:00 am on June 8, 2013. Meanwhile, the bottom concrete (strain gage No. 3) had a maximum of 200 compressive microstrain. Comparing with temperature measurements previously shown in Figure 3-30 through 3-33, it can be observed that top concrete had an approximate temperature of 60 ˚F while that of bottom concrete was 65 ˚F. As a result, top concrete was cooler than bottom so that slab curled up, in agreement with the strain readings of Figure 3-36.

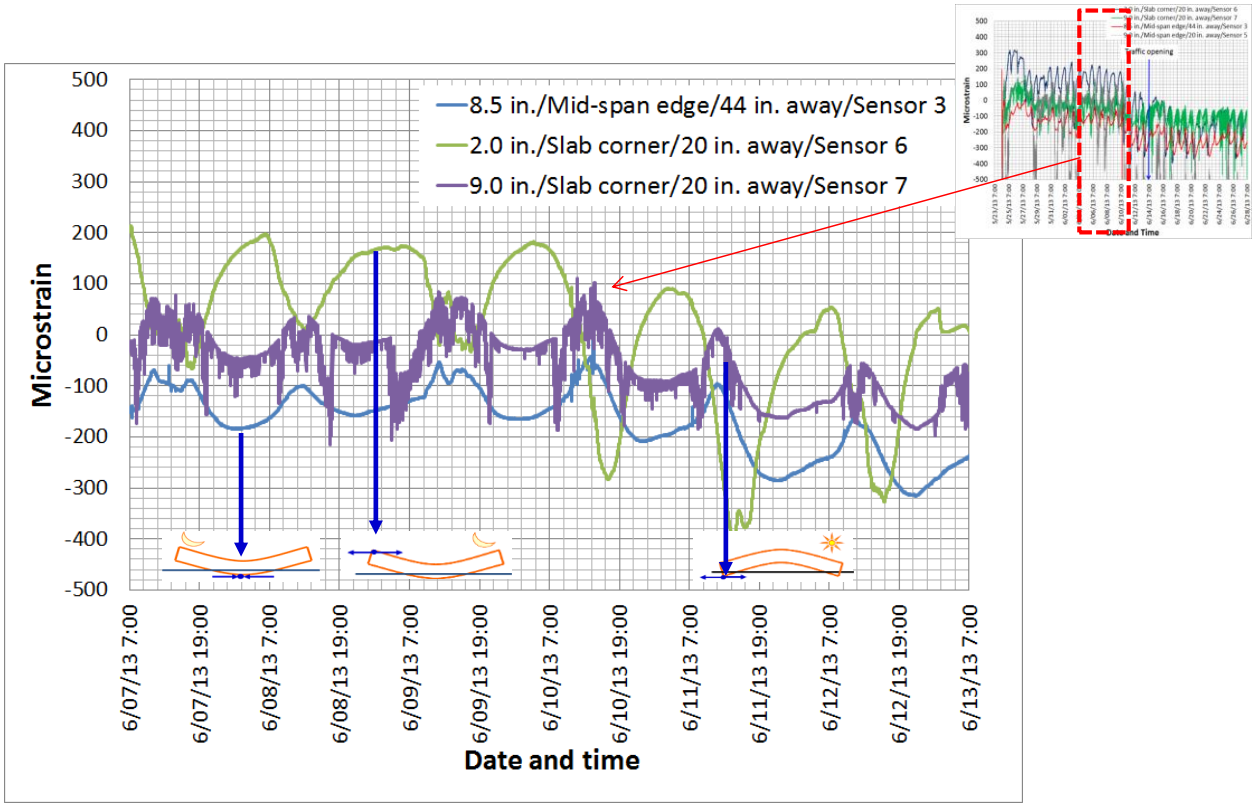

Figure 3-36. Strain measurement: curling and warping.

Two Months after Traffic Opening (June 2013 to July 2013)

Figures 3-37 through 4-42 illustrate the temperature and RH behavior approximately two months after traffic opening, i.e., from July 25 through 27, 2013. According to these figures, it was discovered that an additional 26% of sensors were not functional at the end of July 27, 2013. These sensors were RFID extended probes No. 1, 4, and 6, embedded probes No. 10 and 12, iButton No. 4, MEMS digital humidity sensor No. 3, and strain gage No. 5. Furthermore, these sensors were distributed in everywhere throughout the slab so there was no "concentrated location" where the sensors stopped functioning.

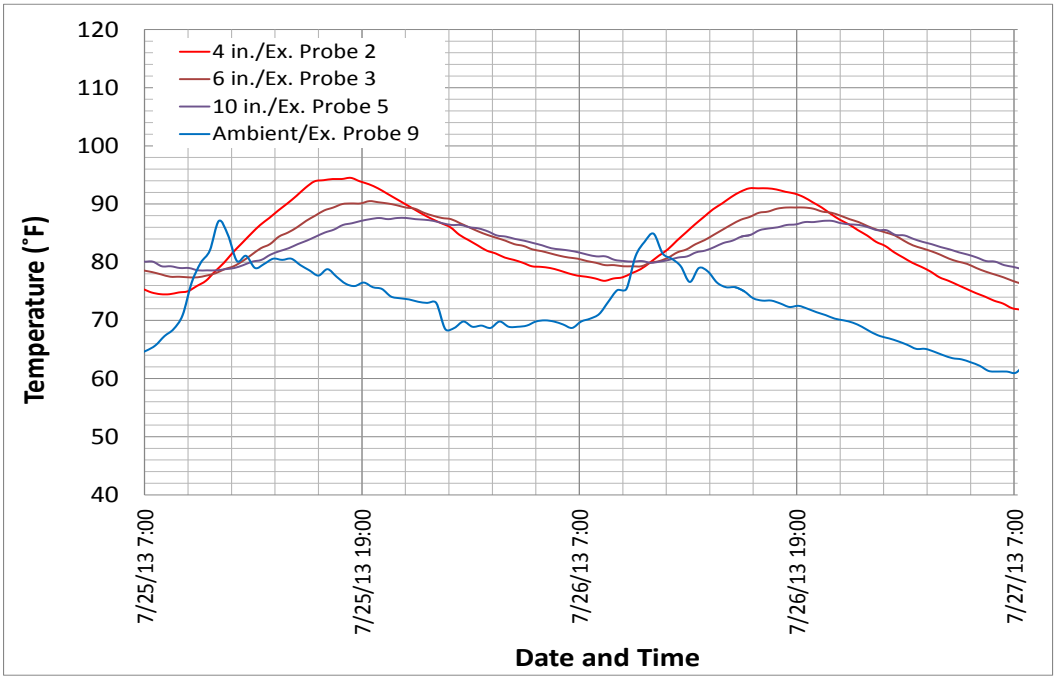

Figure 3-37. Measurement of RFID extended probes in the corner at two months after traffic opening.

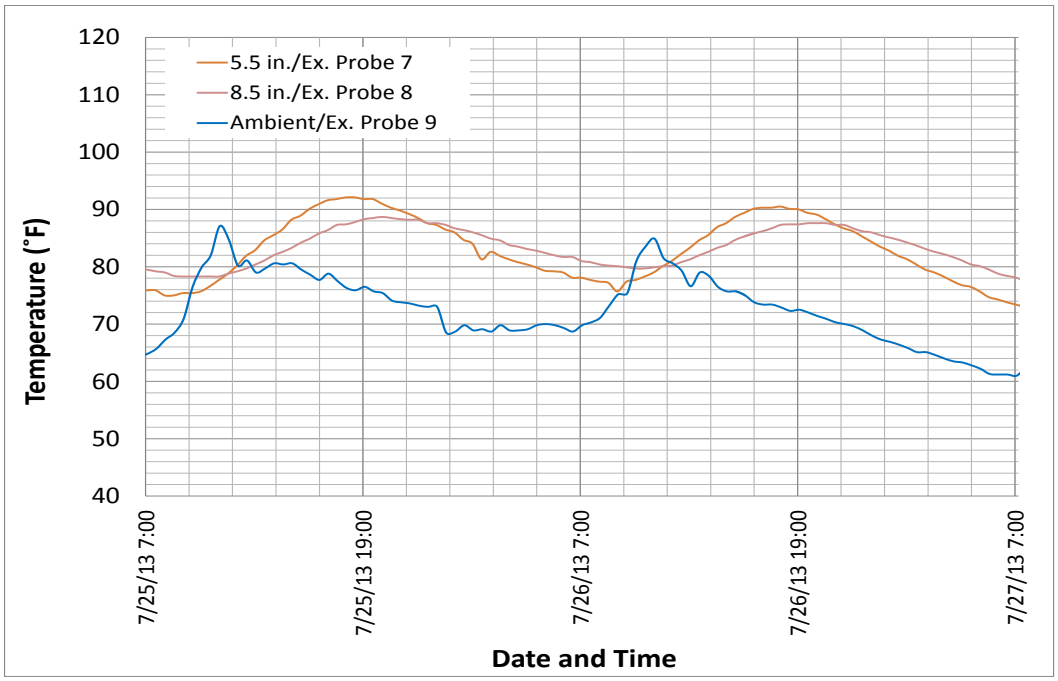

Figure 3-38. Measurement of RFID extended probes in the center at two months after traffic opening.

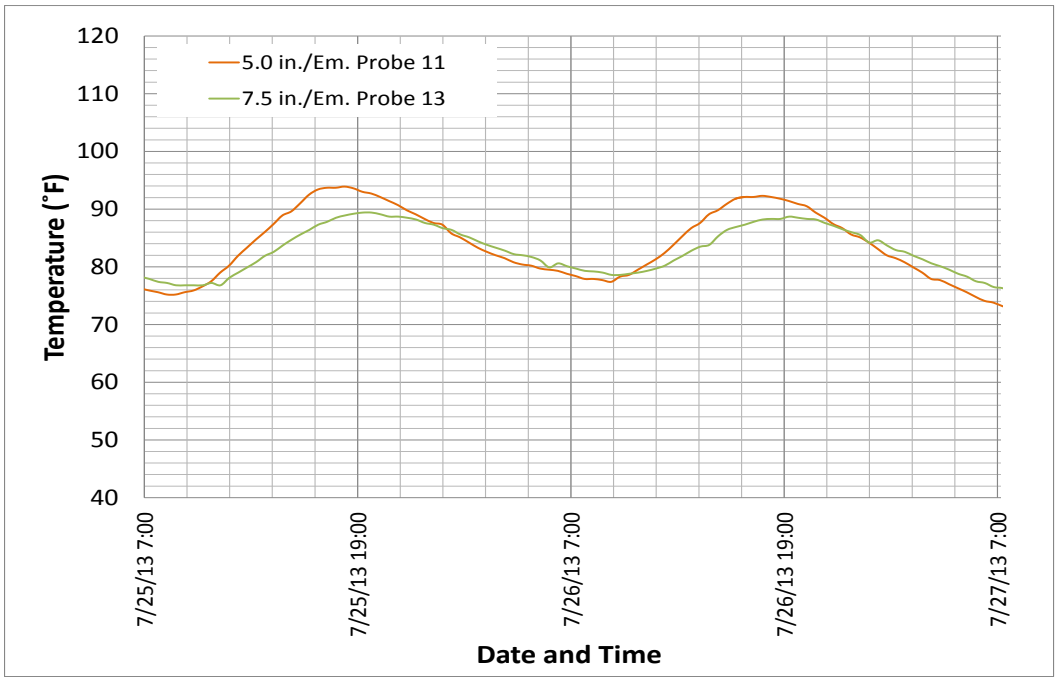

Figure 3-39. Measurement of RFID embedded probes at two months after traffic opening.

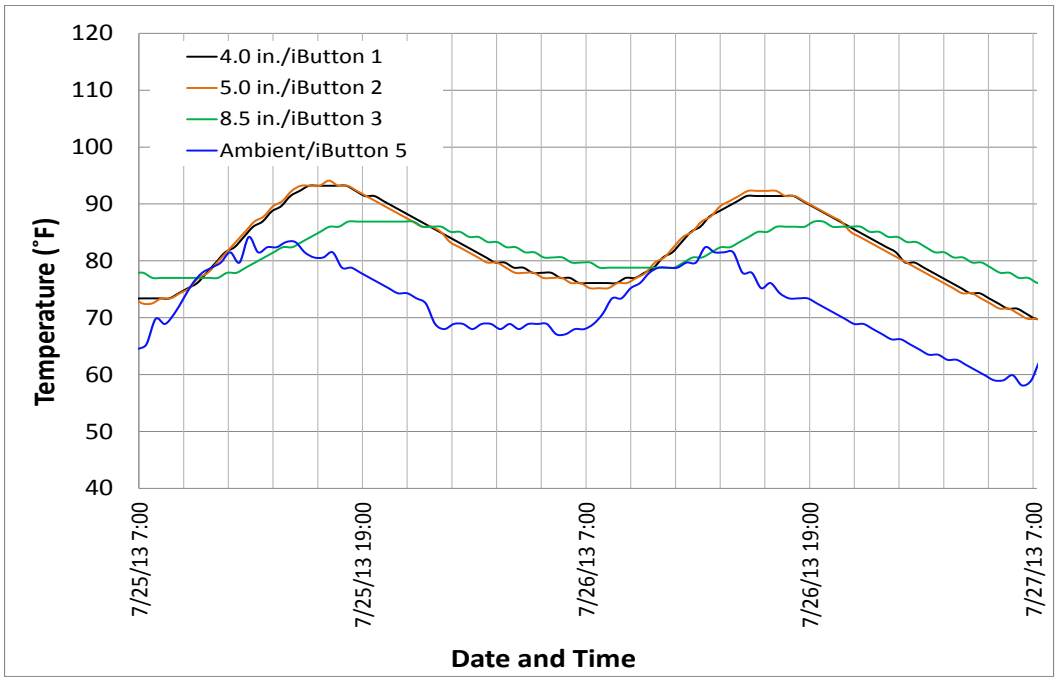

Figure 3-40. Measurement of iButtons at two months after traffic opening.

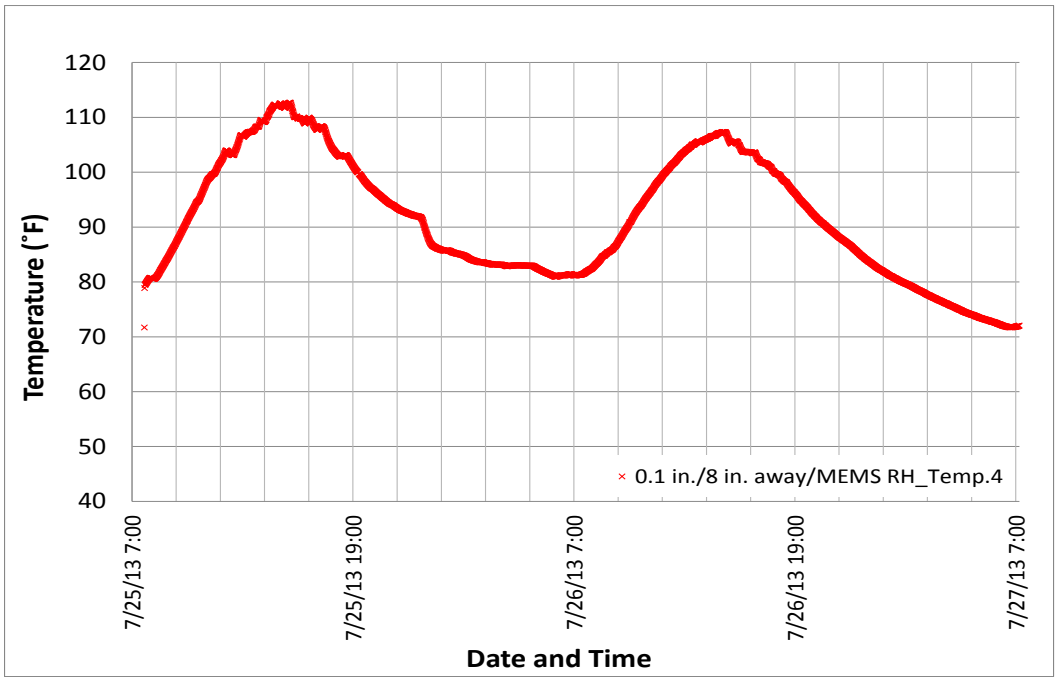

Figure 3-41. Temperature measurement of MEMS digital humidity sensor at two months after traffic opening.

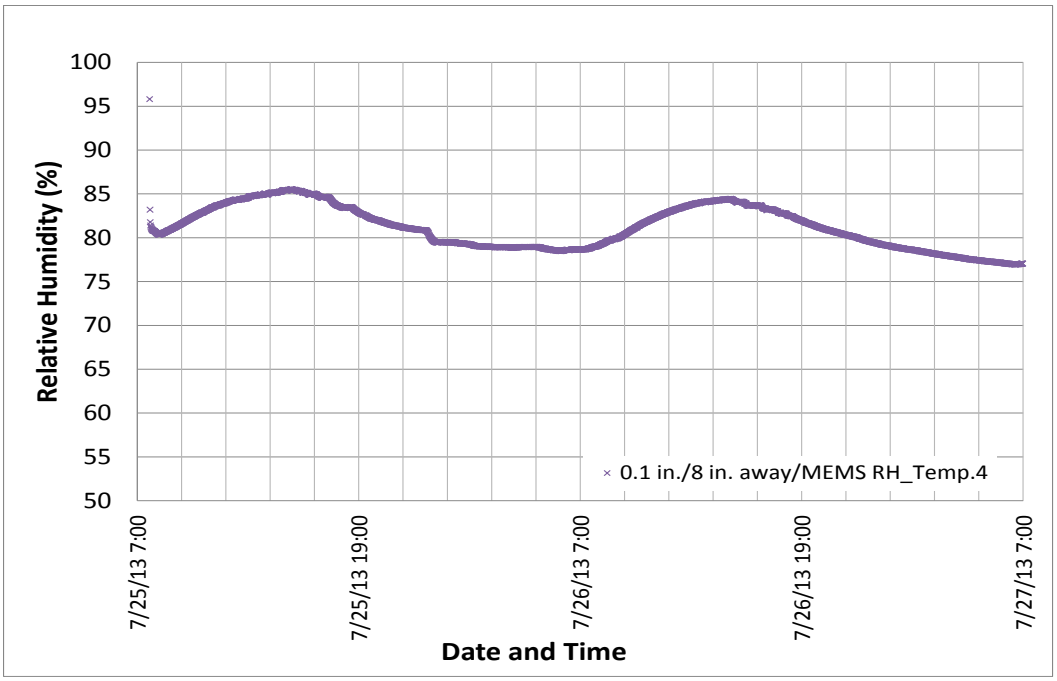

Figure 3-42. RH measurement of MEMS digital humidity sensor at two months after traffic opening.

Figure 3-37 through 3-40 show that the average temperature mainly was in a range from 74 to 94 ˚F. According to Figure 3-41, the MEMS digital humidity sensor exhibited a higher temperature than other sensors, ranging from 80 to 110 ˚F, probably due to strong solar radiation at noon because the MEMS digital humidity sensor was just 0.1 in. below pavement surface. Furthermore, it's obvious that the ambient temperature was lower than that of concrete, and it reached its peak earlier as well, as previously discussed.

Six Months after Traffic Opening (December 2013)

Figures 3-43 through 3-46 illustrate temperature and RH measurements in winter. By the end of December 6, 2013, RFID extended probes No. 5, 7, 8, and 9 and RFID embedded probes No. 13 had stopped functioning. According to these figures, the MEMS digital humidity sensor also reported a temperature more than 50 ˚F higher than the RFID tags and the iButton that reported maximum temperatures of approximately 40 ˚F. The RH value in

winter was maintained between 80 and 90% and that sensor followed a similar temperature pattern.

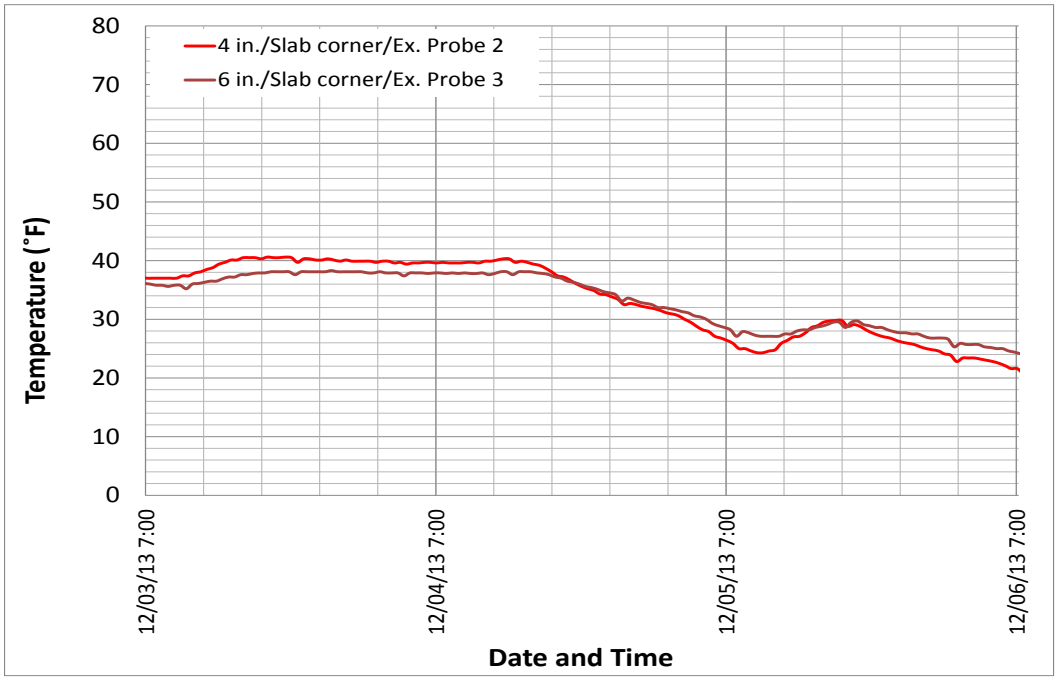

(a)

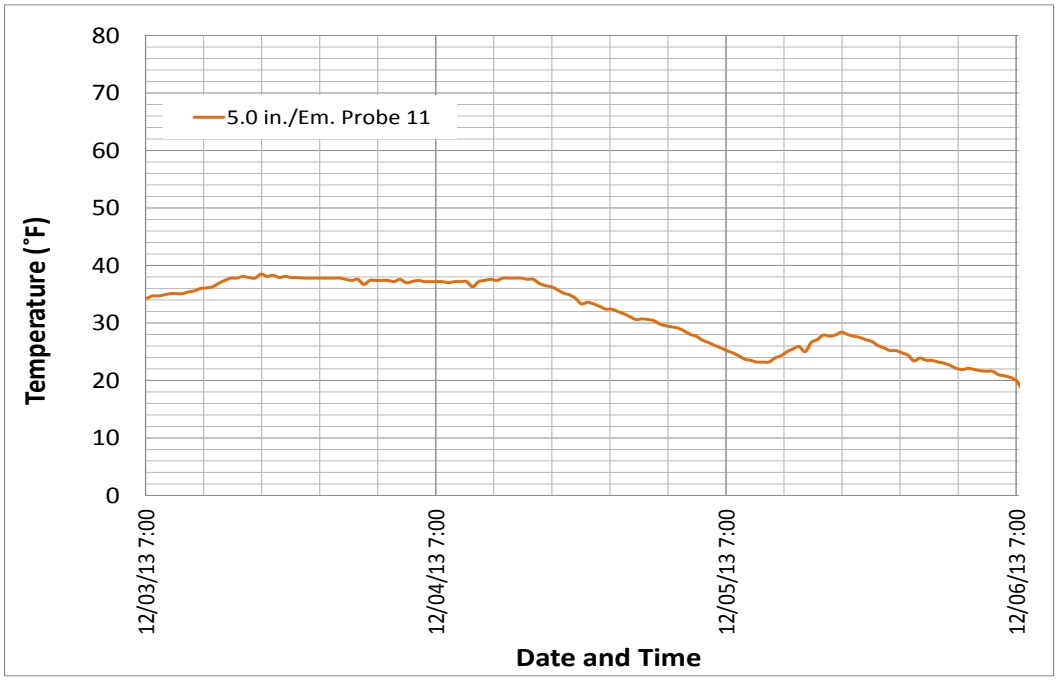

(b)

Figure 3-43. Measurement of RFID extended probes at six months after traffic opening: (a) in the corner; (b) in the center.

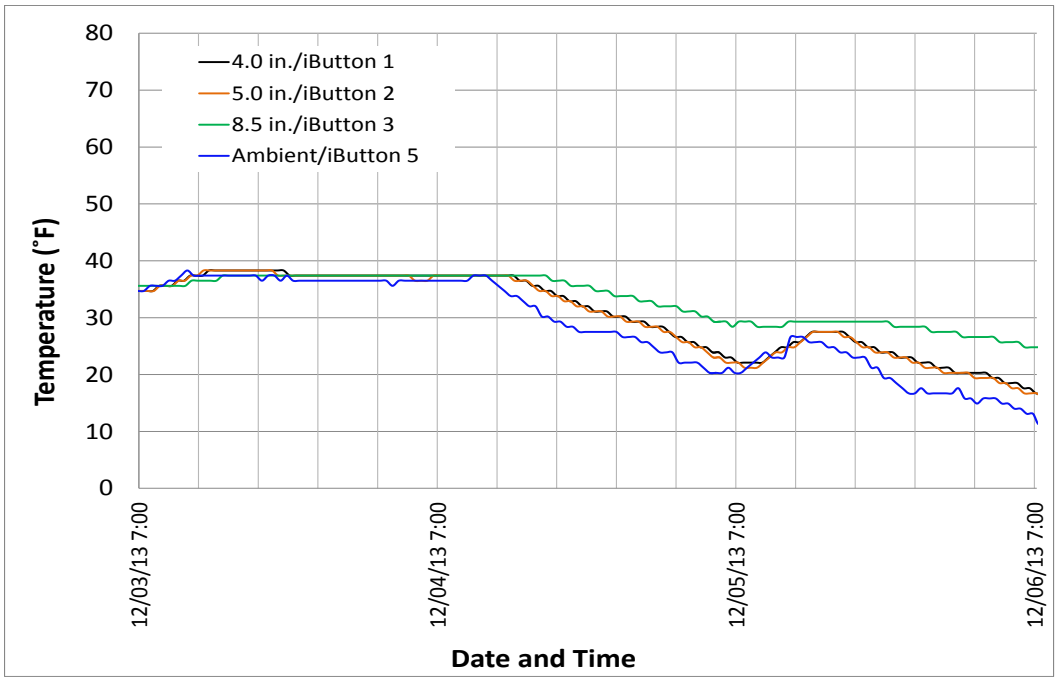

Figure 3-44. Measurement of iButtons at six months after traffic opening.

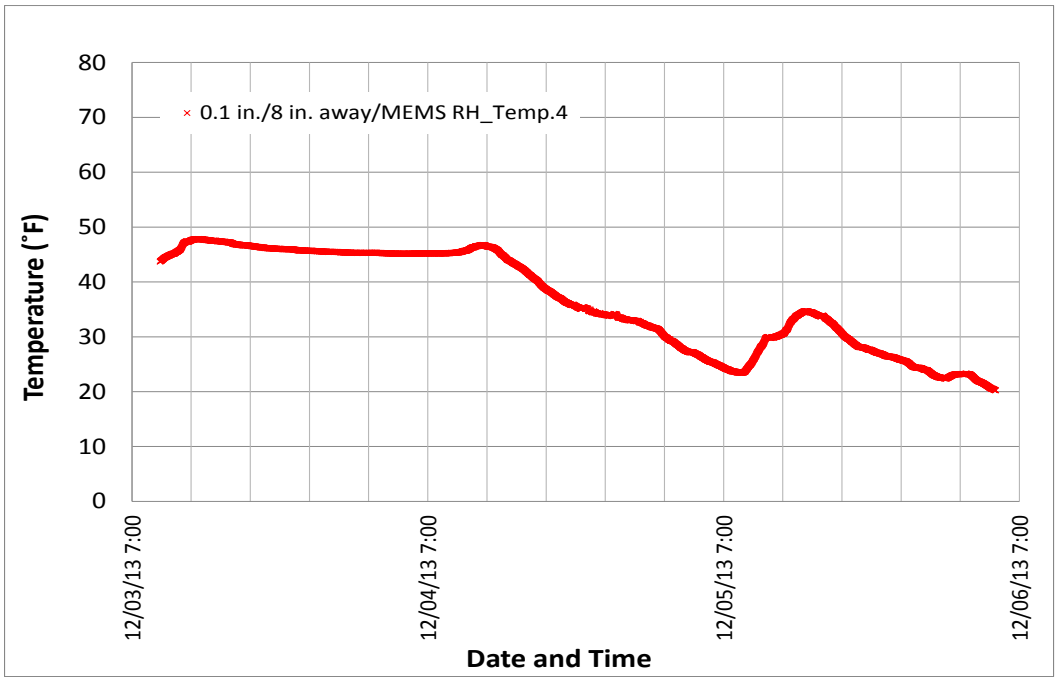

Figure 3-45. Temperature measurement of MEMS digital humidity sensor at six months after traffic opening

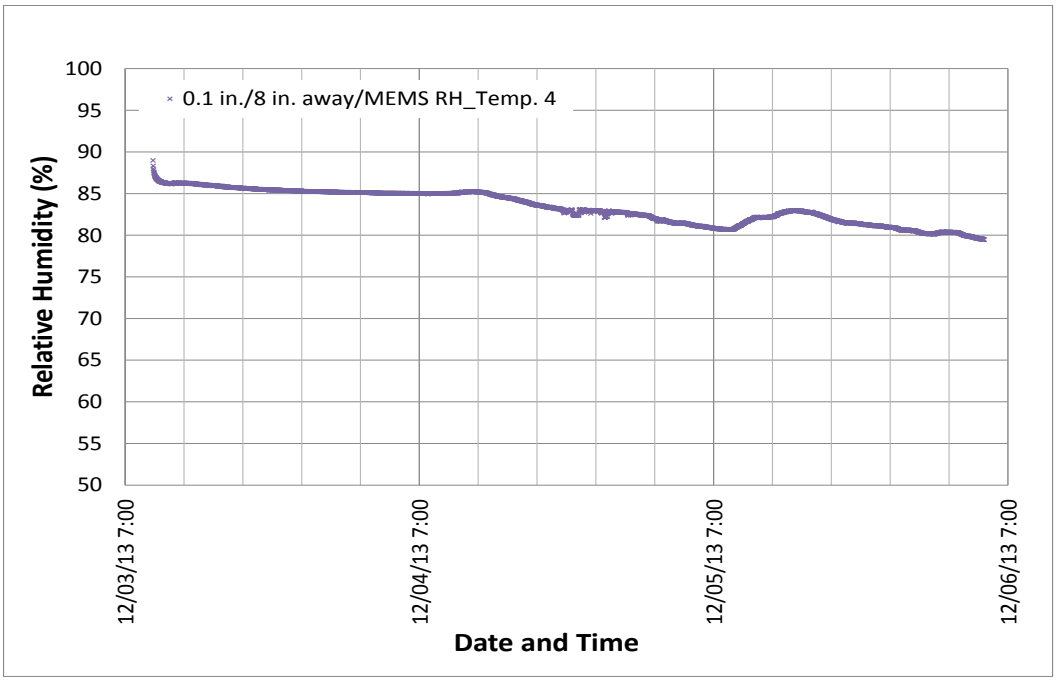

Figure 3-46. RH measurement of MEMS digital humidity sensor at six months after traffic opening.

Concrete Maturity

Laboratory Tests

During concrete construction, a total of 72 cylinders (4 in. ×8 in.) were collected from the project site, and 63 of these were used in laboratory concrete tests, including a compressive strength test, a split tensile strength test, an elastic modulus test, and a coefficient of thermal expansion (CTE) test. Table 3-2 and Figures 3-47 through 3-50, respectively, illustrate the detailed test plan and the test results.

Table 3-2. Concrete testing plan summary.

Type of Test	Age	Repeatability	Standards
Compressive Strength	1, 3, 7, 14, 28, and 90 days	3	ASTM C39
Split Tensile Strength	1, 3, 7, 14,28, and 90 days	3	ASTM C496
Elastic Modulus	1, 3, 7, 14, 28, and 90 days	3	ASTM C469
CTE	7, 28, and 56 days	3	AASHTO T336-11

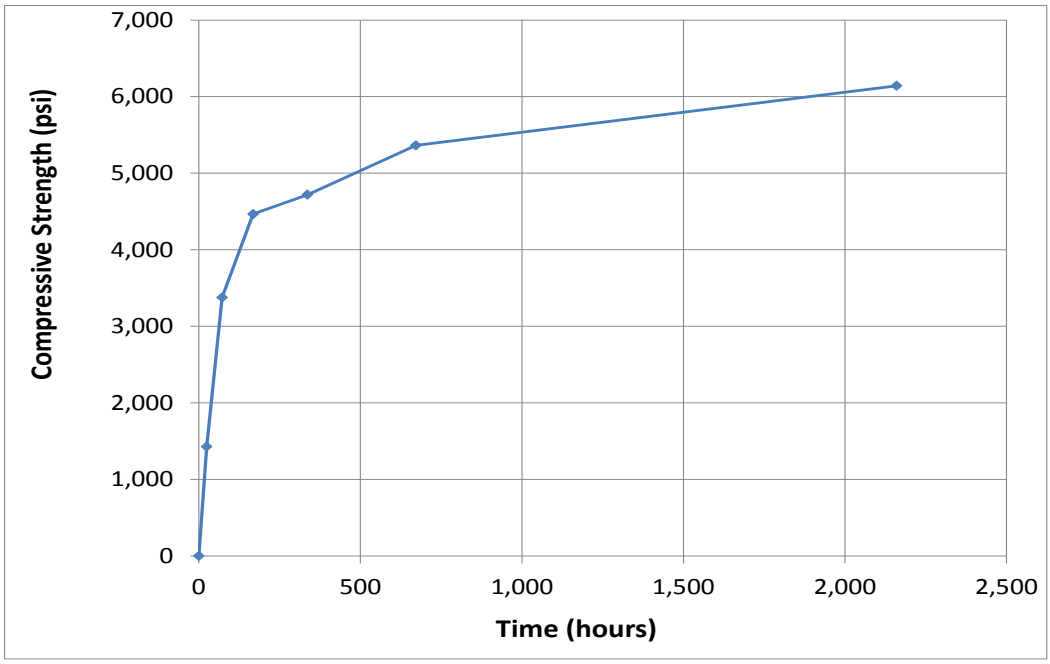

Figure 3-47. Compressive strength test results

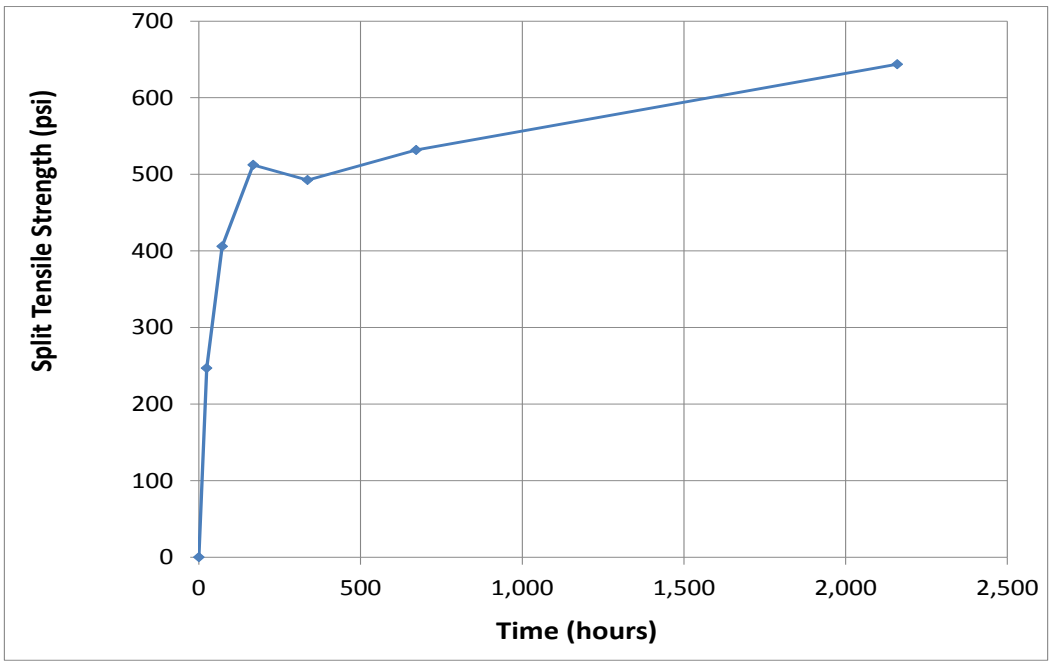

Figure 3-48. Split tensile strength test results.

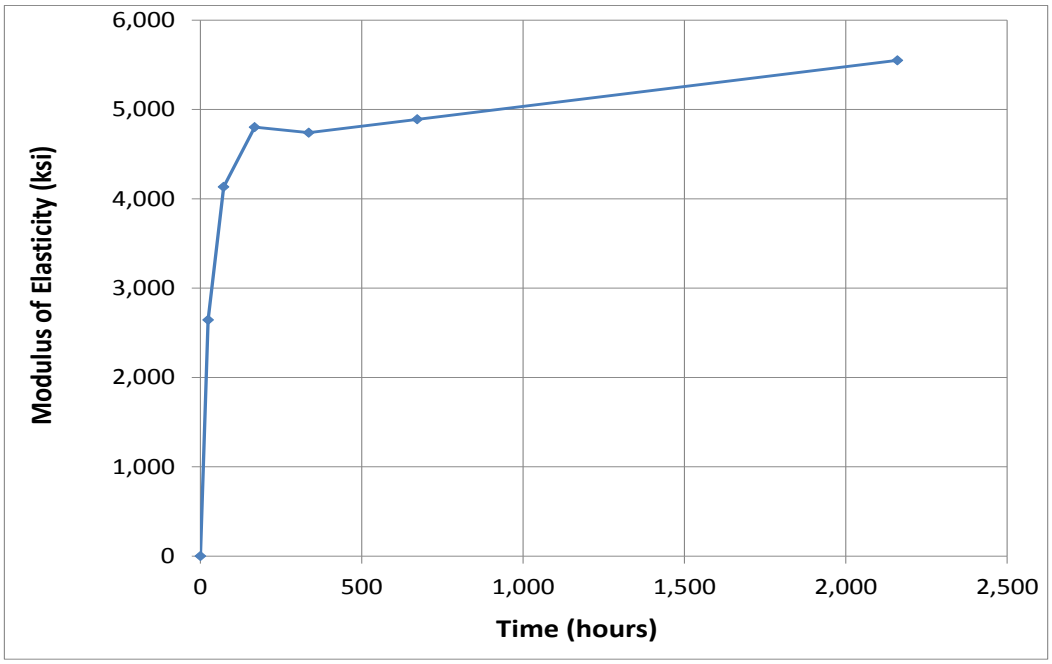

Figure 3-49. Modulus of elasticity test results.

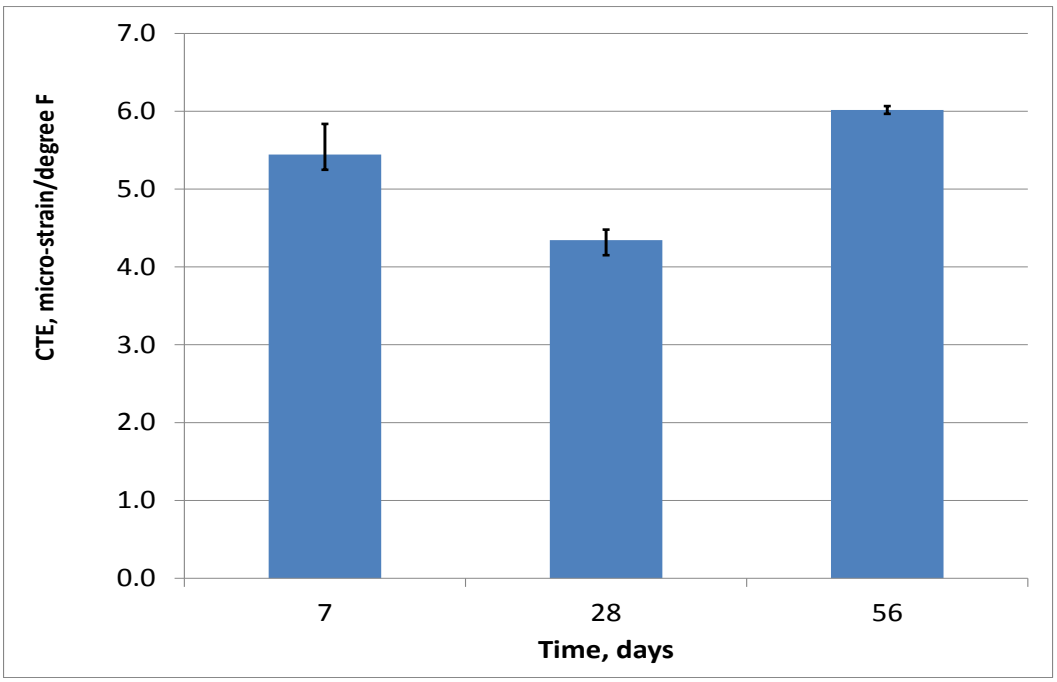

Figure 3-50. Coefficient of thermal expansion test results.

Figure 3-47 through 3-50 illustrate the results of common laboratory concrete tests conducted in accordance with corresponding related standards. It can be seen that the strength increased rapidly during an initial period of 7 days after which the speed of strength increase became slower. However, a slight decrease in split tensile strength and modulus of elasticity were recorded by the 14-day test, and the results of the 28-day coefficient of thermal expansion test exhibited a slight decrease as well. These differences were probably due to variation in different concrete specimens and machine calibration errors. Nevertheless, all the test data were in a reasonable range and met minimum construction requirements. Estimated initial set time and final set time were also obtained in accordance with ASTM C 403. The detailed test results are shown in Appendix C.

Maturity Calculation

The concrete maturity method is a simple and reliable quality control approach for estimating in-place concrete strength. This method accounts for both time and temperature effects on strength development. According to ASTM C1074 (1998), the maturity method is defined as "*a technique for estimating concrete strength that is based on the assumption that samples of a given concrete mixture attain equal strengths if they attain equal values of the maturity index*." The method can help engineers determine appropriate times for form removal, traffic opening, and joint sawing so that the money can be saved through more efficient construction.

ASTM C1074 provides two alternative equations for maturity index calculation: the temperature-time-factor-based Nurse-Saul function and the equivalent age-based Arrhenius function. The Nurse-Saul function assumes a linear relationship between the rate of strength development and temperature, while the Arrhenius function assumes an exponential

relationship between the rate of strength development and temperature. This study adopted the Nurse-Saul function that can be expressed as

$$M = \sum_0^t (T - T_0)\Delta T \qquad (1)$$

where

M = maturity index, ˚C-hours (or ˚C-days),

T = average concrete temperature, ˚F, during the time interval ΔT,

T_0 = datum temperature,

ΔT = time interval (hours or days).

The equation above can be used to calculate the maturity index by utilizing monitored temperature history. The maturity index is an indicator of concrete maturity that can be used to estimate the corresponding in-place strength. The datum temperature is 10 ˚C based on the recommendation given in ASTM C1074. The in-place strength estimation can be calculated from:

$$S = S_u \frac{K(t-t_0)}{1+K(t-t_0)} \qquad (2)$$

where

S = in-place compressive strength at age t,

t = test age,

S_u = limiting strength,

t_0 = age when strength development is assumed to begin,

K = the rate constant.

According to equation (2), in-place strength can be calculated by using the estimated limiting strength, the rate constant, the test age, and the assumed age at which cement hydration began. The limiting strength and the rate constant can be found by developing the

plots described in ASTM C1074. Equation (3) below shows how to calculate the A-value for y-axis in the plot to determine the K-value, and Figures 3-51 and 3-52, respectively, show the concrete maturity curve and the relationship between the estimated in-place strength and the maturity index.

$$A = \frac{s}{(S_u - s)} \qquad (3)$$

where

s = compressive strength from laboratory test.

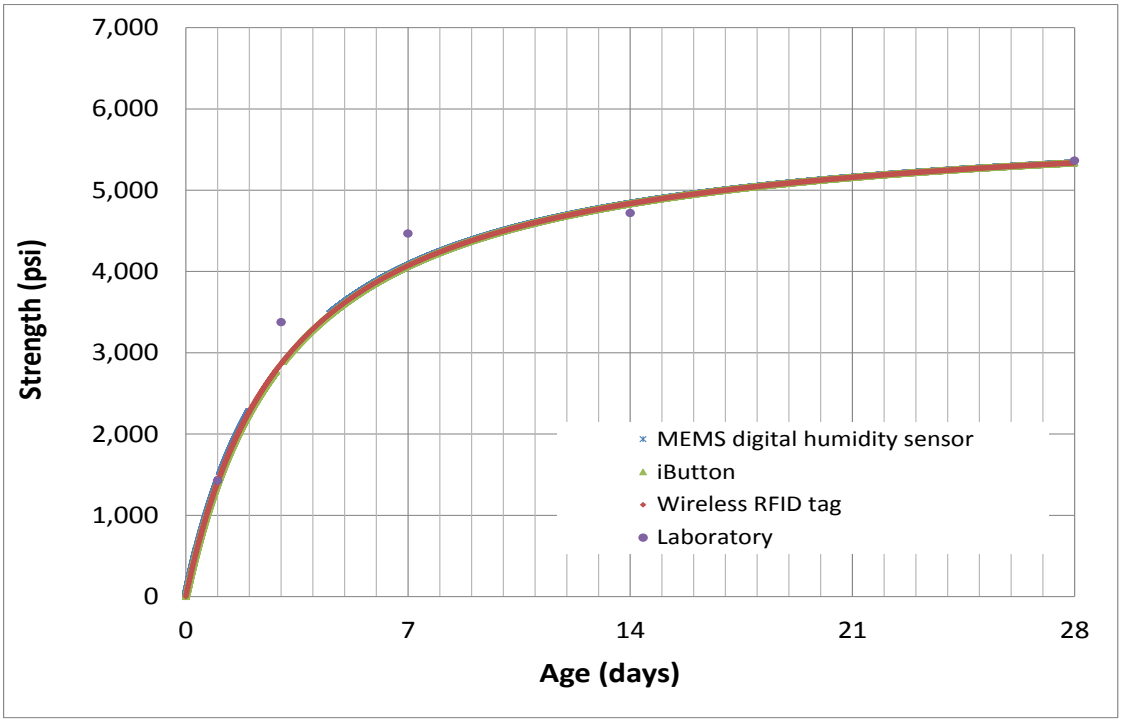

Figure 3-51. Concrete maturity curve.

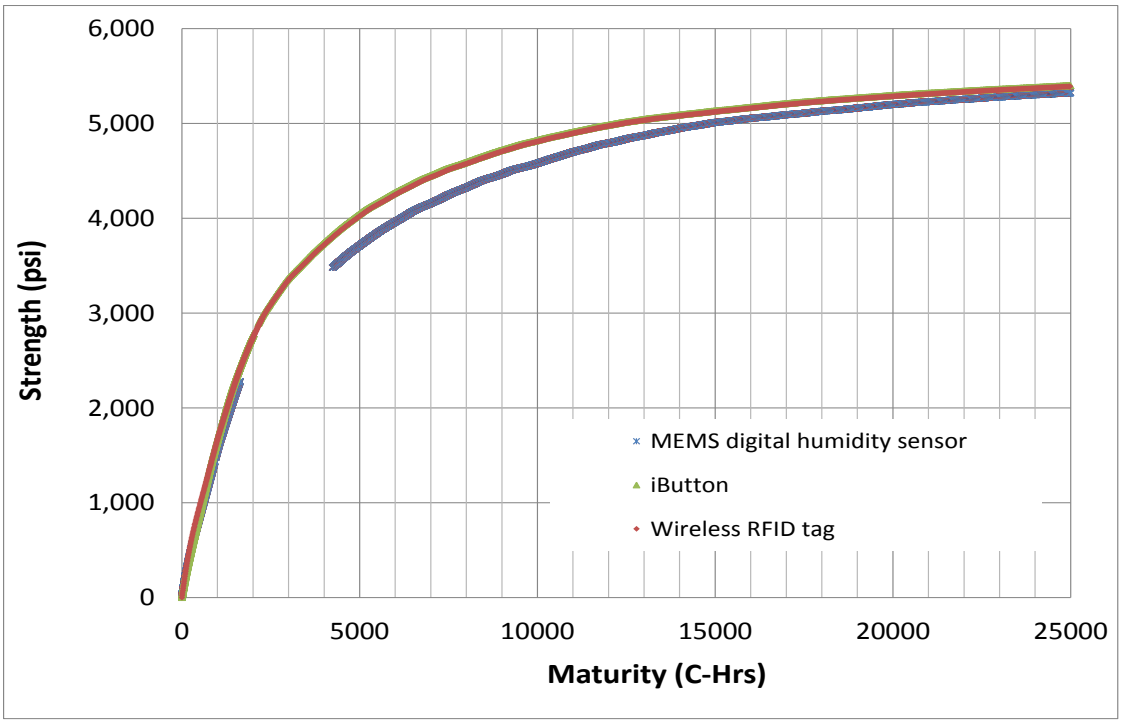

Figure 3-52. Relationship between in-place strength and maturity index.

The concrete maturity curves shown in Figure 3-51 were determined from the sensor data and compressive strength data described earlier. Figure 3-52 shows the relationship between in-place strength and maturity index derived from different sensors. However, the RFID tags and the iButtons had similar average temperature readings, so their curves overlap one another. MEMS digital humidity sensors indicate higher average temperatures due to different sensor position and temperature measurement methods, so they lead to a relatively lower curve. The gap shown in the curve for the MEMS digital humidity sensor is due to power recharging.

Discussion

As stated earlier, this project was conducted to evaluate the performance of MEMS sensors and wireless sensors that had shown promise in helping to achieve Smart Pavement SHM and overcome limitations of traditional wired sensor-based SHM. The MEMS sensors

nicely captured temperature variation for different pavement depth, weather, and seasons, and produced results consistent with early-age curling and warping behaviors of concrete pavement. However, as in earlier projects, some embedded sensors stopped functioning both during road construction and during the pavement-monitoring period. Table 3-3 depicts the number of embedded sensors surviving at various times throughout the entire monitoring period. According to this table, it can be seen that 19% of the sensors had stopped functioning after concrete paving and approximately 63% of the sensors gradually stopped functioning during the 10 months following traffic opening. Possible reasons for these malfunctions can be attributed to

- Damage of sensors due to high alkali environment in concrete
- Damage of sensors and wires incurred by paving and vibration operations of concrete paver
- Corrosion of wires in concrete
- Battery issues
- Harsh climate and slab movement

High temperature, moisture, and adverse pH values all represent challenges to embedded-sensor survivability in plastic concrete. The high alkali environment in concrete is critical to sensors, especially moisture sensors, because their operation requires exposure of their sensing elements to the water vapor in concrete. In US Highway 30 road construction, two out of four MEMS digital humidity sensors directly failed and another MEMS digital humidity sensor could measure temperature only after concrete paving, probably due to alkali environment and extreme moisture content (liquid water) in the concrete. In addition to high alkali environment, other road construction activities can be considered as primary sources of

sensor malfunction as well, as happened in MnROAD construction. The paving and vibration operations of concrete pavers will generate huge lateral forces that can damage a sensor, loosen wire connections, and change the sensor position; the spreading plow or auger at the front of a paver used to spread concrete might also cut the sensor or its wiring, as shown in Figure 3-18. Wire also has potential for corrosion due to the chemical environment inside of concrete. Figure 3-53 shows the winter data acquisition process for RFID tags. During this process, the portable handheld transceiver "Pro" was generally able to identify tags but could not download data from some tags. Even though the distance between the "Pro" and RFID extended probes was only 2 ft., it's still difficult to download data even though a range of 300 ft. was claimed by the manufacturer. This difficulty could be related to battery issues such as reduction of battery capacity and battery life under severe temperature changes and harsh climate conditions such as repeated freezing-thawing cycles that might lead to sensor malfunction or low signal strength. Even the ambient RFID tags stopped functioning during winter time. Slab movement could also be a source of sensor damage.

Table 3-3. Sensor survivability evaluation.

Sensor	Number of Sensor Survived					
	May 23 2013	May 24 2013	Jun. 14 2013	Aug. 22 2013	Dec. 6 2013	Apr. 1 2014
RFID temp (Ex. Probe)	8	8	7	3	2	1
RFID temp (Em. Probe)	4	4	4	2	1	0
EMS RH/Temp.	4	2	2	1	1	1
ibutton (Temp)	4	4	4	3	3	3
Longitudinal strain gage	7	4	4	3	3	0
Total	27	22	21	12	10	5

Figure 3-53. Data acquisition of RFID extended probes in winter.

Although several sensors malfunctioned after road construction, the 81% sensor survival rate at the beginning of opening to traffic could still be regarded as successful instrumentation in comparison to previous pavement instrumentations (Sebaaly et al., 1991). Furthermore, the result of the concrete maturity calculation shows the benefit of using the SHM of pavement. By using MEMS sensors, maturity could be directly calculated on-site and immediately generated as one of the sensor-system outputs. However, the performance of the off-the-shelf MEMS sensors deployed on US Highway 30 illuminated the current limitations, i.e., packaging, wires, signal strength, etc., when using them in pavement health-monitoring systems. A wireless communication system with robust packaging for the MEMS digital humidity sensor was thus implemented to demonstrate a preliminary design for a wireless sensor system.

CHAPTER 4

IMPLEMENTATION OF WIRELESS COMMUNICATION SYSTEM TO MEMS SENSOR

Implemented Wireless System Overview

The wireless system discussed in this study was a preliminary design mainly focusing on the wireless transmission function motivated by field instrumentation in US Highway 30. In this study, an Institute of Electrical and Electronics Engineers (IEEE) standard-based wireless system was utilized because of both its low price and low power consumption. A MEMS digital humidity sensor was used as sensing unit; this pin-based sensor had no packaging for its sensing element so an additional robust packaging was also required.

This wireless system could be subdivided into two parts: wireless transmitter and wireless receiver. The wireless transmitter was interfaced with a MEMS digital humidity sensor to transfer the data captured, while the wireless receiver received transmitted data and downloaded it to a computer through a USB port. Microcontrollers and XBee-PRO modules were used for both the transmitter and the receiver.

Wireless Protocols

As described earlier, wireless network protocols are used to define or standardize the rules and conventions for communication between devices (Lee et al., 2007). The wireless protocol implemented in this design was ZigBee, used to construct a decentralized self-healing wireless mesh network. In this mesh network, nodes can find a new route when an original route fails (Texas Instruments, 2013). ZigBee is the standard IEEE 802.15.4-based protocol; in addition to ZigBee, there are also other possibilities, including Bluetooth, Wi-Fi, cellular, etc. Table 4-1 gives a comparison between different wireless technologies by

evaluating their total scores derived from weighted scores considering various aspects such as data rate, range, energy consumption, etc. In this table, the weighted score of each aspect is calculated by multiplying its weight by the score of each specific wireless technology; a higher total score represents a better wireless technology for this application. Based on this table, it can be seen that ZigBee is more energy-efficient, cost-effective, and easier to work with than the other technologies.

Table 4-1. Comparison of wireless technologies (Al-Khatib et al., 2006).

Aspects		Score (0 to 10)			
Factors	***Weight***	*Bluetooth*	*ZigBee*	*Wifi*	*Cellular*
Multi-node network support	**100**	5	10	10	10
Throughput	**60**	7	6	8	3
Data rate	**60**	7	6	10	10
Range	**50**	6	5	7	10
Ease of implementation	**50**	6	8	6	4
Power consumption	**-80**	6	2	8	6
Cost	**-100**	5	3	7	8
Total Score		460	910	390	200

Microcontrollers

Arduino board is a single-board microcontroller consisting of an Atmel AVR® 8-bit or 32-bit microcontroller which can be wirelessly programmed by a device utilizing the ZigBee protocol (Atmel, 2014). In this study, Arduino Uno and Arduino Mega 2560, respectively, shown in Figure 4-1, were used for the wireless transmitter and receiver.

The Arduino Uno is a microcontroller using an ATmega328 processor with 32 KB of flash memory, 2 KB of static random-access memory (SRAM), and 1 KB of electrically-erasable programmable read-only memory (EEPROM). The board has 14 digital input/output pins, 6 analog inputs, a 5-volt linear regulator, a 16 MHz ceramic resonator, a USB connection, a power jack, an In-Circuit Serial Programming (ICSP) header, and a reset

button. The Arduino Mega 2560 is similar to the Arduino Uno but it has an ATmega2560 processor with 54 digital input/output pins, 16 analog inputs, 4 hardware serial ports (UARTs), and a 16 MHz crystal oscillator. The Arduino Mega 2560 is compatible with most shields designed for the Arduino Duemilanove or Diecimila and it has 256 KB of flash memory, 8 KB of SRAM, and 4 KB of EEPROM for storing code and data. These two microcontrollers were selected because of their high reliability and low cost. Furthermore, Arduino 1.0.4 (open-source software) can be used for program coding such as setting up a time interval, changing the format of exported data, etc., to control both the Arduino Uno and the Arduino Mega 2560.

(a) (b)

Figure 0-1. Microcontrollers: (a) Arduino Uno for wireless transmitter; (b) Arduino Mega 2560 for wireless receiver.

XBee-PRO Modules

XBee-PRO RF module (series 1) as shown in Figure 4-2 is a wireless device, which can offer low cost wireless connectivity in ZigBee mesh networks. It is reliable in point-to-point, multipoint wireless transmission and is designed to conform to the IEEE 802.15.4 standard. Furthermore, the XBee-PRO module has an easy set-up process; its software is called X-CTU, and it can adjust frequency, signal strength, energy consumption, etc. An XBee Explorer Regulated board can also be used to help regulate the voltage input.

(a) (b)

Figure 4-2. XBee device: (a) XBee-PRO modules; (b) XBee Explorer Regulated.

Wireless Transmitter

The wireless transmitter shown in Figure 4-3 consists of a MEMS digital humidity sensor, an XBee-PRO module, an XBee Explorer Regulated, an Arduino Uno microcontroller, and twelve 1.5V AA batteries. Among these devices, the XBee Explorer Regulated is a board that can be pinned onto the XBee-PRO to help it regulate the voltage input. At the wireless transmitter, both a SHT71 sensor and an XBee-PRO with XBee Explorer Regulated were pinned to the digital port and power port on the Arduino Uno board. Meanwhile, twelve 1.5V AA batteries were placed in a plastic holder and connected to the microcontroller to power the entire wireless transmitter through the board's voltage output pin. Furthermore, because the entire wireless transmitter will be buried in concrete, a robust packaging framework is needed, as will be discussed later.

Figure 4-3. Wireless transmitter.

Wireless Receiver

Figure 4-4 is a photograph of the wireless receiver; it consists of an XBee-PRO module, an XBee Explorer Regulated, and an Arduino Mega 2560 microcontroller. The XBee Explorer Regulated used here plays the same role as in wireless transmitter. However, there was no battery used on the Arduino Mega 2560 because it is computer-powered through a USB cable. The XBee-PRO on the Arduino Mega 2560 was paired with the other XBee-PRO on the Arduino Uno in the wireless transmitter to receive the transmitted data. The data was then stored on the Arduino Mega 2560 in a data-storage module with 4096 bytes of non-volatile memory.

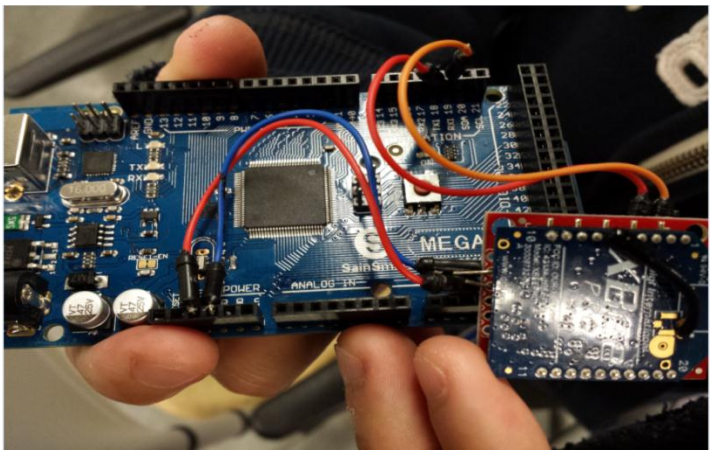

Figure 4-4. Wireless receiver.

Packaging

Robust packaging is required to protect both the sensor and wireless transmission devices like the XBee-PRO module and the microcontroller to ensure that they can work properly inside the concrete. The packaging functions include protecting the wireless transmitter during sensor installation and pavement construction processes, protecting the sensor from alkali-cement hydration reaction, and protecting the wireless transmitter under harsh climate and traffic condition.

Two types of in-house packaging were designed to protect the sensor, the microcontroller, and the XBee-PRO module. For the MEMS sensor, a piece of adhesive tape, a protection filter cap, and steel wool comprised a protective package to prevent direct contact between the raw sensor and fresh concrete, as shown in Figure 4-5. In this packaging, a filter cap was attached to the top of the MEMS sensor using adhesive tape, and steel wool was used to attach the sensor. For the microcontroller and the XBee-PRO module, a small box with an open bottom was prepared; it was comprised of a 0.5 in. thick wooden board and a wooden board nailed to a 7.1 in. long sharp-edged wood stick, A hole was drilled on the board nailed to the stick to permit a sensor cable to pass through and be connected to the Arduino Uno microcontroller. The size of the box was 6.3 in. × 4.1 in. ×3.5 in., sufficient to contain the entire wireless transmission system, as shown in Figure 4-6. Silicon glue and adhesive tape were additionally used to seal the small gap in the box. However, it should be noted that the basic design concept for the packaging for the moisture sensor was to use the material like a filter to allow only water vapor to pass through. Furthermore, an extra eight sensors packaged in the same way were first tested in mortar specimens, and seven out of the eight were able to continuously capture data, indicating that this packaging was successful.

Figure 4-5. MEMS sensor with packaging.

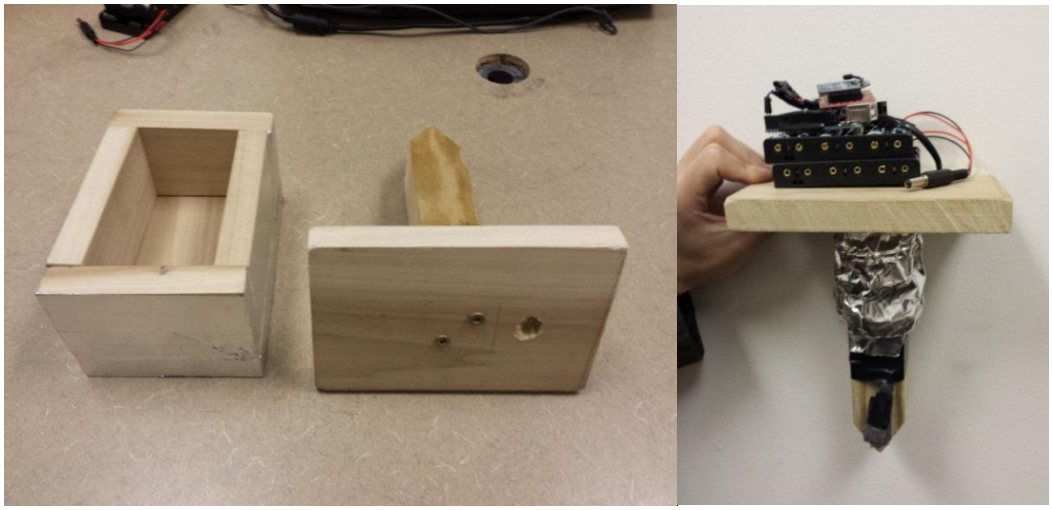

Figure 4-6. Packaging for wireless transmitter.

Evaluation of Implemented Wireless Communication System

Working Principle of Implemented Wireless System

The data-exchange principle of this wireless system is based on the ZigBee protocol. This system requires no external cables. When it is turned on, the MEMS sensor will sense temperature and RH and transfer that data to the XBee-PRO through the Arduino Uno microcontroller. Then the XBee-PRO, at the wireless transmitter, will transmit data to the paired XBee-PRO at the wireless receiver through an antenna; this data will be stored in the Arduino Mega 2560, so the wireless receiver and a computer must be placed nearby because only the Arduino Mega 2560 microcontroller is used to store data in this wireless system. The data can finally be downloaded to the computer through software called "CoolTerm", a simple freeware serial port terminal application without terminal emulation that supports data exchange with hardware connected through serial ports (Sparkfun Electronics, 2014). Temperature, relative humidity, and dew point are the data elements exported from the system.

Comparison between Wired MEMS System and Implemented Wireless MEMS System

Figure 4-7 provides an overall system-level comparison between a wired MEMS system and the wireless MEMS system developed for this study. In the wired MEMS system, the sensor must be connected to the data reader and the computer through cables to continuously monitor concrete properties and the data. As a consequence, both the data reader and the computer require an electrical power supply. However, the implemented wireless system requires no external cables and can thereby save installation time and reduce the risk of sensor malfunction.

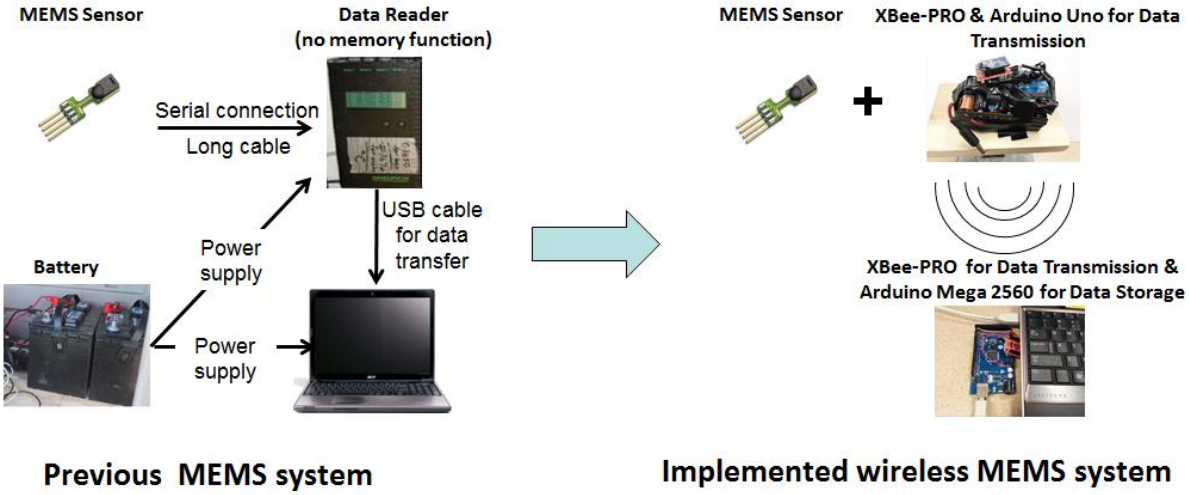

Figure 4-7. Comparison between previous wired MEMS system and implemented wireless system.

Evaluation of Wireless Communication Capability

To test the reliability and survivability of the wireless communication system inside the concrete, both wireless transmitter and receiver were embedded in concrete as shown in Figure 4-8 to conduct a success rate test. Success rate refers to the rate of data transmitted from the transmitter in successfully reaching the receiver. The higher this rate, the more reliable the system will be.

Figure 4-8. Wireless MEMS system inside concrete.

The success rate test was conducted for the wireless MEMS system inside concrete buried underground by gradually increasing horizontal and vertical distances between wireless transmitter and receiver, as shown in Figure 4-9. The test results indicated that the wireless communication system was able to successfully transmit temperature and RH measurements with a nearly 100% success rate when the receiver was horizontally positioned approximately 150 ft. away from transmitter.

(a) (b)

Figure 4-9. Success rate test: (a) wireless MEMS system inside concrete buried underground; (b) vertical distance measurement for data transmission.

Future Improvement

The objective of this study was to investigate the feasibility of implementing wireless based MEMS for concrete pavement structural health monitoring. The system requirements for the wireless MEMS system were derived from field experiences from the wired MEMS system used in US Highway 30. In this design, a wireless communication system was integrated with off-the-shelf MEMS sensors originally designed to be wired. The wireless MEMS system developed was capable of providing reliable temperature and RH measurement data over a distance of more than 150 ft. from the receiver when embedded in concrete. However, the entire system was still energy consuming for the current-limited energy source. It could work for just a few days at a reasonable data-sampling rate using twelve 1.5AA batteries. The lifetime of these batteries could easily be diminished by harsh environmental factors like high temperatures occurring during concrete hydration; extremes of both temperature and humidity can reduce the lifetime and capacity of such batteries. Furthermore, future research should focus on increasing memory capacity and making the whole system smaller. Some recommendations for resolving the aforementioned issues are:

- A power management circuit called Texas Instruments Debuts TPL5000 power timer can be used to control power output of battery; this can possibly extend the current working time to as much as several years under ideal conditions.
- A micro-SD card or QuadRam Shield can be added to the microcontroller to tremendously increase its memory capacity.
- A smaller microcontroller called an Arduino Fio with an XBee plug, shown in Figure 4-10, can be used to replace the original microcontroller to reduce overall system size.

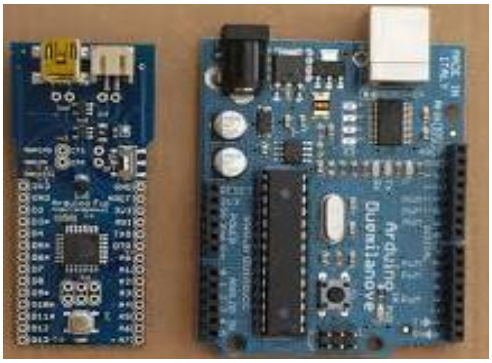

Figure 4-10. Arduino Fio (left) and Arduino Mega 2560 (right).

CHAPTER 5

REQUIREMENTS FOR STRUCTURAL HEALTH MONITORING (SHM) SYSTEM USING SMART SENSING TECHNOLOGIES

This chapter summarizes the issues of using MEMS and wireless sensors in pavement health monitoring system based on previous literature review, field instrumentation, and implementation of a wireless communication system. The requirements of advanced SHM of pavement system are addressed to generate some ideas regarding the strategies that can be effectively used in resolving related issues. A cost evaluation for pavement SHM system and the architecture of advanced pavement SHM system are presented.

Issues on SHM of Pavement System

Over the decades of pavement instrumentation, the general issues related to pavement SHM systems can be mainly divided into four categories: sensor selection, sensor installation, sensor packaging to prevent damage from road construction, and monitoring. These issues exist in the beginning of planning a SHM system for pavement infrastructures until the end of monitoring period. Each of these categories can be crucial to SHM of pavement, so relative strategies must be identified to develop Micro-Electromechanical Systems (MEMS)-based smart wireless sensing technologies for structural health monitoring of concrete pavement. Table 5-1 summarizes the issues related to each category. The corresponding requirements of the advanced SHM of pavement system are discussed in the latter part of this chapter.

Table 5-1. Issues on SHM of pavement system.

Aspect	Issues
Sensor selection	Effect of asphalt/concrete medium, temperature and moisture effects, battery life (measurement frequency), placement, sensor specifications and operating characteristics, cost, hardware architecture, packaging, delivery time
Sensor installation	Optimal number, optimal locations to capture critical responses, orientation/direction, read/write range (placement depth), repeatability and reproducibility, the way of installation (embedded or surface-mounted), training sensor instrumentation personnel off site
Road construction	Design and cost of durable sensor packaging, packaging for moisture sensor
Monitoring	Monitoring period, data measuring interval, frequency of data collection, data signal interference, wireless communications ("hop" network architecture), off-site power, data transfer and storage, protection of equipment, data acquisition systems, embedded software

Cost Evaluation for SHM of Pavement System

The cost to implement SHM systems in similar projects can vary a great deal because it is associated with design, materials, labor and many other factors that depend on the scale and type of structure, number and type of sensors, site location, monitoring period, etc. There is therefore no standard cost for a typical pavement SHM system at this time. However, the typical factors contributing to total SHM cost are:

- Type and number of sensors (traditional sensor /MEMS based, wired/wireless, static/dynamic, active/passive, etc.)
- DAS (automatic or manual)
- Sensor and DAS installation cost
- Travel cost (site investigation, sensor installation, data collection, etc.)
- Software
- Protective equipment (cabinet for DAS, safety vests, helmets, etc.)

Table 5-2 gives a unit sensor cost comparison between traditional sensors and MEMS sensors. In general, unit sensor cost depends on the number of sensors procured; a larger number of sensors typically will be associated with lower per-unit cost. According to Table 5-2, MEMS sensors generally have a lower unit cost, varying perhaps from $3 to a few tens of dollars per sensor. Traditional sensor prices are usually range from $50 to $500. However, the cost of a DAS is much higher than that of a sensor. Table 5-3 illustrates the cost of DAS (The PC is not included) for some of the sensors from Table 5-2. It can be seen that the DAS is much more expensive and may cost $500 to $3,000 per unit. Furthermore, DAS using wired sensors usually have a limited number of connection ports so that a more comprehensive DAS must be purchased if large number of sensors are needed. When using MEMS sensors the cost of a DAS would be relatively lower because many MEMS sensors can use an evaluation kit/board equipped with a USB cable to read and transmit data to a PC, usually resulting in a relatively lower cost compared to a traditional data-logger. However, sensors can be interfaced with different data acquisition devices and their prices vary quite a lot over different models and accessories, so there is not a well-defined standard value for DAS cost.

In addition to sensor and DAS cost, SHM expense also includes labor cost. According to a report from Titi et al. (2012), the typical labor cost of an instrumentation plan/design with construction drawings ranges from $5,000 to $10,000. Furthermore, the maintenance cost per trip due to electrical storms or vandalism could be as much as $2,500 to $5,000, and the data processing cost depends on frequency.

Table 5-2. Sensor unit cost comparison as of 2014.

Categories	Traditional Sensors		MEMS Sensors	
	Manufacture (Model)	Price ($)	Manufacture (Model)	Price ($)
Strain or Soil Pressure	Geokon (4000 series)	120~600	Melexis (90809)	7~8
	Geokon (3900 series)	605		
	Vishay (EGP)	44		
	Tokyo Sokki (PML)	143		
	Encardio Rite (EDS)	65~90		
	Endevco Corp.	5~10		
	Marton Geotechnical Services	150~500		
	Micron Optic (os3600)	649		
	RST Instruments	70~90		
	Smartec	65~90		
	Omega (KFH)	110~290		
	LTD	150~500		
	Applied Geomechanics	150~500		
	CTL (ASG)	500		
Temperature	Omega (Thermocouple)	65~260	Analog Device (ADT7320)	3
	Geokon (Vibrating Wire Temperature Sensor)	200	iButton (DS1921)	15~23
	Applied Geomechanics	200	MEMS VISION (MVH3000D)	N/A
	Slope Indicator	200	RFID tag Q350 series*	30~50
	Omega (RTD)	50~110	Sensirion (SHT71)	25
	Omega (Infrared temperature sensors)	65~260	STMicroelectronics (HTS221)	4~3
	Omega (TT-K-24-100)	78	MEMS VISION (MVH3000D)	N/A
Moisture	Vaisala Inc. (SHM40)	635	Hygrochron iButton	4~3
	Decagon Devices (GS3)	260	Sensirion (SHT71)	25
	Irrometer Watermark (200SS)	90	STMicroelectronics (HTS221)	4~3
	Campbell Scientific (CS616-L25)	140		
	Stevens (Hydraprobe II)	360	MEMS VISION (MVH3000D)	N/A
	Hydronix (Hydro-Probe II)	5,000		
	Innovative Sensor Technology (MK33)	32~50		

Note: * means wireless sensors, and the other sensors shown in the table are wired sensors.

Table 5-3. DAS cost comparison as of 2014.

	Traditional Sensors		MEMS Sensors	
	Sensor Type	DAS Cost ($)	Sensor Type	DAS Cost ($)
Strain or Soil Pressure	Geokon strain gage	1,760	Melexis (90809)	N/A
	Micron Optic (os3600)	24,000		
	Tokyo Sokki (PML)	3,000		
	Vishay (EGP)	708		
Temperature	Omega (Thermocouple)	549	Analog Device (ADT7320)	45~60
			iButton	40
			MEMS VISION (MVH3000D)	N/A
	Omega (TT-K-24-100)	450	RFID tag Q350 series	2,000
			Sensirion (SHT 71)	640
			STMicroelectronics (HTS221)	31.5
Moisture	Campbell Scientific (CS616-L25)	1,465	Hygrochron	40
			MEMS VISION (MVH3000D)	N/A
	Stevens (Hydra probe II)	3,270	Sensirion (SHT 71)	640
			STMicroelectronics (HTS221)	31.5

Requirements for Smart Pavement SHM

Sensor Selection

Selection of sensors can be crucial for pavement health monitoring. When assessing potential sensors, the following factors must be considered:

- Capability of measuring pavement response
- Reliability (i.e., accuracy, life time, survivability in pavement)
- Availability (i.e., shipping time)
- Cost
- Practicality for field instrumentation

Previous pavement instrumentation projects have disclosed the limitations of traditional wired sensors, including high cost, low reliability, complexity of field instrumentation, etc. Furthermore, traditional sensors usually have relatively large size and many external wires, so locating large numbers of sensors of different types to obtain continuous data may very likely cause logistical problems and potential damage to the structure. In addition, data acquisition systems must be placed in close proximity to the pavement, causing more problems in such elements as power supply and data storage and transmission. However, an on-site data acquisition system for a test track may not have such problems because on-site office structures are usually built alongside the test track in projects like MnROAD and Virginia Smart Road; this is not realistic for an actual highway. All these drawbacks combine to limit the use of SHM for pavement systems. Therefore, it is important that sensors used in pavement health monitoring should have small size, be wireless, have low cost, and include an on-board CPU. However, it should be noted that a sufficiently long strain gage length is required to precisely capture the strain values in a concrete matrix. Based on Copley (1994), a gage length three to five times the maximum aggregate size should be sufficient.

It's already universally accepted that MEMS-sensor technology can provide improved system performance, reliability, longevity, and safety compared to existing traditional wired-sensor systems. Their on-board CPUs support a more efficient type of data interrogation. Compared to a traditional sensor, a MEMS sensor has a lower unit cost and smaller size, making it possible to increase in-pavement array density to obtain more data. Furthermore, through the micro-fabrication of MEMS technologies, a highly-integrated multifunction sensor capable of simultaneously measuring several parameters such as

temperature, RH, and strain can be developed. This multifunctional MEMS sensor can also reduce the number of sensors needed, further reducing installation cost.

A wireless sensor system has many benefits such as low installation cost and time, elimination of wire damage, good flexibility, etc. The common wireless technologies used in civil infrastructure include the earlier-described RFID and ZigBee. However, the main challenge for a wireless sensor system is related to the battery issue. In general, pavement has a designed life from 20 to 50 years and maintenance and rehabilitation can be scheduled every 5 to 15 years (Luhr et al., 2010). Therefore, the monitoring period should extend over decades ideally. However, current commercial battery life can only be extended as much as about 10 years under ideal conditions and common sensors equipped with internal batteries have only a 2 to 6 year continuous working time (Roberts, 2006). For example, the iButton and the active RFID tag used in the US-30 Highway project have maximum battery lifetimes of 2 and 6 years, respectively. The harsh climate in a real highway can greatly reduce battery life, and there is no feasible way to replace embedded-sensor batteries in concrete. Accordingly, a passive wireless system should be more suitable for long-term pavement health monitoring.

The aforementioned passive RFID tag usually uses an antenna to convert the wireless signal from the RFID reader into operating power; the idea is to convert electromagnetic wave or RF radiation into DC electrical power. Other potential energy scavenging sources that might be used by self-energy-harvesting systems include wind, solar, thermoelectricity, and physical vibration (Yildiz, 2009). Among these options, physical vibration could be an ideal energy source for pavement health monitoring because it uses strain changes caused by passing vehicles. Therefore, piezoelectric material can be used to make the accelerometer or

transducer for harvesting energy from the physic vibration. In addition to using passive systems, the computational capabilities provided by logical blocks on a board-mounted CPU can be incorporated into the sensor by MEMS technologies to manage power. In this situation, energy might be conserved by putting the device into a sleep mode, as described earlier.

To summarize, the Smart Pavement SHM needs to have MEMS-based sensors, wireless capability, multifunctionality, and be self-powered. Therefore, a wireless MEMS multifunctional sensor containing a self-energy harvesting system represents a promising solution for a Smart Pavement SHM. Durable packaging is also required in this system to protect the sensor from concrete. This kind of wireless multifunctional MEMS sensor is, however, not yet commercially available, because fully integrating all the sensing elements may result in relatively excessive device dimensions and high unit cost due to complex fabrication, assembly and implementation. More importantly, energy consumption may be large because of the need to simultaneously measure a number of parameters.

Sensor Installation

In planning a SHM system, questions always emerge like how many sensors are needed and where the sensors should be installed. Installing sensors throughout the entire structure can produce a superior database but may not be realistic because of cost, logistics, and potential cracking issues. For that reason the number and locations of sensors should be optimized at the planning stage.

Temperature, moisture, and strain sensors are the most common types installed in pavement infrastructure. Vertical displacement gauges such as linear variable differential transformers (LVDTs) placed at the pavement bottom are often used to measure vertical

movement of a concrete slab. Pavement sensors can be grouped into pavement response sensors such as strain gages and LVDTs and pavement environmental-condition-monitoring sensors such as temperature and moisture sensors. In optimizing the number of sensors and their locations, critical locations within the pavement should be determined.

A rigid pavement consists of a series of concrete slabs. The critical locations at which to monitor concrete slab response under load are at the middle of longitudinal joint, the middle of transverse joint, and slab corner, where suffer more from load than other positions (Darestani, 2007). The PCC pavement response sensors should be installed at these locations. Strain gages are usually installed at top and bottom positions location while LVDTs are usually installed at the bottom, as shown in Figure 5-1. As for flexible pavement, critical locations are pavement surface and bottom layer, top of intermediate layer, and top of subgrade (Timm et al., 2004). PCC Pavement environmental-condition-monitoring sensors should be installed at center, but also at various depths to record temperature and moisture variation with depth, as shown in Figure 5-2.

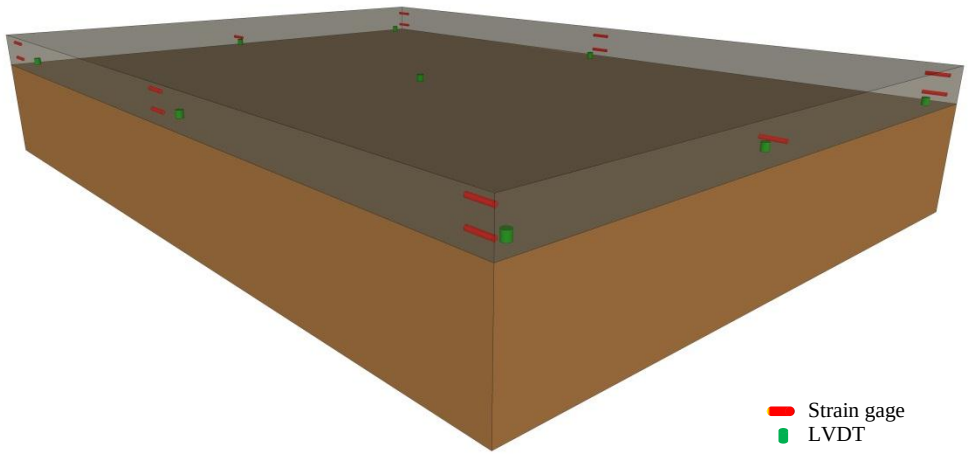

Figure 5-1. Typical PCC pavement response sensors installation layout.

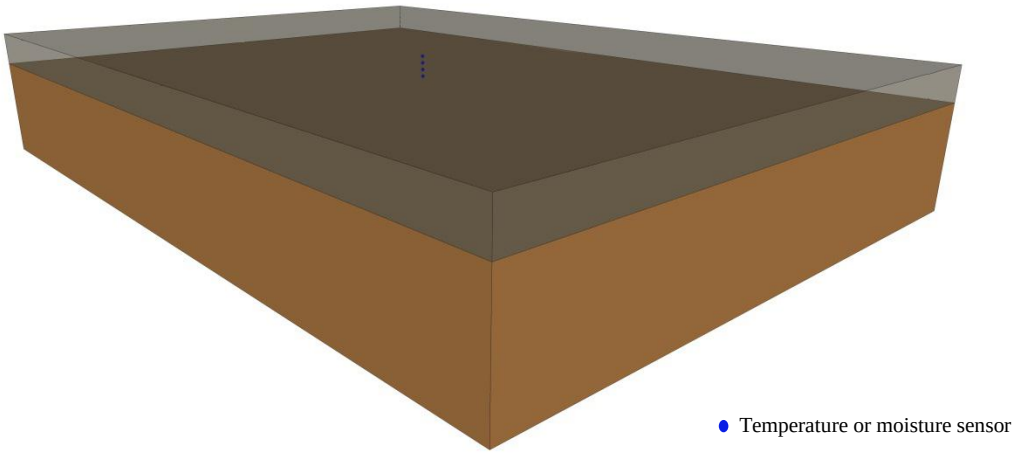

Figure 5-2. Typical PCC pavement environmental-condition-monitoring sensors installation layout.

It should be noted that the installation plan may require modification based on specific conditions such as project purpose, sensor types, sensor size, budget, etc. However, it is recommended that temperature and moisture sensors always be installed every 2 in. along the depth from top to bottom. The highest sensor embedded in the concrete pavement should be only 1 to 2 in. away from the surface. If a sensor needs to be installed at lesser depths, it is probably better to install it after concrete paving.

Pavement sensors are delicate so they must be very well-protected to increase their survivability. Previous projects using sensors anchored on wooden bars did not work well and led to a time-consuming process. Instead, a pre-manufactured cage may be useful in making the installation process both easier and faster. The sensor packaging and the wooden bar used to fix the location of sensors can be equipped with multiple screw holes to permit flexible mounting and increased reliability. An oblong rather than a cylindrical bar shape might be more stable during concrete spreading. A sensor might be installed in an instrumented core or even inside a hollow wooden bar so that the core or wooden bar could

act as a shell and protect the sensor. A sensor might also be installed in a specially-designed gyroscopic frame so that its angle of orientation resulting from concrete paving could be measured. It is notable that the sheet metal boxes (See Figure 5-3) used in the pavement instrumentation conducted by the Ohio University had a 90% strain gage survival rate, so that approach might also be useful (Sargand and Khoury, 1999).

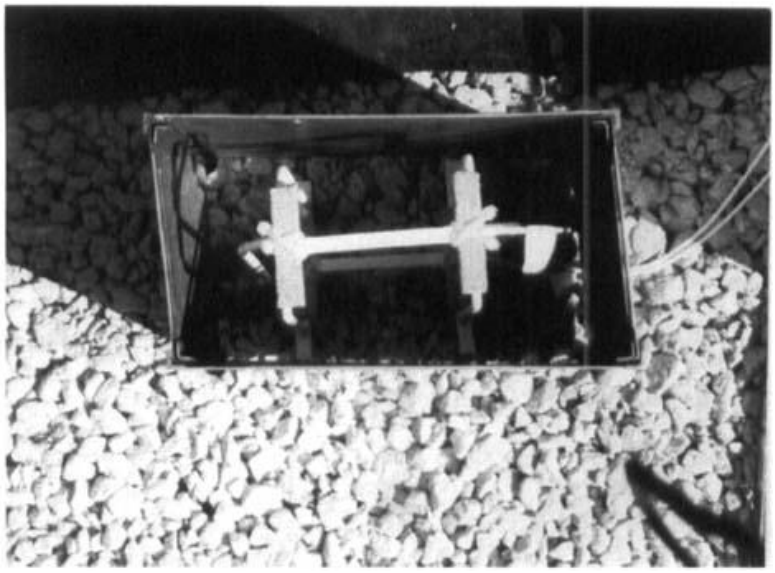

Figure 5-3. Sheet metal boxes (Sargand and Khoury, 1999).

The quality of sensor installation directly affects sensor survivability in pavement, so training installers in advance will increase the survivability rate and save time. Furthermore, maintaining the vertical distance from the top sensor to the paver and vibrator to be greater than at least 1 in. will reduce vibration effects due to the construction equipment; pouring some fresh concrete on the top of sensor prior to paver operation can also mitigate the force from concrete spreading. The instrumented location should be remote from power lines to avoid electro-magnetic noise, and protection of the sensors and wires from shoulder paving and drainage system layout operation should also be considered. It is essential to communicate with the construction crew in developing an optimal installation plan.

Sensor Packaging to Prevent Damage from Road Construction

As previously mentioned, packaging is crucial in establishing a reliable sensor system, particularly one with moisture sensors, to be used in pavement health monitoring. The cost of packaging can represent 75% to 95% of the overall product cost (Attoh-Okine, 2003). Sensor packaging involves more than just choosing standard chip packages; it includes packaging for the whole sensor system. One therefore must take into account different system and assembly requirements, especially when using multifunctional sensors (Wang, 2010; Frank, 2013).

In general, packaging a system of MEMS sensors can be divided into three levels: die packaging, device packaging, and system packaging. The sensor die refers to the actual silicon chip containing the integrated circuit (IC) whose packaging system includes wafer packaging, sometimes considered to be another level of packaging (SILICON LABS, 2014b). Device packaging provides protection for micromechanical components immediately after their manufacture, and the system package protects the entire system, including battery, antenna, etc. (Chiao and Lin, 2006).

In the packaging process, the structure of a MEMS sensor is first encapsulated by bonding the device wafer to a second wafer to protect it from moisture contamination and particle impingement before assembling it into a standard packaging module. During assembly of die packaging, to reduce potential packaging-material-induced stress on the sensor die, cavity packaging, specially-designed die coating, and transfer-molding processes are used to minimize such effects. Then die bonding and wire bonding complete device-level packaging, and insertion into a metal or plastic case accomplishes system-level packaging.

Figure 5-4 and Table 5-4 provide detailed descriptions for each level of packaging (IMEGO, 2014, Amkor, 2014).

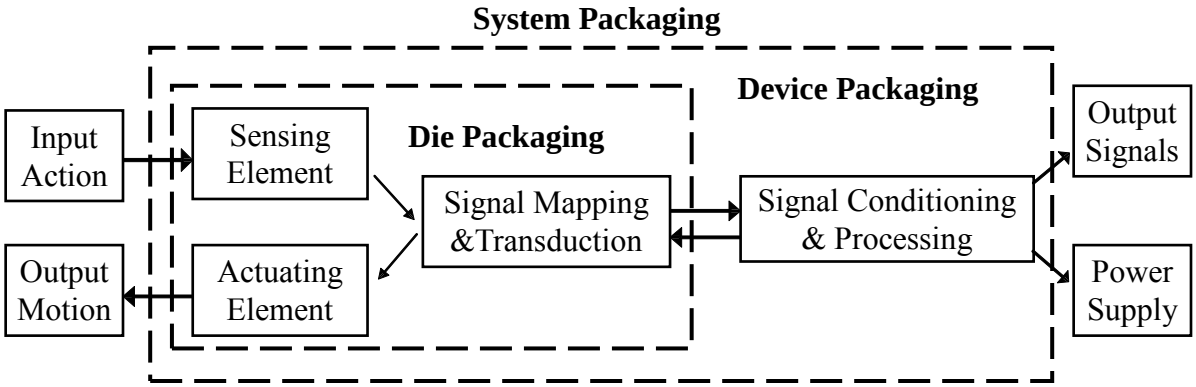

Figure 5-4. MEMS sensor packaging system (Hsu, 2008).

Table 5-4. MEMS sensor packaging methods and materials.

Levels	Packages
Die	Cavity packaging (CSP-cavity LGA package), CERDIP, Ceramic LCC, SOIC, and MLF® derivatives
Device	Die bonding, wire bonding, interconnect, etc.
System	Ceramic packages (basic dual in-line packages, chip carriers, flat packs, and multilayers packages), plastic packages (leadframe materials include copper alloy, nickel-iron, composite strip, etc.), metal packages (Kovar, cold rolled stell, copper, molybdenum, silicon carbide reinforced aluminum, etc.)

New packaging materials and methods emerge virtually every day, but MEMS sensors are application-specific so it is hard to develop "one size fits all" packaging and sensor systems. Among the various sensors, the moisture sensor is most vulnerable to environment because to measure water vapor it must have access to its outside environment via an open pore, representing a severe challenge for MEMS sensor encapsulation (Wang, 2010). The most common packaging for moisture sensors is a pre-molded open-cavity package. In concrete, both the high pH environment and excessive water exposure can damage moisture sensors through their open pores. Therefore, a hand-made simple packaging

approach is usually used for the moisture sensor to improve its performance, as described by Ye et al. (2006), Choi and Won (2008), and Wells (2005). However, there are no 100% reliable moisture sensors with robust packaging yet available, and most moisture sensors do stop functioning in concrete pavement a few weeks after road construction. As a result, engineers continue to pursue a reliable moisture-sensor packaging method to be used in pavement applications. There are also companies specializing in sensor-packaging design and manufacture. The following paragraphs give a summary of past packaging methods for moisture sensors used in pavement.

Simple Packaging Used in the Field

Ye et al. (2006) conducted a literature review about curing in PPC pavement and a moisture sensor called Hygrochron was evaluated in that study. Choi and Won (2008) performed a similar study to identify compliance-testing methods for curing, and a plastic pipe with Gore-Tex was used to protect the Hygrochron sensor in concrete pavement, as shown in Figure 5-5. However, the pore size or the configuration of this fabric may have influenced the RH measurements and the readings in concrete therefore may not have been consistent (Choi and Won, 2008). Near the end of their study, an RH value over 100% was observed.

Figure 5-5. Hygrochron packaged in the field (Ye et al., 2006; Choi and Won, 2008).

Figure 5-6 illustrates a packaging method from Wells (2005) used in a field pavement construction project, similar to Choi and Won (2008). The University of Pittsburgh conducted a study in 2002 to investigate early-age concrete pavement behavior. In this study, a Sensirion SHT75 humidity sensor was used to monitor RH value; this was the same sensor used in the US Highway 30 study. During road construction, the moisture sensor was inserted into a plastic cylindrical tube and the enclosure was sealed with a circular Gore™ membrane vent using ordinary superglue. The idea behind this kind of packaging was to protect sensors from direct contact with the concrete mixture, but the majority of the sensors later stopped functioning and unrealistic RH measurement values above 100% were also observed. The reason for these failures was probably due to condensation along the sensor tips.

Figure 5-6. Moisture sensor packaging (Wells, 2005).

Wang (2013) performed a study of sensor network applications in building construction. He used polyoxymethylene plastic to make a package for prevention of direct contact with liquid in fresh concrete, as shown in Figure 5-7. A Gore screw-in vents was used to provide a protective seal over the sensor to allow diffusion of moisture vapor only.

Furthermore, the final dimensions of this packaging were 65 mm in diameter and 45 mm in height.

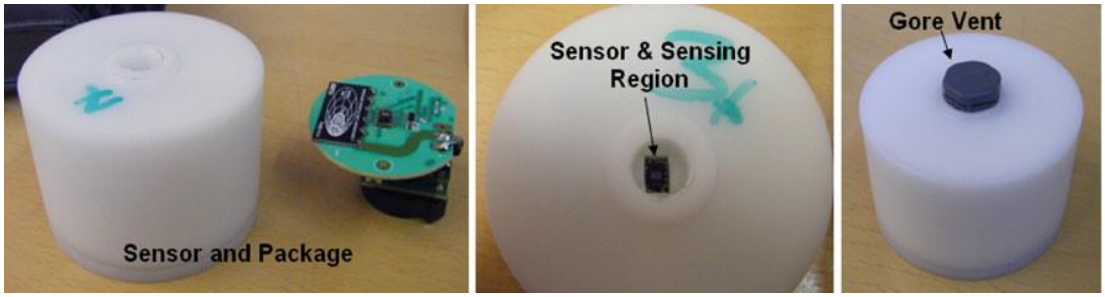

Figure 5-7. Moisture sensor packaging (Quinn and Kelly, 2010; Wang, 2013).

Spherical Steel Platform

Lian et al. (2010) have developed the embedded wireless strain/stress/temperature sensor platform for highway applications shown in Figure 5-8. This steel platform was spherical in shape with a 3-inch diameter. The top half of this platform contained an RF data acquisition/control/communication board along with pressure, strain, moisture, temperature, and three-axial acceleration sensors, and the bottom half contained a rechargeable battery and Faraday energy-harvesting devices. The platform has large power consumption and is still in the testing stage.

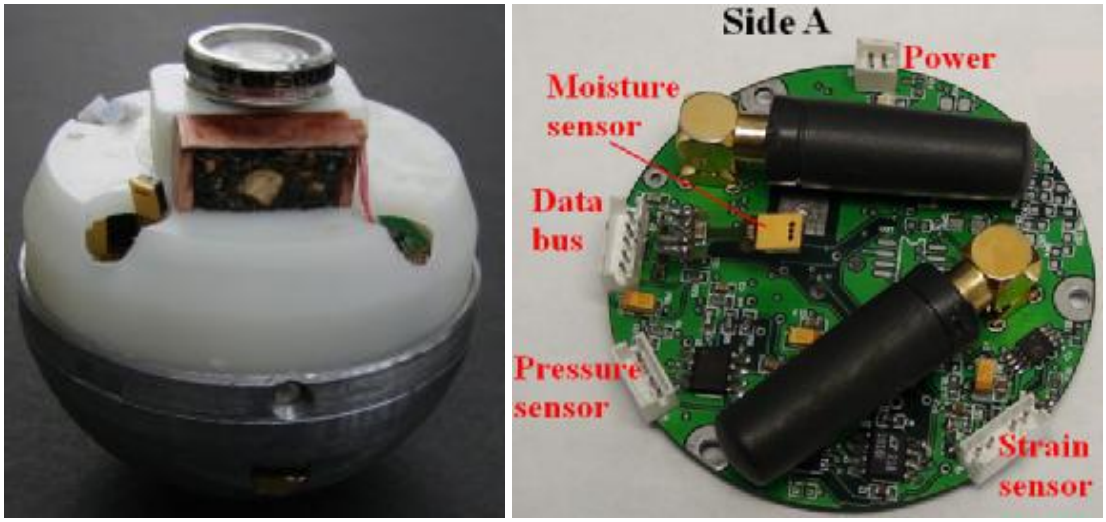

Figure 5-8. Wireless strain/stress/temperature sensor platform (Lian et al., 2010).

Porous Cement Paste

Bennett et al. (1999) installed temperature sensors in an instrumented core to measure temperature of pavement as described in the literature review of Chapter 2. Barroca et al. (2013) used a similar approach to embed the moisture sensor in a porous mortar cube, as shown in Figure 5-9. In this study, the moisture sensor was fabricated by first welding a filter cap and a filter membrane and it was then buried in a porous 2 in. mortar cube made with coarse sand using a low water/cement ratio of 1:3. In this packaging system, the mortar worked as a shell to protect sensor wire connections during concrete casting, and the high porosity of this cube allowed the sensor to measure the RH level of concrete through the pores.

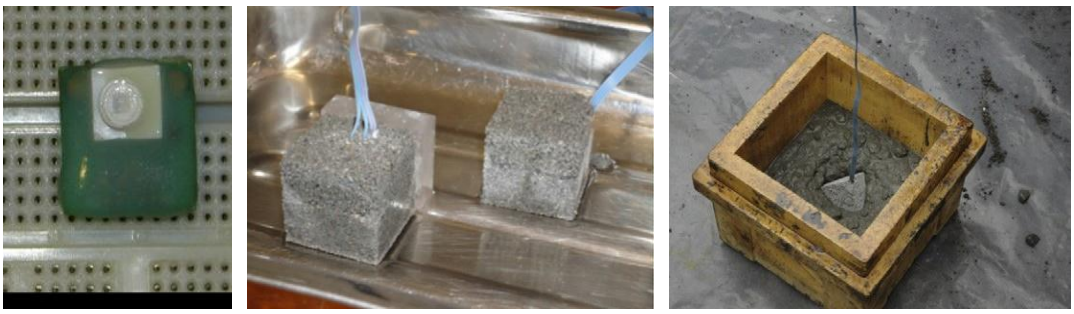

(a) (b) (c)

Figure 5-9. Sensor packaging made by Barroca et al. (2013): (a) sensor fabrication; (b) Porous mortar shell; (c) concrete casting.

Stainless Steel Jacket

Sarrfi and Romine (2005) conducted a study to develop a sensor capable of measuring both temperature and moisture. The sensor die was protected by a polymeric coating and the whole chip was encapsulated in a stainless steel jacket equipped with a ceramic filter for RH measurement, as shown in Figure 5-10 (Saafi and Romine, 2005; Jackson et al., 2008; Norris et al., 2008). The dimensions of the completed sensor are 3 mm in height and 5 mm in diameter.

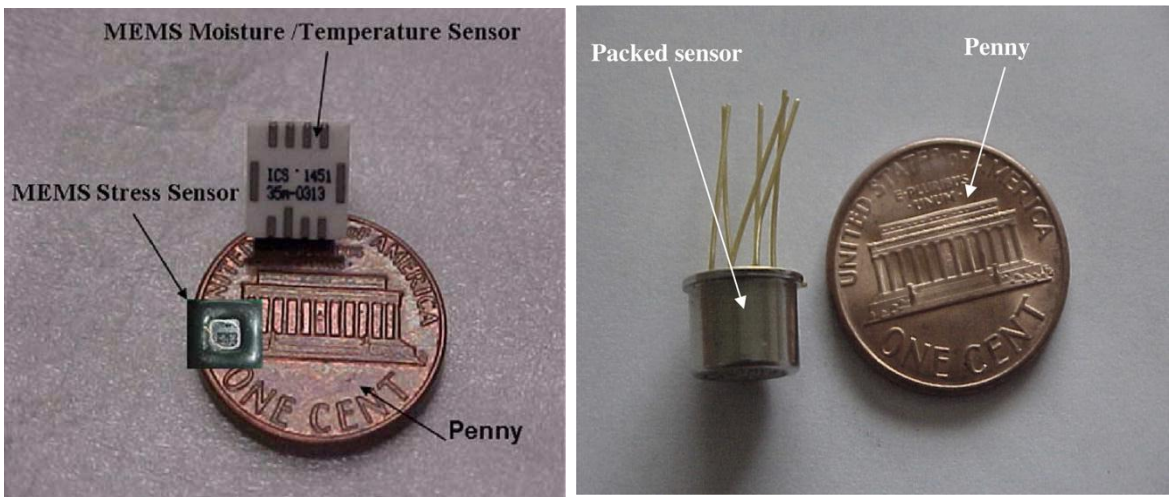

(a) (b)

Figure 5-10. Stainless steel jacket packaging: (a) Sensor die by polymeric coating (Saafi and Romine, 2005); (b) stainless jacket packaging (Norris et al., 2008).

Moisture Sensor with Detecting Probe

There have been several probe-based moisture sensors, including the MK33 and the Hydro-Probe II Moisture Sensor, claimed to be applicable to internal concrete RH measurement. The MK 33 is a capacitive sensor that could be directly embedded in concrete mixture because of its high solvent and hot water resistance, as shown in Figure 5-11 (a) (Every and Deyhim, 2009). The Hydro-Probe II moisture sensor is a sensor using digital microwave to measure RH in concrete, as shown in Figure 5-11 (b). Similarly to MK 33, the Hydro-Probe II moisture sensor can be directly placed in plastic concrete to provide reliable RH measurement. However, this sensor is very expensive with a unit cost of more than $5,000 (Sebesta, 2013). In addition to the MK33 and the Hydro-Probe II Moisture Sensor, other probe-based moisture sensors such as Time Domain Reflectometer (TDR) and the Stevens Hydra Probe are often used in soil-moisture detection. These probe-based moisture sensors are, however, unable to provide an RH profile versus pavement depth.

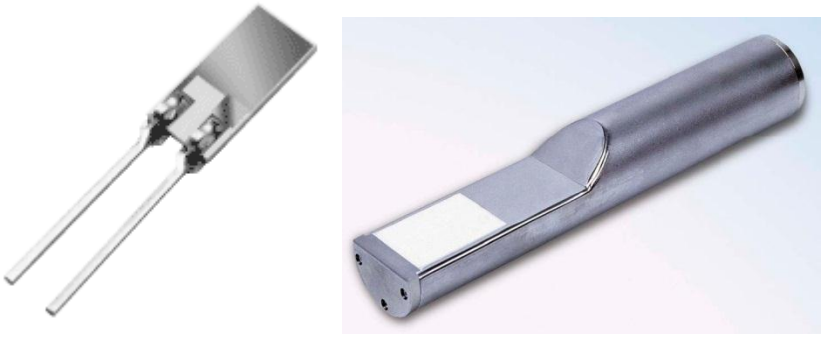

(a) (b)

Figure 5-11. Moisture sensor with detecting probe: (a) MK33 humidity sensor (Every and Deyhim, 2009); (b) Hydro-Probe II moisture sensor (Hydronix, 2014).

Monitoring

The monitoring period can be divided into either short-term or long-term intervals depending on project objectives, sensor survivability, and battery life. A short-term period might be just few months while a long-term period could be several years; a longer monitoring period is usually desirable even it's hard to achieve. Data-measuring intervals can vary from one minute up to one hour. Typically, one-half hour should be sufficient for temperature and moisture measurements while strain can be measured each minute. Short intervals can, however, provide more detailed data while consuming more power, so a balance point between size of the data-measuring interval and battery life should be established. One strategy is to adjust the interval depending on changes in situation. It's well known that early-age behavior of concrete pavement may impact long-term performance, so at early age a short measuring interval might be applied (Ruiz et al., 2005). Then longer intervals can be used for the time remaining to consume less energy; they might be shortened when a critical situation is detected. Early age is defined as the first 72 hours after pavement construction by the Federal Highway Administration guidelines, although sometimes the term may refer to the time before traffic opening (Ruiz et al., 2005).

Daily data collection and backup is preferred to guard against accidental data loss, but this may depend on specific situations affected by weather, distance, cost, etc. Onsite DAS and power sources should be protected from harsh climate and local animals. However, if wireless sensors are used, a moving truck mounting a DAS could be used for data collection. To achieve this goal, reliable wireless transmission technology is required to provide a strong signal and eliminate electronic interference, as shown in Figure 5-12 (Lajnef et al., 2013). In addition to a vehicle mounted with DAS, a two-level wireless communication system for remote data collection might be employed. The first level would use a wireless communication device at the data collection site. This device would act as a transfer station to transmit data via the internet to the second level. Figure 5-13 shows an example of this kind of wireless device, an "i-TOWER" used in the HardTrack concrete-monitoring system. It can transmit data via cellular internet with a built-in 3G/4G Hot-Spot. Furthermore, it can be powered with either turbine or solar power (Wake, Inc., 2014).

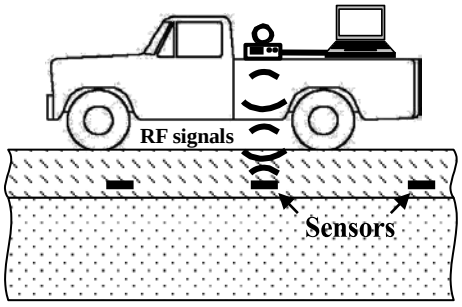

Figure 5-12. RF reader mounted on a moving vehicle (Lajnef et al., 2013).

Figure 5-13. i-TOWER with turbine & solar panel (Wake, Inc., 2014).

Architecture of Smart Pavement SHM System

Smart Pavement SHM is defined as long-term, continuous, sustainable pavement system providing information about in-situ pavement conditions to prevent multi-faceted safety concerns, including pavement deterioration. The previous literature review in Chapter 2 has described the need of Smart Pavement SHM for both highway and airfield pavement. The basic concepts of the Smart Pavement SHM systems are similar for both highway pavement and airfield pavement. For airfield pavement, a SHM system can be combined with a Foreign Object Debris (FOD) detection system to provide in-time warning for appearance of FOD, which is the foreign substance or debris that could cause aircraft damage (Ang, 2013).

Figures 5-14 (a) and (b) illustrate conceptual designs of highway and airport health monitoring systems, respectively. In both Figures 5-14 (a) and (b), the embedded smart MEMS sensor subsystem is a wireless multifunction MEMS sensor able to simultaneously

measure strain, temperature, and moisture. A robust packaging subsystem should also be implemented to protect the embedded smart MEMS sensors from pavement construction, high alkali environment of concrete, and harsh climactic and traffic conditions. A reliable DAS, mounted either on a moving vehicle for highway pavement or a control tower for airfield pavement, can be used for data collection, storage, and transfer from embedded MEMS sensors. An intelligent data-mapping model subsystem employing sensing data fusion and geo-spatial analysis approach can be utilized in data mapping of collected data from sensors installed at specific locations. Realistic characterization of pavement-layer properties and responses through an intelligent data-mapping model subsystem can be used to provide early warning about critical distress initiation, accurate airport pavement-life predictions, and planning pavement management activities, as well as calibration and validation of mechanistic-based pavement-response prediction models. Unlike highway pavement SHMs, smart MEMS sensor subsystem for airfield pavement SHM can be integrated with Electro-optical (EO) based distress and FOD detectors to monitor actual pavement surface condition.

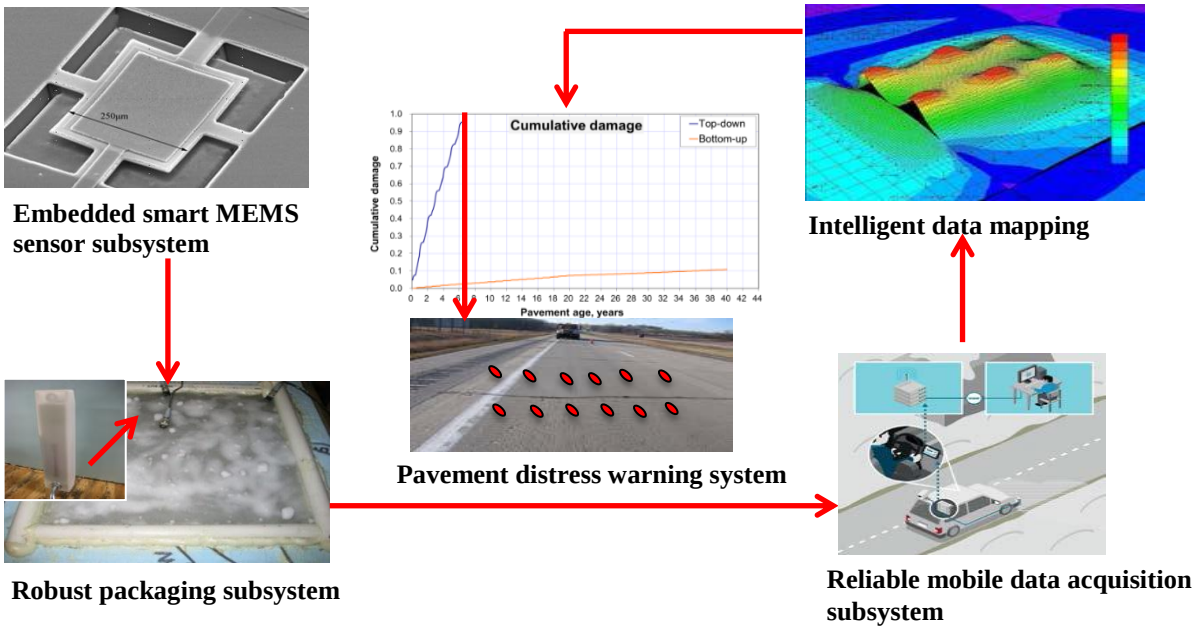

(a)

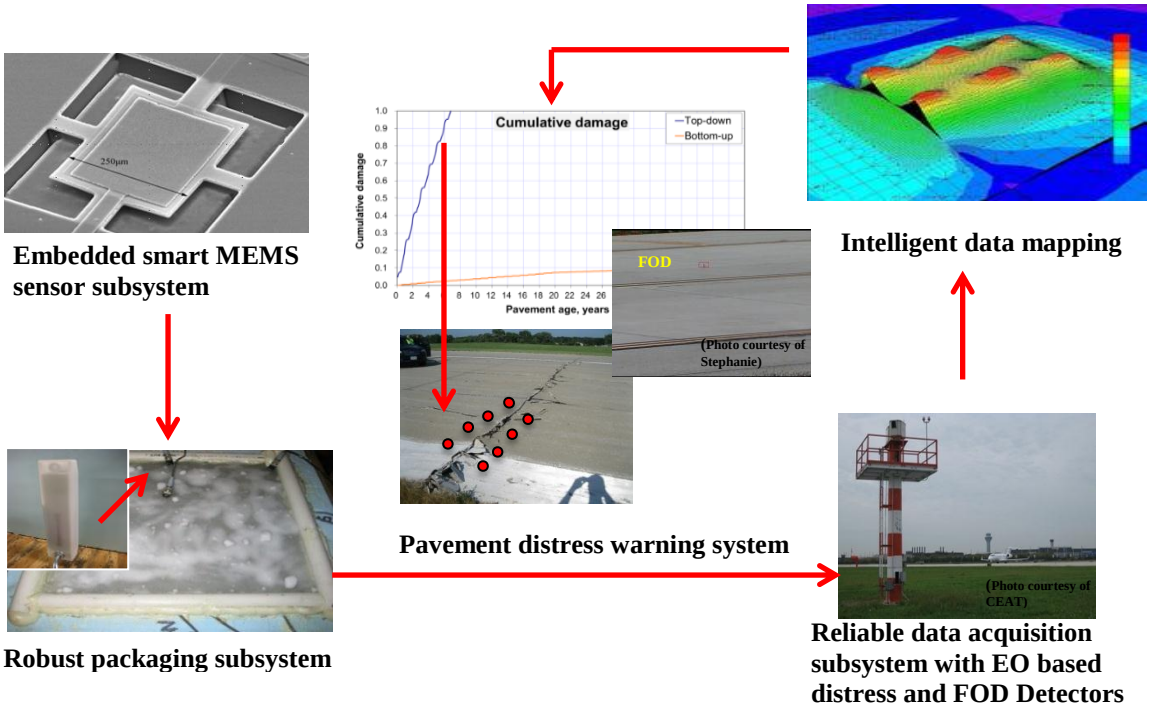

(b)

Figure 5-14. Smart pavement monitoring systems for: (a) highway pavement; (b) airfield pavement.

Other Potential technologies for Development of Smart Sensing and Smart SHM on Pavement Infrastructure

Fiber Optic Sensor System

A fiber optic sensor is a type of sensor that can either monitor environmental conditions or transmit data using fiber optic communication that modulates a light beam within the fiber. In general, fiber optic sensors have small size and weight and can be used in explosive and corrosive environments. They can also be used to provide distributed sensing along the optical fiber. Theoretically, hundreds of locations along a fiber just 1-m long can be measured. Furthermore, fiber optic sensors can be used to measure strain, temperature, humidity, pH, etc. (Balageas et al., 2006; Glisic and Inaudi, 2007; Rice, 2014). Figure 5-15 illustrates a typical fiber optic sensor.

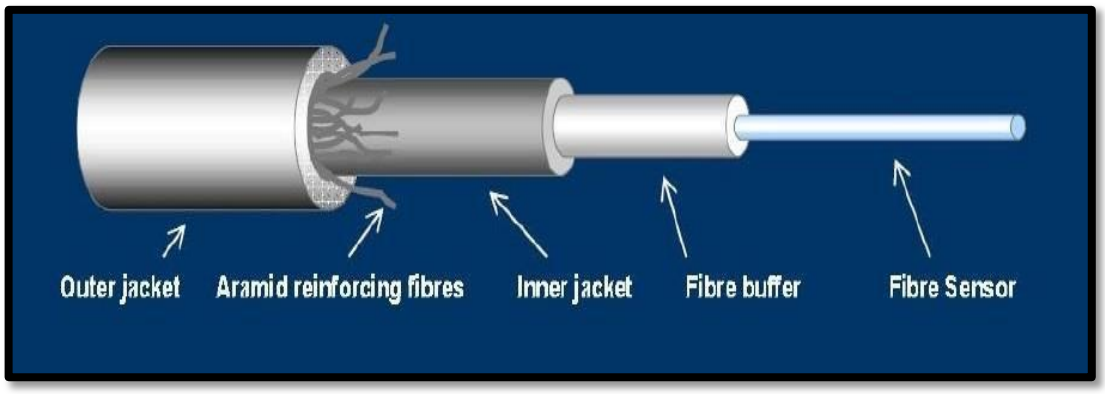

Figure 5-15. Typical fiber optic sensors (Kottiswaran et al., 2014).

Self-Sensing Concrete

Self-sensing concrete is a new alternative for Smart Pavement SHM relying on making measurements based on electrical resistivity, impedance, capacitance and so on (Han et al., 2014). It utilizes conductive materials such as nanotubes to configure an internal electric network inside the concrete, so properties such as stress and strain can be measured

based on piezoresistivity effects; the data can be acquired using either wired or wireless methods (Li and Ou, 2009; Sun et al., 2010; Han et al., 2014; Ubertini et al., 2014). Self-sensing concrete can also be used to monitor traffic or melt snow in transportation infrastructures. Figure 5-16 illustrates a self-sensing concrete system for strain measurement.

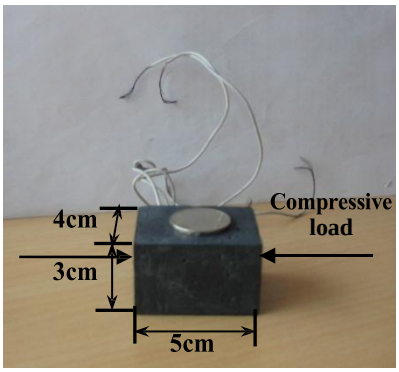

Figure 5-16. Self-sensing concrete for strain measurement (Han et al., 2014).

Micro Battery with Nuclear Power

Battery life is a key factor for active wireless sensors used in health monitoring, and traditional battery technology may extend the work life by as much as 10 years (Roberts, 2006). Micro batteries using nuclear energy may provide a solution that can increase battery life to several decades with sizes at the micro or even nano scale. This technology, still in the research stage, has its main concept that uses radioisotopes rather than fossil or chemical fuels (Guo et al., 2008).

Vehicle Noise Based Roadway Health Monitoring

Vehicle noise based roadway health monitoring systems use a noise-based data collection system to evaluate infrastructure for proactive maintenance, operation, and safety. In such a system, a vehicle is used as mobile sensor to measure noise, vibration, and harshness. Sensing devices such as accelerometers can be mounted on the vehicle for such

data measurement and they generate less congestion than other methods (Yousuf and Morton, 2014). Figure 5-17 illustrates a versatile onboard traffic-embedded roaming-sensor (VOTERS) test van equipped with sensors, camera, and millimeter-wave radar to measure pavement surface conditions.

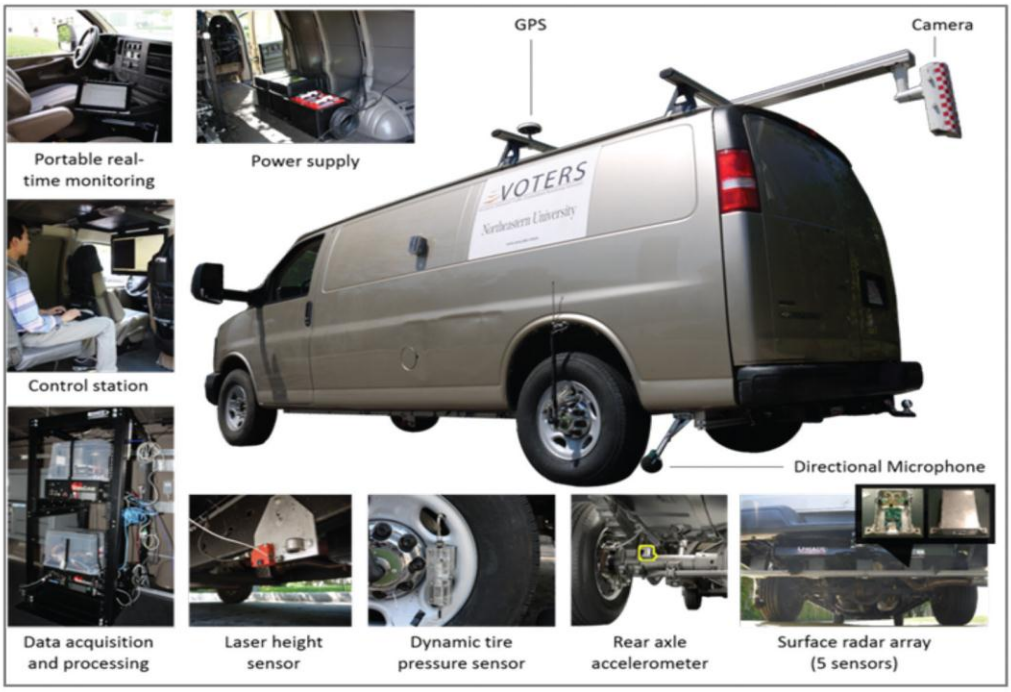

(a)

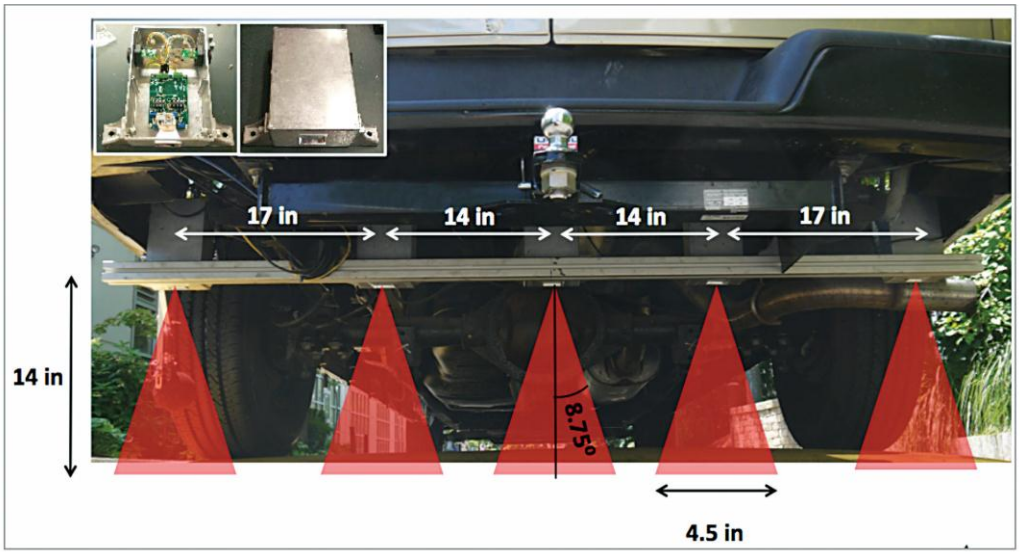

(b)

Figure 5-17. Vehicle noise based roadway health monitoring: (a) VOTER test van; (b) Millimeter-wave radar (Yousuf and Morton, 2014).

CHAPTER 6

SUMMARY, FINDINGS, RECOMMNEDATIONS

Summary

Early damage detection in transportation infrastructure systems could provide better pavement maintenance and rehabilitation strategies to give such system longer operational life. To perform such early damage detection inn transportation infrastructure, the Structural Health Monitoring (SHM) was conceived, has been implemented or is currently being implemented. Recent advancements in sensing technology make SHM more evolving and driving to develop the next generation of SHM, so called as Smart SHM. As considering current shift changes in SHM through applications of new sensing technologies, this study discusses the use of Micro-Electromechanical Systems (MEMS) based smart wireless sensing technologies on health monitoring of concrete pavement. The literature review results pertain to SHM of pavement infrastructure system was discussed to evaluate the current pavement SHM practices and to identify how terms of "Smart Sensor" and "Smart SHM" applied to transportation infrastructure systems have been defined in the literature.

MEMS and wireless sensing technologies and their applications to pavement SHM reported in the literature were reviewed and documented as these have been considered as promising technologies to meet requirements of "Smart Sensor". A field demonstration of off-the-shelf MEMS and wireless sensor system applications under actual in-service concrete pavement site was conducted to evaluate their performance, identify their limitations, and demonstrate how their sensed data can be utilized to monitor concrete pavement behaviors. The feasibility of implementation of a wireless communication system into the MEMS sensor

has been investigated. As following up literature review, field demonstration, and implementation of wireless communication system, issues regarding concrete pavement SHM using current available MEMS and wireless sensor system were synthesized and enumerated and the requirements for achieving Smart Pavement SHM were explored to develop the conceptual design of smart health monitoring of both of highway and airport pavement systems as the next generation of Pavement SHM. The findings and recommendations drawn from this study can be summarized as follows:

Literature Review

- SHM can be useful for civil infrastructure to save both money and time by turning schedule-based maintenance into condition-based maintenance. However, the traditional sensor based SHM approach has limitations such as high installation cost and time, high array density, wire damage, and low survivability of sensors for long-term application. Therefore, the traditional approach may provide neither continuously long-term monitoring for pavement structural behavior changes nor real-time warning indications of in-service pavement failure.
- MEMS based sensor system is a type of promising smart-sensing technology that could be used to achieve Smart Pavement SHM. Most MEMS-based sensors for SHM purpose are still in the research stage and have not yet been commercialized.
- Wireless sensors can save both installation time and cost and they do not present wire-damage concerns. Even though they represent a potentially huge benefit for SHM, they have not yet been widely applied to pavement health monitoring, and most research studies are still in the proof-of-concept stage.

Field Instrumentation and Evaluation

- Sensor survivability is critical for long-term SHM of pavement systems. In the field instrumentation studied, about 78% of the embedded sensors remained functional one month after traffic opening, but only 20% were still functional ten months after traffic opening.
- Temperature, moisture, and strain profiles were developed from the monitored data, and they accurately reflected weather and seasonal change, including effects of thunderstorms, heat waves, summer, and winter. Furthermore, curling and warping behaviors of concrete resulting from different temperatures at different concrete depths was observed and analyzed. According to the strain curve, the top concrete and bottom concrete showed opposite patterns of curvature.
- The main reasons for cessation of sensor functioning included concrete paver operation, alkali-cement hydration reaction in concrete, corrosion of sensor wires, battery issues, harsh climate, and slab movement. The moisture sensor was more sensitive to chemical environment. Furthermore, the RFID tags had a low wireless communication range, probably due to battery issues, cold weather, and steel reinforcement in concrete.
- Normal concrete tests were conducted in the laboratory and a concrete maturity curve was developed to estimate in-place concrete strength gain. However, MEMS digital humidity sensors showed a higher maturity index for same-design in-place strength because they indicated higher average temperatures.

Implementation of Wireless Communication System

- The ZigBee based wireless network implemented for the MEMS sensors demonstrated reliable communication and achieved a high success rate over a 150 ft. span.
- The Power consumption of the system was still high, mainly due to the microcontrollers, so a power-saving mechanism such as power management circuit could be added to extend its working time.

Requirements for Smart Pavement Structural Health Monitoring System

- Procedures and strategies for pavement instrumentation must be considered well in advance. Communication with the construction manager is important in increasing sensor survivability in pavement.
- Use of MEMS sensors usually produces lower unit sensor cost and DAS purchase fee.
- Robust packaging, especially for moisture sensors, is a key element for sensor survivability. However, no 100% reliable moisture sensor is yet available.

Recommendations

Based on the findings of this research, the followings recommendations are proposed for future development of "Smart Sensor" and "Smart SHM" for pavement infrastructure systems.

- A wireless multifunctional MEMS sensor with an energy-harvesting system and durable packaging is recommended for Smart Pavement SHM. A power-management circuit could also be used to reduce device power consumption.

- An active RFID system has a long communication range but limited lifetime and relative large size, while a passive RFID system has unlimited lifetime but a short communication range. Therefore, a semi-passive RFID system with internal batteries that can be also self-powered may be a solution combining the advantages of both active and passive RFID systems.
- Several types of wireless communication systems given in Chapter 5 are recommended for data collection. The first system would use a vehicle-mounted DAS system to collect data using a passive wireless-sensor system. Wireless communication range and on-board data storage capacity would be critical factors in this whole system. The second system would use a two-level wireless system with a local data-transfer station powered by solar or wind. The data-transfer station could both collect data from embedded sensors and transmit data to a remote office. For example, a small scale-structure and near an office site could use an RFID system for first-level communication and a ZigBee network as a second level. Such a combined RFID and ZigBee-based monitoring system could improve monitoring efficiency and promise low cost.
- For a large structure where data must be transmitted to a remote office, the data can be transmitted via the Internet (second level) so a technician could download data at either home or office.
- RF communication usually has a limited range. The data can be lost if the transmission distance is too long, so a "Hop network" can be used to resolve this problem and save power (Zhao and Guibas, 2004).

- Sensor installation should use smart strategies to eliminate effects of road construction activities, as described in Chapter 5. Communicating with the construction manager as soon as possible to optimize the installation method is critically important. An easy sensor-installation method should also be investigated in the future. Specially-designed tools or packaging of sensors may be needed.
- Other sensing technologies such as fiber optic sensor systems, self-sensing concrete, micro battery using nuclear power, and vehicle noise for roadway health monitoring are recommended for future investigation.

REFERENCES

Adams, D. (2007). *Health Monitoring of Structural Materials and Components: Methods with Applications*. John Wiley & Sons, Ltd., Chichester, UK.

Ahlborn, T. M., Shuchman, R., Sutter, L. L., Brooks, C. N., Harris, D. K., Burns, J. W., and Oats, R. C. (2010). *The State-of-the-Practice of Modern Structural Health Monitoring for Bridges: A Comprehensive Review*, Michigan Tech, MI.

Al-Khatib, Z., Yu, J., Al-Khakani, H. G., and Kombarji, S. (2009). A Wireless Multivariable Control Scheme for A Quadrotor Hovering Robotic Platform Using IEEE® 802.15.4. Concordia University, Canada.

AllAboutMEMS. (2002). What is MEMS? http://www.allaboutmems.com/whatismems.html (accessed July 15, 2014).

Al-Qadi, I. L., Loulizi, A., Elseifi, M., and Lahouar, S. (2004). The Virginia SMART ROAD: The Impact of Pavement Instrumentation on Understanding Pavement Performance. *Journal of the Association of Asphalt Paving Technologists*, Vol. 73.

Amkor Technology. (2014). MEMS & Sensors Packaging Technology Solutions. http://www.amkor.com/go/mems (Accessed Oct 11, 2014)

Andò, B., Baglio, S., Savalli, N., and Trigona, C. (2011). Cascaded "Triple-Bent-Beam" MEMS Sensor for Contactless Temperature Measurements in Nonaccessible Environments. *IEEE Transactions on Instrumentation and Measurement*. 60(4), pp. 1348-1357.

Ang, L. (2013). Research and Design of an Airfield Runway FOD Detection System Based on WSN. *International Journal of Distributed Sensor Networks*, Hindawi Publishing Corporation.

ARDUINO. (2014). Products http://arduino.cc/en/Main/Products#.UxTTlfm9l8E (Accessed in March 29, 2014).

Atmel. (2014). Atmel AVR 8-bit and 32-bit Microcontrollers http://www.atmel.com/products/microcontrollers/avr/ (Accessed in March 29, 2014).

Attoh-Okine, N., and Mensah, S. (2003). MEMS Application in Pavement Condition Monitoring-Challenges. *NIST SPECIAL PUBLICATION SP*, pp. 387-392.

Asbahan, R. E. (2009). Effects of the Built-In Construction Gradient and Environmental Conditions on Jointed Plain Concrete Pavements. Dissertation, University of Pittsburgh, PA.

ASCE. (2013). 2013 Report Card for America's Infrastructure. http://www.infrastructurereportcard.org/a/documents/2013-Report-Card.pdf (Accessed Oct 28, 2014)

ASTM. (2007). Standard Practice for Estimating Concrete Strength by the Maturity Method. *Annual Book of ASTM Standards* (Vol. ASTM C1074). West Conshohocken, PA.

Aygun, B., and Gungor, V. C. (2011). Wireless Sensor Networks for Structure Health Monitoring: Recent Advances and Future Research Directions. *Sensor Review*, 31(3), pp. 261-276.

Baker, H. B., Buth, M. R., and Van Deusen, D. A. (1994). *Minnesota Road Research Project Load Response Instrumentation Installation and Test Procedures*. Technical Report No. MN/PR-94/01, Minnesota Department of Transportation, MN.

Balageas, D., Fritzen, C. P., and Güemes, A. (2006). *Structural Health Monitoring*. ISTE Ltd., Newport Beach, CA.

Barroca, N., Borges, L. M., Velez, F. J., Monteriro, F., Gorski, M., and Castro-Gomes, J. (2013). Wireless Sensor Networks for Temperature and Humidity Monitoring within Concrete Structures. *Construction and Building Materials*, Vol.40, pp. 1156–1166.

Bennett, R., Hayes-Gill, B., Crowe, J. A., Armitage, R., Rodgers, D., and Hendroff, A. (1999). Wireless Monitoring of Highways. *Smart Systems for Bridges, Structures, and Highways*, *Proceedings of the SPIE*, Newport Beach, CA, March 1–2, Vol.3671, pp. 173–182.

Bouhouche, T., El Khaddar, M. A., Boulmalf, M., Bouya, M., and Elkoutbi, M. (2014). A New Middleware Architecture for the Integration of RFID Technology into Information Systems. *In Multimedia Computing and Systems (ICMCS)*, International Conference, IEEE, pp. 1025-1030.

Bremer, K., Wollweber, M., Guenther, S., Werner, G., Sun, T., Grattan, K. T. V., and Roth, B. (2014). Fiber Optic Humidity Sensor Designed for Highly Alkaline Environments. *Processing of SPIE*, Vol. 9157, pp. 9571A4-1.

Brownjohn, J. M. (2007). Structural Health Monitoring of Civil Infrastructure. *Phil. Trans. R. Soc. A*, 365(1851), pp. 589-622.

Buenfeld, N., Davis, R., Karmini, A., and Gilbertson, A. (2008). Intelligent Monitoring of Concrete Structures. *CIRIA*, UK, pp. 150.

Cepero, E. D. (2013). Structural Health Monitoring Inside Concrete and Grout Using the Wireless Identification and Sensing Platform (WISP). Dissertation, Florida International University, FL.

Ceylan, H., Gopalakrishnan, K., Taylor, P., Shrotriya, P., Kim, S., Prokudin, M., Wang, S., Buss, A. F., and Zhang, K. (2011). *A Feasibility Study on Embedded Micro-Electromechanical Sensors and Systems (MEMS) for Monitoring Highway Structures*. Iowa Highway Research Board Publication No. IHRB Project TR-575, Iowa State University, Ames, IA.

Ceylan, H., Gopalakrishnan, K., Kim, S., Taylor, P. C., Prokudin, M., and Buss, A. F. (2013). Highway Infrastructure Health Monitoring Using Micro-Electromechanical Sensors and Systems (MEMS). *Journal of Civil Engineering and Management*, Vol.19 (sup1), pp. 188-201.

Chiao, M., and Lin, L. (2006). Device-level Hermetic Packaging of Microresonators by RTP Aluminum-to-Nitride Bonding. *Microelectromechanical Systems, Journal of* 15(3), pp. 515-522.

Cho, S., Yun, C. B., Lynch, J. P., Zimmerman, A. T., Spencer Jr, B. F., and Nagayama, T. (2008). Smart Wireless Sensor Technology for Structural Health Monitoring of Civil Structures. *International Journal of Steel Structures*, 8(4), pp. 267-275.

Choi, K. S., Kim, D. S., Yang, H. J., Ryu, M. S., and Chang, S. P. (2014). A Highly Sensitive Humidity Sensor with a Novel Hole Array Structure Using a Polyimide Sensing Layer. *RSC Advances*, Vol.4, pp. 32075-32080.

Choi, S. and Won, M. (2008). *Identification of Compliance Testing Method for Curing Effectiveness*. FHWA Publication No. FHWA/TX-09/0-5106-2, pp. 21-30, Center for Transportation Research, the University of Texas, Austin, TX.

Chou, C. P., Cheng, H. J., and Lin, S. T. (2004). Analysis of Concrete Joint Movements and Seasonal Thermal Stresses at the Chiang Kai-Shek International Airport. *FAA Worldwide Airport Technology Transfer Conference*, Atlantic City, NJ.

Copley, J. R. (1994). Rout 2 Rigid Pavement Instrumentation Project: Installation and Testing of Selected Instruments and Data Analysis for Slabs 3, 4, 6, 7, & 9. Thesis, Ohio University, OH.

Cortez, N. E., Vieira Filho, J., and Baptista, F. G. (2014). Design and Implementation of Wireless Sensor Networks for Impedance-Based Structural Health Monitoring Using ZigBee and Global System for Mobile Communications. *Journal of Intelligent Material Systems and Structures*, pp. 1-12.

Darestani, M. Y. (2007). Response of Concrete Pavements under Moving Vehicular Loads and Environmental Effects. Dissertation. Queensland University of Technology, Australia.

Das, B. M. (2010). *Principles of Geotechnical Engineering*. 25th Edition, CENGAGE Learning, Stamford, CT.

Deng, F., He, Y., Zhang, C., and Feng, W. (2014). A CMOS Humidity Sensor for Passive RFID Sensing Applications. *Sensors*, 14(5), pp. 8728-8739.

DIgI. (2014). ZigBee Wireless Standards https://www.digi.com/technology/rf-articles/wireless-zigbee (Accessed in March 25, 2014).

Doebling, S. W., Charles R. F., and Prime, M. B. (1998). A Summary Review of Vibration-Based Damage Identification Methods. *Shock and Vibration Digest*, 30(2), pp. 91-105.

Dong, M., and Hayhoe, G. F. (2000). *Denver International Airport Sensor Processing and Database*. Technical Report DOT/FAA/AR-00/17, U.S. Department of Transportation, Federal Aviation Administration, Office of Aviation Research, Washington, DC.

Dong, Z. J., Li, S. L., Wen, J. Y., & Chen, H. C. (2012). Asphalt Pavement Structural Health Monitoring Utilizing FBG Sensors. *Advanced Engineering Forum*, Vol. 5, pp. 339-344.

Enckell, M. (2011). Lessons Learned in Structural Health Monitoring of Bridges Using Advanced Sensor Technology. TRITA-BKN. Bulletin 108, KTH Architecture and the Build Environment.

Every, E. V., Faridazar, F., and Deyhim, A. (2009). Embedded Sensors for Life-time Monitoring of Concrete. *4th International Conference on Structural Health Monitoring on Intelligent Infrastructure (SHMII-4)*, July 22-24, 2009, Zurich, Switzerland.

Farrar, C. R. (2001). Historical Overview of Structural Health Monitoring. *Lecture Notes on Structural Health Monitoring Using Statistical Pattern Recognition*, Los Alamos Dynamics, Los Alamos, NM.

Farrar, C. R., Hemez, F. M., Shunk, D. D., Stinemates, D. W., Nadler, B. R., and Czarnecki, J. J. (2004). A Review of Structural Health Monitoring Literature: 1996-2001. Los Alamos National Laboratory, NM.

Farrar, C. R., & Worden, K. (2007). An Introduction to Structural Health Monitoring. *Phil. Trans. R. Soc. A*, 365(1851), pp. 303-315.

Federal Aviation Administration. (2011). *Development of Standards for Nonprimary Airports*. Advisory Circular AC 150/5100-13B, U.S. Department of Transportation.

Federal Aviation Administration. (2007). *Guidelines and Procedures for Maintenance of Airport Pavements.* Advisory Circular AC 150/5380-6B, U.S. Department of Transportation.

Federal Aviation Administration. (2009). *Airport Foreign Object Debris (FOD) Detection Equipment.* Advisory Circular AC 150/5220-24, U.S. Department of Transportation.

Federal Highway Administration. (2012a). Highway statistics, 2012, Section 4—Highway Infrastructure, Table HM-12. http://www.fhwa.dot.gov/policyinformation/statistics/2012/ (Accessed Oct 11, 2014).

Federal Highway Administration. (2012b). Pavement Assessment. Federal Highway Administration Broad Agency Announcement No. DTFH61-12-R-00055.

Frank, R. (2013), Smart Sensors: Packaging, Testing, and Reliability. http://www.memsjournal.com/2013/09/smart-sensors-packaging-testing-and reliability.html (Accessed Oct 11, 2014)

Garg, N., Guo, E., and McQueen, R. (2004). *Operational Life of Airport Pavements*. Technical Report DOT/FAA/AR-04/46, U.S. Department of Transportation, Federal Aviation Administration, Office of Aviation Research, Washington, DC.

Geokon, Inc. (2014). Concrete Embedment. http://www.geokon.com/4200-Series. (Accessed August 6, 2013).

Glisic, B., and Inaudi, D. (2007). *Fibre Optic Methods for Structural Health Monitoring*. John Wiley & Sons Ltd., Chichester, UK.

Granja, J. L., Azenha, M., de Sousa, C., Faria, R., and Barros, J. (2014). Hygrometric Assessment of Internal Relative Humidity in Concrete: Practical Application Issues. *Journal of Advanced Concrete Technology*, 12(8), pp. 250-265.

Graves, S. W. (2012). Electro-optical Sensor Evaluation of Airfield Pavement. Thesis, University of Illinois at Urbana-Champaign, Urbana, Illinois, IL.

Guo, H., Li, H., Lal, A., and Blanchard, J. (2008). Nuclear Microbatteries for Micro and Nano Devices. *In Solid-State and Integrated-Circuit Technology (ICSICT),* 9th International Conference, IEEE, pp. 2365-2370.

Han, J., Cheng, P., Wang, H., Zhang, C., Zhang, J., Wang, Y., Duan, L., and Ding, G. (2014). MEMS-based Pt Film Temperature Sensor on an Alumina Substrate. *Materials Letters*, Vol.125, pp. 224-226.

Hansen, W., Arbor, A., and Surlaker, S. (2006). *Embedded Wireless Temperature Monitoring Systems for Concrete Quality Control*. Ann Arbor, MI.

Haque, M. E., Zain, M. F. M., Hannan, M. A., Jamil, M., and Johari, H. (2012). Recent Application of Structural Civil Health Monitoring Using WSN and FBG. *World Applied Sciences Journal*, 20(4), pp. 585-590.

Hayhoe, G. F. (2004). Traffic testing results from the FAA's national airport pavement test facility. *Proceedings of the 2nd International Conference on Accelerated Pavement Testing*. Minneapolis, MN.

Herricks, E. E., Lazar, P., Woodworth, E., and Patterson, J. (2012). *Performance Assessment of an Electro-optical-based Foreign Object Debris Detection System*. Technical Report DOT/FAA/AR-11/13, U.S. Department of Transportation, Federal Aviation Administration, William J. Hughes Technical Center, Aviation Research Division, Atlantic City International Airport, NJ.

Hsu, T. R. (2008). *MEMS & Microsystems: Design, Manufacture, and Nanoscale Engineering*. John Wiley & Sons, Inc., NJ.

Hugo, F., and Epps, A. L. (2004). NCHRP Synthesis 325: Significant Findings from Full-scale Accelerated Pavement Testing. *National Cooperative Highway Research Program*.

Hydronix. (2014). Hydro-Probe II Moisture Sensor for Bins, Chutes and Conveyor Belts. http://www.hydronix.com/products/hydroprobe.php. (Assess June 6, 2014).

IDENTEC SOLUTIONS. (2008). Technology Rises with New York Skyline. http://www.wakeinc.com/PDF/FreedomTowerRelease.pdf (Accessed in March 27, 2014).

IMEGO. (2005). Sensor-System Packaging. http://www.imego.com/Expertise/electronic-packaging/sensor-system-packaging.aspx (Accessed Oct 11, 2014)

Islam, T., Khan, A., Akhtar, J., and Rahman, M. (2014). A Digital Hygrometer for Trace Moisture Measurement. *IEEE Transactions on Industrial Electronics*, 61(10), pp. 5599-5605.

Jackson, T., Mansfield, K., Saafi, M., Colman, T., and Romine, P. (2008). Measuring Soil Temperature and Moisture Using Wireless MEMS Sensors. *Measurement*, 41(4), pp. 381-390.

Jang, J. H., Jeong, J. H., Kwon, S. M., and Park, H. G. (2005). Long-term Monitoring Operation of the Test-Road in Korea Highway Corporation (KHC). *In Sensing Issues in Civil Structural Health Monitoring*, Springer Netherlands, pp. 505-514.

Kang, I., Schulz, M. J., Kim, J. H., Shanov, V., and Shi, D. (2006). A Carbon Nanotube Strain Sensor for Structural Health Monitoring. *Smart materials and structures*, 15(3), pp. 737-748.

Kaur, N., and Bhalla, S. (2014). Combined Energy Harvesting and Structural Health Monitoring Potential of Embedded Piezo-Concrete Vibration Sensors. *Journal of Energy Engineering*, ASCE.

Kim, S. K., Pakzad, S., Culler, D., Demmel, J., Fenves, G., Glaser, S., and Turon, M. (2007). Health Monitoring of Civil Infrastructures Using Wireless Sensor Networks. *IPSN'07*, pp. 254-263.

Kottiswaran, N., Jayabalaji, K. A., Deepak, S., and Priyadarshini, S. (2007). Health Monitoring of Civil Infrastructures Using Wireless Sensor Networks. *IJIRSET*, 3(2) pp. 226-231.

Krüger, M., Große, C. U., and Marrón, P. J. (2005). Wireless Structural Health Monitoring using MEMS. *Key Engineering Materials*, Vol. 293, pp. 625-634.

Kuang, K. S. C. (2014). Development of a Wireless, Self-Sustaining Damage Detection Sensor System Based on Chemiluminescence for Structural Health Monitoring. *Processing of SPIE, Smart Sensor Phenomena, Technology, Networks, and Systems Integration*, Vol. 9062.

Lajnef, N., Chatti, K., Chakrabartty, S., Rhimi, M., and Sarkar, P. (2013). *Smart Pavement Monitoring System*. FHWA Publication No. FHWA-HRT-12-072, Michigan State University, MI.

Lajnef, N., Rhimi, M., Chatti, K., Mhamdi, L., and Faridazar, F. (2011). Toward an Integrated Smart Sensing System and Data Interpretation Techniques for Pavement Fatigue Monitoring. *Computer-Aided Civil and Infrastructure Engineering*, 26(7), pp. 513-523.

Lary, J. (2009). Airport Pavement Maintenance and Management. Airfield Safety, Sign Systems and Maintenance Management Workshop, Pavement Consultants Inc.

Lazar, P., and Herricks, E. E. (2010). Procedures for FOD Detection System Performance Assessments: Electro-optical FOD Detection System. *FAA Worldwide Airport Technology Transfer Conference*, Atlantic City, NJ.

Lee, H. S., Cho, M. W., Yang, H. M., Lee, S. B., and Park, W. J. (2014). Curing Management of Early-age Concrete at Construction Site Using Integrated Wireless Sensors. *Journal of Advanced Concrete Technology*, 12(3), pp. 91-100.

Lee, J. (2004). *Use of MEMS Sensors in Structural Engineering*. Final Project of CEE 619 Advanced Structural Dynamics and Smart Structures, University of Michigan, MI.

Lee, J. S., Su, Y. W., and Shen, C. C. (2007). A Comparative Study of Wireless Protocols: Bluetooth, UWB, Zigbee, and Wi-Fi. Industrial Electronics Society (IECON), 33rd Annual Conference of the IEEE, Nov. 5-8, Taipei, Taiwan.

Lee, J., Kim, J., Kim, D., and Lee, K. (2003). Improvement of Field Installation Method for Asphalt Concrete Pavement Strain gage. *Journal of the Korean Society of Road Engineers*, (5)3. pp. 31-42.

Lee, X. G., Hovan, M., King, R., Dong, M. Y., and Hayhoe, G. F. (1997). Runway Instrumentation at Denver International Airport Development of Database. *Aircraft/pavement technology: in the midst of change*, pp. 348.

Lewis, F. L. (2004). Wireless Sensor Networks. *Smart Environments: Technologies, Protocols, and Applications*, pp. 11-46.

Li, H., and Ou, J. P. (2009). Smart Concrete, Sensors and Self-Sensing Concrete Structures. *Key Engineering Materials*, Vol. 400, pp. 69-80.

Lian, K. (2010). *Developing Embedded Wireless Strain/Stress/Temperature Sensor Platform for Highway Applications*. Report No. NCHRP IDEA Project 129, Highway IDEA Program, Louisiana State University, LA.

Lin, C. H., Fu, L. M., and Lee, C. Y. (2014). MEMS-based Humidity Sensor Based on Thiol-coated Gold Nanoparticles. *Proceedings of the 9th IEEE International Conference on Nano/Micro Engineered and Molecular Systems*, HI.

Liu, C. R., Guo, L., Li, J., and Chen, X. (2007). Weigh-in-motion (WIM) Sensor Based on EM Resonant Measurements. *Antennas and Propagation Society International Symposium*, IEEE, pp. 561-564.

Lloret, J. (2009). Introduction to Network Protocols and Algorithms. *Network Protocols and Algorithms*, Macrothink Institute™, (1)1, pp. 1-6.

Loh, K. J., Zimmerman, A. T., and Lynch, J. P., (2007). Wireless Monitoring Techniques for Structural Health Monitoring. In proceeding of the International Symposium of Applied Electromagnetics & Mechanics, Lansing, MI.

Lu, Y. F., Lou, W. Z., and Guo, M. R. (2014). Rapid Temperature Measurement of Meteorological Detection System Based on MEMS. *Key Engineering Materials*, Vol.609, pp. 1185-1188.

Luhr, D., Kinne, C., Uhlmeyer, J. S., and Mahoney, J. P. (2010). What We Don't Know about Pavement Preservation. In First International Conference on Pavement Preservation, Chapter 8, Newport Beach, CA.

Lynch, J. P. (2002). *Decentralization of Wireless Monitoring and Control Technologies for Smart Civil Structures*. Technical Report No.140, John A. Blume Earthquake Engineering Center. Stanford, CA.

Lynch, J. P., (2007). An Overview of Wireless Structural Health Monitoring for Civil Structures. *Phil. Trans. R. Soc. A*, 365(1851), pp. 345-372.

Lynch, J. P., and Loh, K. J. (2006). A Summary Review of Wireless Sensors and Sensor Networks for Structural Health Monitoring. *The Shock and Vibration Digest*, Vol.38, No.2, pp. 91–128.

Lynch, J. P., Sundararajan, A., Law, K. H., Kiremidjian, A. S., and Carryer, E. (2003). Power-efficient Wireless Structural Monitoring with Local Data Processing. In proceedings of the International Conference on Structural Health Monitoring and Intelligent Infrastructure, Tokyo, Japan, Vol.1, pp. 331–338.

Maser, K., Egri, R., Lichtenstein, A., and Chase, S. (1996). Field Evaluation of a Wireless Global Bridge Evaluation and Monitoring System. In proceedings of the 11th Conference on Engineering Mechanics, Fort Lauderdale, FL, May 19–22, Vol.2, pp. 955–958.

Maxim Integrated. (2014). Overview of Ibutton Sensors and Temperature/Humidity Data Loggers. http://www.maximintegrated.com/en/products/ibutton/ibuttons/thermochron.cfm (Accessed April 2, 2014)

Mccarter, W. and Vennesland, O. (2004). Sensor Systems for Use in Reinforced Concrete Structures. *Construction and Building Materials*, 18(6), pp. 351–358.

MEMSnet. (2014). What is MEMS Technology? https://www.memsnet.org/about/what-is.html (Accessed March 26, 2014).

Modares, M. and Waksmanski, N. (2012). Overview of Structural Health Monitoring for Steel Bridges. *Practice Periodical on Structural Design and Construction*,18(3), pp. 187-191.

Mohammed, A. A., Moussa, W. A., and Lou, E. (2011). High-performance Piezoresistive MEMS Strain Sensor with Low Thermal Sensitivity. *Sensors*, 11(2), pp. 1819-1846.

Moradi, M., and Sivoththaman, S. (2013). Strain Transfer Analysis of Surface-Bonded MEMS Strain Sensors. *Sensors Journal*, IEEE, 13(2), pp. 637-643.

MnROAD Brochure. (2014). MnROAD: Safer, Smarter, Sustainable Pavement through Innovative Research http://www.dot.state.mn.us/mnroad/pdfs/2014MnROADBrochure.pdf (Accessed June 30, 2014)

MNX. (2014). What is MEMS Technology. https://www.mems-exchange.org/MEMS/what-is.html. (Accessed in February 20, 2014).

Mullen, M. (2011). Special Inspections of Paved Areas during Excessive Heat Periods. *Central Region Airport Certification Bulletin*, Federal Aviation Administration, Central Region, Airports Division, Kansas City, MO.

Nagayama, T., and Spencer Jr, B. F. (2007*). Structural Health Monitoring Using Smart Sensors*. Technical Report No. NSEL-001, Newmark Structural Engineering Laboratory. University of Illinois at Urbana-Champaign, IL.

Nassiri, S. (2011). Establishing Permanent Curl/Warp Temperature Gradient in Jointed Plain Concrete Pavements. Dissertation, University of Pittsburgh, PA.

National Instruments. (2012). Five Factors to Consider When Implementing a Wireless Sensor Network (WSN). http://www.ni.com/white-paper/10789/en/ (Accessd in September 5, 2014).

Norris, A., Saafi, M., and Romine, P. (2008). Temperature and Moisture Monitoring in Concrete Structures Using Embedded Nanotechnology/Microelectromechanical Systems (MEMS) Sensors. *Construction and Building Materials*. 22(2), pp. 111-120.

Ong, J. B., You, Z., Mills-Beale, J., Tan, E. L., Pereles, B. D., and Ong, K. G. (2008). A Wireless, Passive Embedded Sensor for Real-Time Monitoring of Water Content In Civil Engineering Materials. *Sensors Journal,* IEEE, 8(12), pp. 2053-2058.

Oppenheim, I. J., Garrett, J. H., and Gabriel, K. J. (2000). Potential MEMS Applications in Civil Engineering. *Space 2000,* ASCE, pp. 495-501.

Park, S., Ahmad, S., Yun, C. B., and Roh, Y. (2006). Multiple Crack Detection of Concrete Structures Using Impedance-based Structural Health Monitoring Techniques. *Experimental Mechanics*. Vol. 46, pp. 609–618.

Pasko, T. J. (1998). Concrete Pavements-Past, Present, and Future. *Public Roads*, 62(1), pp. 7-15.

Phares, B. M., Wipf, T. J., Greimann, L. F., and Lee, Y. S. (2005). *Health Monitoring of Bridge Structures and Components Using Smart-Structure Technology*, Volume I. Technical Report No. 0092-04-14, Bridge Engineering Center, Center for Transportation Research and Education, Iowa State University, IA.

Pei, J. S., Ivey, R. A., Lin, H., Landrum, A. R., Sandburg, C. J., King, T., Zaman, M. M., Refal, H. H., Mal, E. C., Oshlake, O., Heriba, A., and Hurt, E. (2007). Monitoring Pavement Condition Using "Smart Dust" under Surge Time Synchronization. *Sensors and Smart Structures Technologies for Civil, Mechanical, and Aerospace Systems 2007, Proceedings of the SPIE*, Vol.6529, pp. 173–182.

Pei, J. S., Ivey, R. A., Lin, H., Landrum, A. R., Sandburg, C. J., Ferzli, N., and Mai, E. C. (2009). An Experimental Investigation of Applying Mica2 Motes in Pavement Condition Monitoring. *Journal of Intelligent Material Systems and Structures*. Vol.20, pp. 63-85.

Plankis, A., and Heyliger, P. (2013). *Off-Grid MEMS Sensors Configurations for Transportation Applications*. Technical Report No. MPC-13-257.

Potter, J. F., Mayhew, H. C., and Mayo, A. P. (1969). *Instrumentation of the full scale experiment on A1 trunk road at Conington, Huntingdonshire*. Rrl Report, Transport Research Laboratory (Road Research Laboratory), Wokingham, Berkshire, U.K.

Qi, G. Z., Xun, G., Qi, X. Z., Dong, W., and Chang, P. (2005). Local Measurement for Structural Health Monitoring. *Earthquake Engineering and Engineering Vibration*, 4(1), pp. 165-172.

Qin, Y. (2011). Numerical Study on the Curling and Warping of Hardened Rigid Pavement Slabs. Dissertation, Michigan technological University, MI.

Quinn, B., and Kelly, G. (2010). Feasibility of Embedded Wireless Sensors for Monitoring of Concrete Curing and Structural Health. *Processing of SPIE, Sensors and Smart Structures Technologies for Civil, Mechanical, and Aerospace Systems*, Vol.7647.

Read more: CoolTerm - Free Download and Software Reviews - CNET Download.com http://download.cnet.com/CoolTerm/3000-2383_4-10915882.html#ixzz2ueTEGqCd (Accessed March 3, 2014).

Rice, J. A., and Lloyd, J. (2014). *Optimization of A Pavement Instrumentation Plan for A Full-Scale Test Road: Evaluation*. Florida Department of Transportation, FL.

Roberts, C. M. (2006). Radio frequency identification (RFID*). Computers & Security*, 25(1), pp. 18-26.

Rollings, R. S., and Pittman, D. W. (1992). Field Instrumentation and Performance Monitoring of Rigid Pavements. *J. Transp. Eng.*, ASCE, 118(3), pp. 361-370.

Ruan, Q., Xu, W., and Wang, G. (2011). RFID and ZigBee Based Manufacturing Monitoring System. *Electric Information and Control Engineering (ICEICE), 2011 International Conference on*. IEEE. pp. 1672-1675.

Rufino, D., Roesler, J., and Barenberg, E. (2004). *Mechanistic Analysis of Pavement Responses from Denver International Airport*. FAA Center of Excellence (COE) for Airport Technology Report No.26, Department of Civil and Environmental Engineering, University of Illinois at Urbana-Champaign, IL.

Ruiz, J. M., Rasmussen, R. O., Chang, G. K., Dick, J. C., and Nelson, P. K. (2005). *Computer-Based Guidelines for Concrete Pavements, Volume II--Design and Construction Guidelines and HIPERPAV II User's Manual*. Technical Report No. FHWA-HRT-04-122, The Transtec Group, Inc., Austin, TX.

Saafi, M., and Romine, P. (2005). Preliminary Evaluation of MEMS Devices for Early Age Concrete Property Monitoring. *Cement and Concrete Research*, 35(11), pp. 2158-2164.

Saboonchi, H. and Ozevin, D. (2012). Numerical Simulation of Novel MEMS Strain Sensor for Structural Health Monitoring. *20th Analysis and Computation Specialty Conference*, ASCE, pp. 139-150.

Sackin, D., Garret, J., Gabriel, K., and Patton, M. (2000). MEMS for Civil Infrastructure: Smart Aggregate for Concrete. *Advanced Technology in Structural Engineering*, ASCE, pp. 1-8.

Salman, N., Rasool, I., and Kemp, A. H. (2010). Overview of the IEEE 802.15. 4 Standards Family for Low Rate Wireless Personal Area Networks. *Wireless Communication Systems (ISWCS), 7th International Symposium*, IEEE, pp. 701-705.

Sargand, S. M., and Khoury, I. S. (1999). Sensor Installation in Rigid Pavement. *Experimental Techniques*, 23(3), pp. 25-27.

Scott, S., Kovacs, A., Gupta, L., Katz, J., Sadeghi, F., and Peroulis, D. (2011). Wireless Temperature Microsensors Integrated on Bearings for Health Monitoring Applications. *Micro Electro Mechanical Systems (MEMS), 2011 IEEE 24th International Conference*. pp. 660-663.

Scott, S., Sadeghi, F., and Peroulis, D. (2012). Highly Reliable MEMS Temperature Sensors for 275 ˚C Applications-Part 1: Design and Technology. *Journal of Microelectromechanical Systems*, 22(1), pp. 225-235.

Sebaaly, P. E., Tabatabaee, N., Kulakowski, B., and Scullion, T. (1991). *Instrumentation for Flexible Pavements-Field Performance of Selected Sensors*. Technical Report No. FHWA-RD-91-094, Federal Highway Administration, Washington, DC.

Sebesta, S., Oh, J., Lee, S. I., Sanchez, M., and Taylor, R. (2013). *Initial Review of Rapid Moisture Measurement for Roadway Base and Subgrade*. Technical Report No. FHWA/TX-13/0-6676-1, Texas A&M Transportation Institute, TX.

Sensirion, Inc. (2014). Datasheet SHT7X Humidity and Temperature Sensor. http://www.sensirion.com/en/technology/humidity/ (Accessed in March 24, 2014).

Shen, K. Y. (2013). Wireless System for Sensors on US-30, Creative Component, Iowa State University, Ames, IA.

Sheridan, V., Tsegaye, B., and Echols, M. (2005). ZigBee-Enabled RFID Reader Network. Dissertation, Worcester Polytechnic Institute, MA.

SILICON LABS. Silicon Laboratories, Inc. *The Evolution of Wireless Sensor Networks.* http://www.silabs.com/Support%20Documents/TechnicalDocs/evolution-of-wireless-sensor-networks.pdf (Accessed in March 25, 2014a).

SILICON LABS. Silicon Laboratories, Inc. *Integrating Raw Die Can Enable Innovative Packaging Solutions for Embedded Systems.* http://www.silabs.com/support%20documents/technicaldocs/mcu-die-sales-enables-innovation.pdf (Accessed in September 23, 2014b).

Smith, D. (2012). Multisensor MEMS for Temperature, Relative humidity, and High-g Shock Monitoring. Thesis, Rochester Institute of Technology, NY.

Southwest Center for Microsystems Education (SCME). (2013). History of MEMS. http://scmenm.org/index.php?option=com_docman&task=cat_view&gid=63&Itemid=162. (Accessed Aug 22, 2014)

Sparkfun Electronics. CoolTerm (Windows, Mac, Linux) https://learn.sparkfun.com/tutorials/terminal-basics/coolterm-windows-mac-linux (Accessed in March 20, 2014).

Spencer, B. F., Ruiz-Sandoval, M. E., and Kurata, N. (2004). Smart Sensing Technology: Opportunities and Challenges. *Structural Control and Health Monitoring*, 11(4), pp. 349-368.

Sun, M., Staszewski, W. J., and Swamy, R. N. (2010). Smart Sensing Technologies for Structural Health Monitoring of Civil Engineering Structures. *Advances in Civil Engineering*, Vol.2010, pp. 13.

Texas Instruments. (2013). ZigBee Wireless Networking Overview. http://www.ti.com/lit/sg/slyb134d/slyb134d.pdf (Accessed in December 5, 2013).

Texas Instruments. (2014). TPL5000 Datasheet http://pdf1.alldatasheet.com/datasheet-pdf/view/530828/TI/TPL5000.html (Accessed in March 22, 2014).

Timm, D. H., Priest, A. L., and McEwen, T. V. (2004). *Design and Instrumentation of the Structural pavement Experiment at the NCAT Test Track*. NCAT Report 04-01, National Center for Asphalt Technology, Auburn University, AL.

Titi, H., Tabatabai, H., Sobolev, K., Crovetti, J., and Foley, C. (2012). *Feasibility Study for a Freeway Corridor Infrastructure Health Monitoring Instrumentation Testbed*. Technical Report No. CFIRE 04-08, National Center for Freight and Infrastructure Research and Education (CFIRE), University of Wisconsin-Madison, WI.

Tompkins, D., and Khazanovich, L. (2007). *MnROAD Lessons Learned*. Technical Report No. MN/RC-2007-06, Minnesota Department of Transportation, University of Minnesota, MN.

Tully, R. (2007). *The use of low cost "iButton" Temperature Logger Arrays to Generate High Spatial Resolution Tidal Inundation Regime Data*. Marine Resource Management, Oregon State University, OR.

Yousuf, M and Morton, T. (2014). *Use of Vehicle Noise for Roadways, Bridge, and Infrastructure Health Monitoring.* Technical Report No. FHWA-HRT-14-059, Workshop Summary Report, Woodward Communication, Inc.

Ubertini, F., Materazzi, A. L., D'Alessandro, A., and Laflamme, S. (2014). Natural Frequencies Identification of A Reinforced Concrete Beam Using Carbon Nanotube Cement-Based Sensors. *Engineering Structures*, Vol. 60, pp. 265-275.

Varadan, V. K., and Varadan, V. V. (2000). Microsensors, Microelectromechanical Systems (MEMS), and Eectronics for Smart Structures and Systems. *Smart Materials and Structures*, 9(6), pp. 953-972.

WAKE, Inc. (2010). The HARD TRACK System. http://www.wakeinc.com/hardtrack.html. (Accessed Oct 19, 2014)

Wang, C. Y., Wang, H. L., and Chen, M. H. (2006). Structural Health Monitoring Activities of Applying Optical Fiber Sensors in Taiwan. *International Workshop on Structural Health Monitoring and Damage Assessment*, National Chung Hsing University, Taichung, Taiwan, ROC.

Wang, L., Bos, A., Van Weelden, T., and Boschman, F. (2010). The Next Generation Advanced MEMS & Sensor Packaging. *In Electronic Packaging Technology & High Density Packaging (ICEPT-HDP), 2010 11th International Conference*, IEEE, pp. 55-60.

Wang, X. T. (2013). Study of Sensor Network Applications in Building Construction. Thesis, Kungliga Tekniska Högskolan Royal Institute of Technology, Sweden.

Watters, D. G., Jayaweera, P., Bahr, A. J., Huestis, D. L., Priyantha, N., Meline, R., and Parks, D. (2003). Smart Pebble: Wireless Sensors for Structural Health Monitoring of Bridge Decks. *Processing of SPIE, Smart Structures and Materials, Mechanical 2003: Smart Systems and Nondestructive Evaluation for Civil Infrastructures*, Vol.5057.

Weinmann, T. L., Lewis, A. E., and Tayabji, S. D. (2004). Pavement Sensors Used at Accelerated Pavement Test Facilities. *In Proceedings of the Second International Conference on Accelerated Pavement Testing*.

Wells, S. A. (2005). Early Age Response of Jointed Plain Concrete Pavements to Environmental Loads. Thesis, University of Pittsburgh, PA.

Wong, K. (2004). Instrumentation and Health Monitoring of Cable-supported Bridges. *Struct. Control Health Monit*, 11(2), pp. 91-124.

Wu, N. C., Nystrom, M. A., Lin, T. R., and Yu, H. C. (2006). Challenges to Global RFID Adoption. *Technovation*, 26(12), pp. 1317-1323.

Varaiya, P. P. (2008). *A Low Cost Wireless MEMS System for Measuring Dynamic Pavement Loads*. California PATH Program, Institute of Transportation Studies, University of California at Berkeley, CA.

Xue, W., Wang, L., Wang, D., and Druta, C. (2013). Pavement Health Monitoring System Based on an Embedded Sensing Network. *Journal of Materials in Civil Engineering*, ASCE, 26(10).

Ye, D., Mukhopadhyay, A. K., and Zollinger, D. G. (2009). *Laboratory and Field Evaluation of Concrete Paving Curing Effectiveness*. Technical Report No. FHWA/TX-10/0-5106-3, Texas Transportation Institute, Texas A&M University System, TX.

Ye, D., Zollinger, D., Choi, S., and Won, M. (2006). *Literature Review of Curing in Portland Cement Concrete Pavement*. FHWA Publication No. FHWA/TX06/0-5106-1, pp. 8-13, Center for Transportation Research, the University of Texas at Austin, TX.

Yildiz, F. (2009). Potential Ambient Energy-Harvesting Sources and Techniques. *The Journal of Technology Studies*, 35(1). http://scholar.lib.vt.edu/ejournals/JOTS/v35/v35n1/yildiz.html (Assessed Oct 5, 2014).

Zhao, F., and Guibas, L. J. (2004). *Wireless Sensor Networks: An Information Processing Approach*. Morgan Kaufmann Publishers Inc., San Francisco, CA.

Zhu, X., Mukhopadhyay, S. K., and Kurata, H. (2012). A Review of RFID Technology and Its Managerial Applications in Different Industries. *Journal of Engineering and Technology Management*, 29(1), pp. 152-167.

Zinck, C. (2013). MEMS & Sensors Packaging Evolution (Power Point Slide). http://www.semi.org/eu/sites/semi.org/files/docs/ASE%20MEMS%20packaging%20-%20SEMI%202013%20C%20Zinck%20final%20new2.pdf (Access Oct 6, 2013).

APPENDIX A: PUBLICATIONS COMING OUT FROM MASTER STUDY

This appendix displays the two conference papers published from master study.

Development of a Wireless Communication System for Concrete Pavement Health Monitoring

by

Shuo Yang, Graduate Research Assistant
Phone: +1-(515) 708-0562, Fax: +1-(515) 294-8216, E-mail: shuoy@iastate.edu
Department of Civil, Construction & Environmental Engineering
24 Town Engineering Building

Keyan Shen, Graduate Research Assistant
Phone: +1-(515) 708-8832, Fax: +1-(515) 294-8432, E-mail: kshenyy@gmail.com
Department of Electrical and Computer Engineering

Dr. Halil Ceylan – Associate Professor
(Corresponding Author)
Phone: +1-(515) 294-8051, Fax: +1-(515) 294-8216, E-mail: hceylan@iastate.edu
Department of Civil, Construction & Environmental Engineering
406 Town Engineering Building

Dr. Sunghwan Kim – Research Assistant Professor
Phone: +1-(515) 292-3475, Fax: +1-(515) 294-8216, E-mail: sunghwan@iastate.edu
Department of Civil, Construction & Environmental Engineering
24 Town Engineering Building

Dr. Daji Qiao, Associate Professor
Phone: +1-(515) 294-2390, Fax: +1-(515) 294-8432, E-mail: daji@iastate.edu
Department of Electrical and Computer Engineering
3214 Coover Hall

and

Dr. Kasthurirangan Gopalakrishnan – Senior Research Scientist
Phone: +1-(515) 294-3044, Fax: +1-(515) 294-8216, E-mail: rangan@iastate.edu
Department of Civil, Construction & Environmental Engineering
354 Town Engineering Building

Iowa State University of Science and Technology
Ames, Iowa 50011-3232
USA

Submitted for the 8th International DUT-Workshop on Research and Innovations for Design of Sustainable and Durable Concrete Pavements, to be held on September 20-21, 2014, in Prague, Czech Republic

June 201

Development of a Wireless Communication System for Concrete Pavement Health Monitoring

Shuo Yang[1], Keyan Shen[2], Daji Qiao[3], Halil Ceylan[4], Sunghwan Kim[5] and Kasthurirangan Gopalakrishnan[6]
Iowa State University, Ames, Iowa, USA

ABSTRACT: In recent years, structural health monitoring and management (SHM) has become a popular approach and is considered essential for achieving well-performing, long-lasting, sustainable transportation infrastructure systems. Key requirements in ideal SHM of road infrastructure include long-term, continuous, and real-time monitoring of pavement behaviors under various pavement geometry-materials-loading configurations and environmental conditions. With advancements in wireless technologies, integration of wireless communications into sensing device is considered an alternate and superior solution to existing time- and labor-intensive wired sensor systems to meet these requirements. This study explored the development and deployment of a wireless communications sub-system into a commercial off-the-shelf concrete pavement monitoring sensor system. The overall goal was to investigate the feasibility of developing wireless based Micro-Electromechanical Sensors and Systems (MEMS) by integrating a wireless network system with off-the-shelf MEMS sensors. A success rate test was performed after the wireless transmission system was buried in the concrete, and the test results indicated that the system was able to provide reliable communications at a distance of more than 46 m (150 ft.). This will be a useful feature for highway engineers performing routine pavement scans from the shoulder without the need for traffic control or road closure.

KEY WORDS: Pavement, wireless, temperature, humidity, concrete, MEMS

1. INTRODUCTION

Like many advanced technologies, wireless sensor technologies were initially developed and deployed for military and industrial purposes. In recent years, these kinds of technologies are extensively applied in civil engineering infrastructure to measure the material and geometric properties changes for serviceability assessment, which is referred to as structural health monitoring (SHM). Over past decades, SHM has been widely used in civil engineering infrastructure to monitor structural integrity failures such as cracks, concrete deterioration, and steel corrosion. An early warning could avoid unnecessary costs to the maintenance programs. Moreover, continuously measured data can contribute to improved modeling and analytics resulting in prolonged system service life and reduced life cycle costs (Buenfeld et al., 2008; Mccarter et al., 2004). Wired sensor systems are widely used in traditional SHM to detect structural damage. However, the use of wired sensors can be very time-consuming and costly if a large number of sensors have to be installed to improve quality of measured

data in SHM. Furthermore, in cases where wires are buried in concrete, wires may be corroded or damaged. Due to these drawbacks, the use of wireless technologies is considered a promising substitute to provide better functionality at a lower price especially when a higher spatial density of sensors is desired (Kim et al., 2007). In addition, Micro-Electromechanical Sensors and Systems (MEMS) technology has been investigated for SHM since MEMS make it possible for systems of all kinds to be smaller, faster, more energy-efficient and less expensive (Ceylan et al., 2011).

Numerous studies have been conducted to apply wireless sensor technologies in bridge system SHM (Maser et al., 1996; Lynch and Loh, 2006). However, only few recent studies have investigated these technologies in pavement system SHM applications. For instance, Lajnef et al. (2013) focused on development of a wireless strain sensing system for asphalt pavement SHM to detect fatigue damage. The sensor system developed in this study contained a low-power consumption wireless integrated circuit sensor interfaced with a piezoelectric transducer. This piezoelectric ceramic transducer was designed with an array of ultra-low power floating gate (FG) computational circuits and it could generate power to supply FG analog processor in the sensor under stress. Each sensor node could store the data and then periodically transmit them to Radio frequency (RF) reader mounted on a moving vehicle.

The objective of this study was to investigate the feasibility of developing a wireless based MEMS for concrete pavement SHM. A wireless network system was integrated with an off-the-shelf MEMS sensor which was originally designed for wired data acquisition. The field performance of commercial wired MEMS sensors was evaluated in a newly constructed concrete pavement under actual traffic load and weather conditions to identify the system requirements for development of the wireless MEMS sensor system. A preliminary design of prototype wireless system with robust packaging was developed to improve the survivability of MEMS sensors. The wireless system utilized XBee-PRO modulus interfaced with Arduino boards to build the transmission system based on ZigBee protocol. The detailed procedure and findings pertaining to the development of wireless based MEMS are discussed.

2. EVALUATION OF COMMERCIAL OFF-THE-SHELF WIRED MEMS SENSORS

2.1. Description of evaluated sensor

Temperature and moisture content are significant factors in the hydration process between cementitious materials and water, which in turn influence early-age concrete properties. Anomalies in the hydration process may result in insufficient strength and durability since the development of early concrete strength mainly depends on the moisture diffusion and hydration temperature (Ye, et al., 2006). Furthermore, concrete pavement can be subjected to deformation due to different temperature and moisture gradients throughout the concrete, commonly referred to as curling (temperature) and warping (moisture/humidity) behaviors. This, when combined with heavy traffic loading, could lead to cracking of slabs. Considering the significant impact of temperature and moisture gradients within the concrete slab on the overall slab behavior and performance, these two properties were selected for sensor-based measurement and health monitoring investigations.

The Sensirion SHT71 digital humidity sensor, classified as a commercial off-the-shelf MEMS device that can simultaneously measure Relative Humidity (RH) as well as temperature, was evaluated in this study. Note that moisture content measured inside concrete is typically expressed as RH which refers to the ratio of moisture content of air compared to saturated moisture level at the same temperature and pressure (Ye et al., 2006).

The commercial MEMS digital humidity sensor integrates sensor elements coupled with signal processing circuitry on a silicon chip by MEMS technology to provide a fully calibrated digital output. A unique capacitive sensor element consisting of paired conductors is built out of the capacitor of MEMS sensor to capture humidity while another band-gap sensor measures temperature. These conductors are separated by a polymer dielectric that can absorb or release water proportional to the relative environmental humidity, and thus can change the capacitance of the capacitor (Sensirion, Inc., 2014). An electronic circuit calculates RH by measuring the capacitance difference. Additionally, the capacitance for the chip of this MEMS sensor is formed by a "micro-machined" finger electrode system with different protective and polymer cover layers, which can simultaneously protect the sensor from interference as well. However, in order to continuously monitor and store measurement data, MEMS sensors have to be connected with a data reader of evaluation kit EK-H4 (see Figure 1) and a computer which require power (battery) supply all the time.

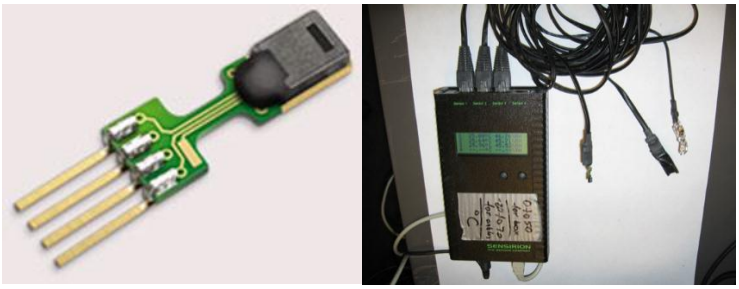

Figure 1: Sensirion SHT71 sensor (left) and evaluation kit EK-H4 (right)

2.2. Field instrumentation and results

A set of four wired commercial MEMS RH/Temperature (RH/T) sensors were instrumented in a newly constructed jointed plain concrete pavement (JPCP) in a US-30 highway section near Ames, Iowa, USA. The instrumented JPCP, constructed at 8:00 am on May 24, 2013, consists of 254 mm (10 in.) thick concrete slab with approximately 6 m (20 ft.) transverse joints spacing. The passing lane and travel lane widths for this JPCP are 3.7 m (12 ft.) and 4.3 m (14 ft.), respectively. A 152-mm (6 in.) thick Hot-Mix Asphalt (HMA) shoulder was constructed approximately 28 days after concrete paving. A set of wireless temperature sensors and longitudinal strain gages were installed in the same section along with the commercial MEMS RH/T sensors for another series of investigations, which is not the focus of this study.

Before the paving of concrete took place, the RH/T sensors were tied on to short wood sticks installed on top of the base course. As seen in Figure 2, all the cables/wires from the sensors were tied together and then placed in a polyvinyl chloride (PVC) pipe buried underground to protect them from damage during concrete paving operations. The cables in

the PVC pipe were connected to a Data Acquisition System (DAS) equipment (laptop, data logger, evaluation kit, and batteries) in a plastic shield box placed near the drainage ditch away from the HMA shoulder (See Figure 3). The installation of these wired sensors required great care, was time consuming and labor-intensive.

Figure 2: Sensor instrumentation on US-30 highway section

Figure 3: Data acquisition system

Figure 4 illustrates measured temperature and RH profiles captured by wired MEMS RH/T sensors one month after concrete paving. This figure shows measurements from MEMS RH/T sensor No. 3 (installed at 51 mm (2 in.) below pavement surface and 711 mm (28 in.) away from shoulder) and MEMS RH/T sensor No. 4 (installed at 2.5 mm (0.1 in.) below pavement surface and 203 mm (8 in.) away from shoulder). Among the four sensors installed before paving, two sensors (No. 3 and No. 4) remained functional in measuring temperature inside concrete while one sensor (No. 4) measured only RH of concrete.

The other two sensors, No. 1 and No. 2 (installed at 216 mm (8.5 in.) and 140 mm (5.5 in.) below pavement surface and 711 mm (28 in.) away from shoulder) malfunctioned several hours after concrete paving operations. This could probably be attributed to damages incurred to the wires/cables from concrete paver and vibrator operations. The sensor itself could also have been damaged because of the high alkali environment prevailing during concrete hydration. Data could not be acquired from May 26 to 28, 2013 since the battery (power supply) for the DAS was not recharged. These practical constraints and limitations of

wired sensor systems with respect to continuous monitoring and storage of measured data highlight the need for a self-powered, wireless sensor system.

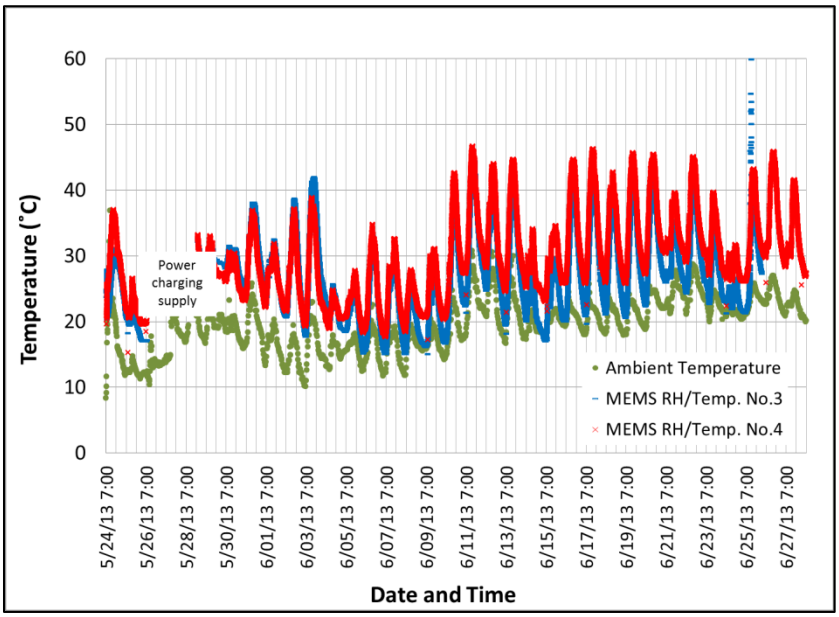

(a)

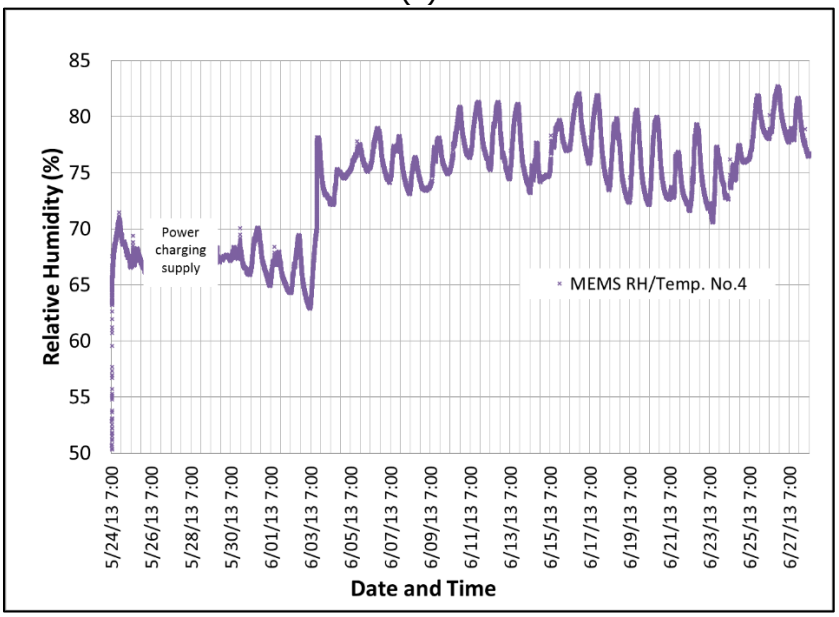

(b)

Figure 4: Commercial off-the-shelf wired MEMS RH/Temperature sensor measurements: (a) Temperature profile, (b) RH profile

2.3. Lessons learned from field evaluation

The on-site experiences from US-30 highway sensor installation and monitoring and the identified limitations of wired sensor systems proved to be resources in identifying the system requirements in the development of wireless MEMS sensor systems. These

limitations include time consuming and labor intensive installation process, poor sensor survivability caused by cable damage, and complicated sensor packaging required to protect sensor from high alkali environment during concrete hydration.

Critical factors to be considered in wireless MEMS sensor systems include hardware architecture, packaging, embedded software, wireless signal strength, and low-power consumption under on-site conditions. Considering these critical factors, a preliminary wireless system with a robust packaging for MEMS sensors was developed. This is discussed in the following sections.

3. DEVELOPMENT OF WIRELESS COMMUNICATIONS SYSTEM

3.1. Overview of wireless system

The wireless system presented in this study was a preliminary design mainly focusing on the wireless transmission function. The wireless system could be divided into two parts: wireless transmission end and wireless receiving end. The wireless transmission end is used to transfer data from MEMS sensors into wireless transmission devices. The wireless receiving end connected with computer is used to download data without the need for a wire. Microcontrollers and XBee-PRO modules are required for the transmission and receiving ends to communicate with each other.

3.2. Wireless network protocol

ZigBee is selected as the wireless networking protocol. It can be used to construct a decentralized self-healing wireless mesh network. In this mesh network, nodes can find a new route when the original route fails (Texas Instruments, 2013). Besides ZigBee, there are also other wireless technologies such as Bluetooth, Wi-Fi, and cellular. However, ZigBee is more energy-efficient, cost-effective, and easy to work with than these other technologies as shown in Table 1. Table 1 compares different wireless technologies by evaluating their total scores, which are sums of weighted scores from all the factors. The weighted score of each factor is to multiply its weight by the score of specific wireless technology. A higher total score represents better wireless technology for this application.

Table 1. Comparison of wireless technologies (Al-Khatib et al., 2006)

Aspects		Score (0 to 10)			
Factors	***Weight***	*Bluetooth®*	*ZigBee®*	*Wifi®*	*Cellular*
Multi-node network support	**100**	5	10	10	10
Throughput	**60**	7	6	8	3
Data rate	**60**	7	6	10	10
Range	**50**	6	5	7	10
Ease of implementation	**50**	6	8	6	4
Power consumption	**-80**	6	2	8	6
Cost	**-100**	5	3	7	8
Total Score		460	910	390	200

3.3. Microcontrollers

Arduino board is a single-board microcontroller consisting of an Atmel AVR® 8-bit or 32-bit microcontroller which can be wirelessly programmed by the device utilizing ZigBee protocol (Atmel, 2014). In this study, Arduino Uno and Arduino Mega 2560, as shown in Figure 5, were used for the wireless transmission end and receiving end, respectively.

Arduino Uno is the microcontroller using processor ATmega328 which has 32 KB of flash memory, 2 KB of static random access memory (SRAM), and 1 KB of electrically erasable programmable read-only memory (EEPROM). It contains 14 digital input/output pins, 6 analog inputs, a 5 volt liner regulator, a 16 MHz ceramic resonator, a USB connection, a power jack, an In Circuit Serial Programming (ICSP) header, and a reset button on its board. As for Arduino Mega 2560, it is similar to Arduino Uno but it has an ATmega2560 processor with 54 digital input/output pins, 16 analog inputs, 4 hardware serial ports (UARTs), and a 16 MHz crystal oscillator. Moreover, the Arduino Mega 2560 is compatible with most shields designed for the Arduino Duemilanove or Diecimila and it has 256 KB of flash memory, 8 KB of SRAM and 4 KB of EEPROM for storing code and data. These two microcontrollers were selected due to their high reliability and low cost. Arduino 1.0.4 (open-source software) can be used for program coding to control both Arduino Uno and Arduino Mega 2560 such as setting up time interval, changing the format of exported data, and etc.

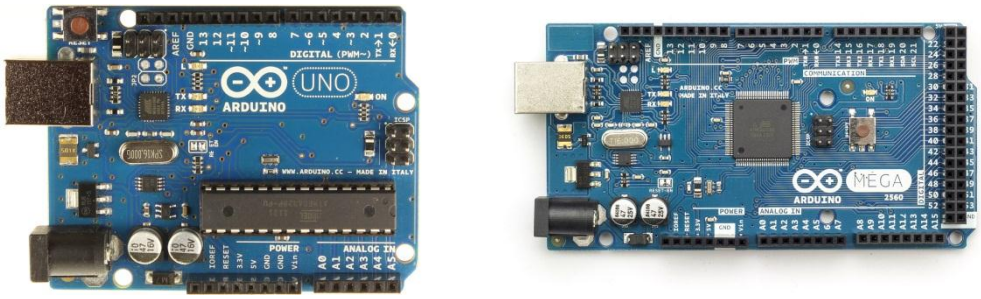

Figure 5: Arduino Uno for wireless transmission end (left) and Arduino Mega 2560 for wireless receiving end (right)

3.4. XBee-PRO modulus

XBee-PRO RF modulus (series 1) as shown in Figure 6 is a wireless device, which can offer low cost wireless connectivity in ZigBee mesh networks. It's reliable in point-to-point, multipoint wireless transmission and it is designed to meet the IEEE 802.15.4 standard. Furthermore, XBee-PRO modulus also has an easy set up process and the software used to program is called X-CTU, which adjusts its frequency, signal strength, energy consumption, and so on. Additionally, an XBee Explorer Regulated board can be used to help it regulate the voltage input.

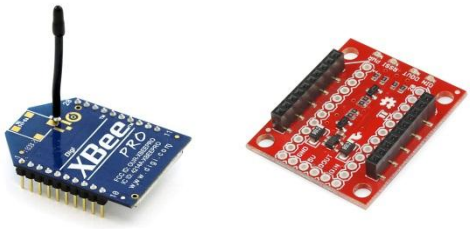

Figure 6: XBee-PRO (left) and XBee Explorer Regulated (right)

3.5. Wireless transmission

The wireless transmission end as shown in Figure 7 consists of a MEMS sensor (SHT71 digital humidity and temperature sensor), an XBee-PRO modulus, an XBee Explorer Regulated, an Arduino Uno microcontroller, and 12×1.5V AA batteries. Among these devices, XBee Explorer Regulated is a board that can be pinned on XBee-PRO to help it regulate the voltage input. In the wireless transmission end, both the SHT71 sensor and XBee-PRO with XBee Explorer Regulated were pinned on the digital port and power port on Arduino Uno board. Meanwhile, twelve 1.5V AA batteries were placed in a plastic holder connected with the microcontroller to power the entire wireless transmission end through the voltage output pin on the board. Furthermore, because the entire wireless transmission end will be buried in concrete, a robust packaging framework is needed for the wireless transmission system which will be discussed later.

Figure 7: Wireless transmission end without batteries

3.6. Wireless reception

The wireless receiving end, as shown in Figure 8, consists of an XBee-PRO modulus, an XBee Explorer Regulated, and an Arduino Mega 2560 microcontroller. The XBee Explorer Regulated here plays the same role as it was used in the wireless transmission end. However, there were no batteries on the Arduino Mega 2560 because it was powered by computer through a USB cable. The XBee-PRO on the Arduino Mega 2560 was paired with the other XBee-PRO on the Arduino Uno in the wireless transmission end to receive the

transmitted data. After that, the data will be stored in a data-storage module with 4096 bytes non-volatile memory on the Arduino Mega 2560.

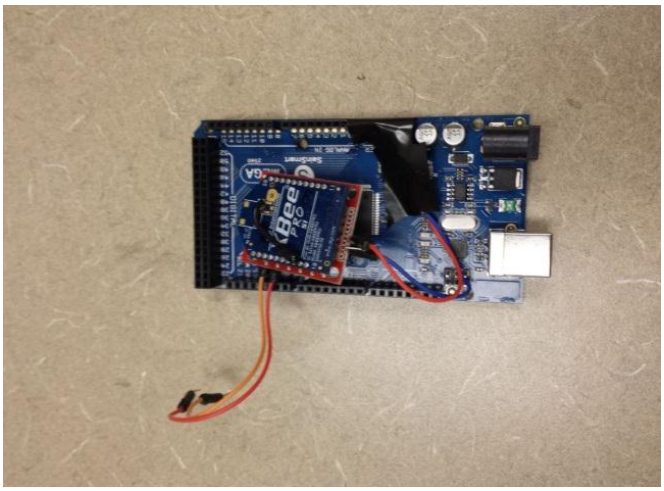

Figure 8: Wireless receiving end

3.7. Packaging

Robust packaging is required to protect both the sensor and wireless transmission devices such as XBee-PRO modulus and microcontroller to make sure they can work properly inside the concrete. The functions of the packaging include protecting the wireless transmission end during the sensor installation and pavement construction process, protecting the sensor from alkali-cement hydration reaction, and protecting the wireless transmission end under harsh climate and traffic conditions.

Two kinds of in-house packaging were designed to protect the sensor, microcontroller and XBee-PRO modulus, respectively. For the MEMS sensor, a piece of adhesive tape, a protection filter cap, and steel wool were used to make the protective package to prevent direct contact between the raw sensor and fresh concrete. In this packaging, a filter cap was placed on the top of the MEMS sensor using adhesive tape. Steel wool was used to attach the sensor. As for the microcontroller and XBee-PRO modulus, a small box with the bottom open, consisting of 12 mm thick wood board and a wood board nailed with a 180 mm long sharp-edged wood stick, was prepared. A hole was drilled on the board nailed with the stick to allow the cable from the sensor to go through to connect the Arduino Uno microcontroller. The size of the box was 160 mm × 105 mm × 88 mm (6.3″×4.1″×3.5″) which was sufficient to place the entire wireless transmission system, as shown in Figure 10. Silicon glue and adhesive tape were used as well to seal the small gap in the box.

Figure 9: MEMS sensor with packaging

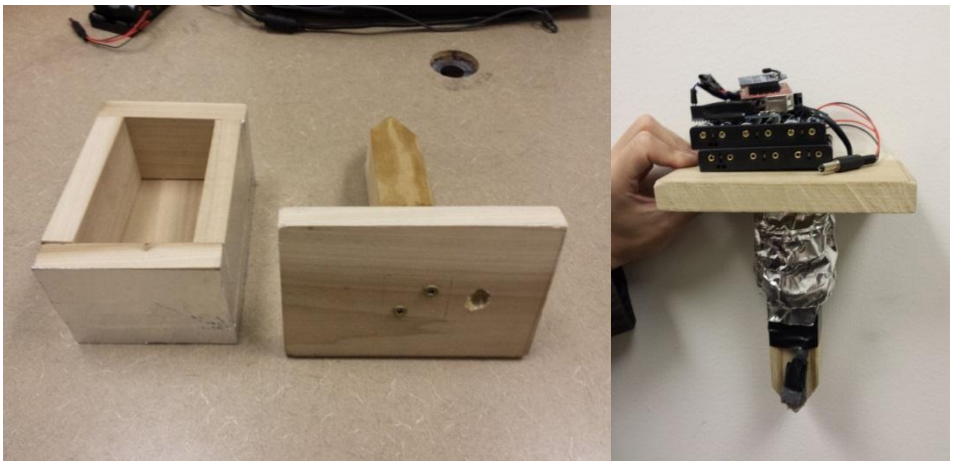

Figure 10: Packaging for wireless transmission end

4. EVALUATION OF DEVELOPED WIRELESS COMMUNICATION SYSTEM

4.1. Working principle of developed wireless system

The data exchange principle of this wireless system is based on ZigBee protocol. This system does not require any external cables. When the system is turned on, the MEMS sensor will sense temperature and RH and then transfer data to XBee-PRO through Arduino Uno microcontroller. Then XBee-PRO in wireless transmission end will transmit data to the paired XBee-PRO in wireless receiving end through antenna. The data captured in wireless receiving end will be stored in Arduino Mega 2560. Thereby, the wireless receiving end with a computer must be placed nearby to receive the data packets because only the Arduino Mega 2560 microcontroller is used to store data in this wireless system. At last, the data can be downloaded to the computer through a software, referred to as "CoolTerm". CoolTerm is a simple freeware serial port terminal application without terminal emulation which allows data exchange with hardware connected to serial ports (Sparkfun Electronics, 2014). The output data exported from the system are temperature, relative humidity, and dew point.

4.2. Comparison between wired MEMS system and wireless MEMS system developed

Figure 11 provides an overall system-level comparison between wired MEMS system and wireless MEMS system developed. In the wired MEMS system, the sensor should be connected to the data reader and the computer through cables to continuously monitor the concrete properties and download the data. As a consequence, both the data reader and the computer require electrical supply for operations. However, the developed wireless system does not require any external cables which can save installation time and reduce the risk of malfunction of sensors.

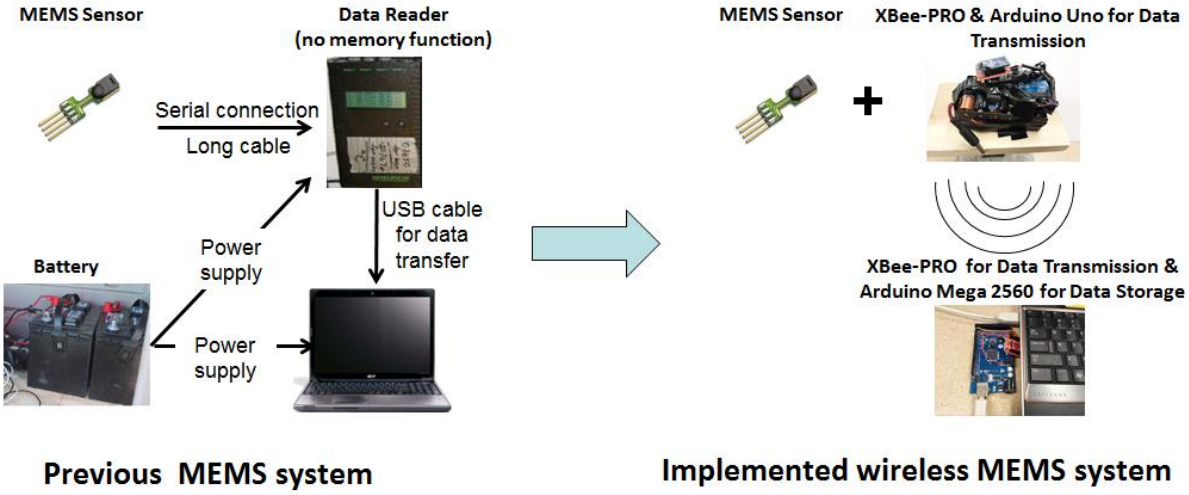

Figure 11: Comparison between pervious MEMS system and implemented wireless system

4.3. Evaluation of wireless communication capacity

To test the reliability and survivability of the wireless communication system inside the concrete, both wireless ends were embedded in the concrete as shown in Figure 12 to conduct a success rate test. Success rate means the success rate of data transmitted from transmission end that can be received by the receiving end. The higher the rate is, the more reliable the system will be.

Figure 12: Wireless MEMS system inside concrete

The success rate test was conducted for wireless MEMS system inside concrete buried underground by increasing horizontal and vertical distances between wireless transmission and receiving ends (See Fig 13).

(a) (b)

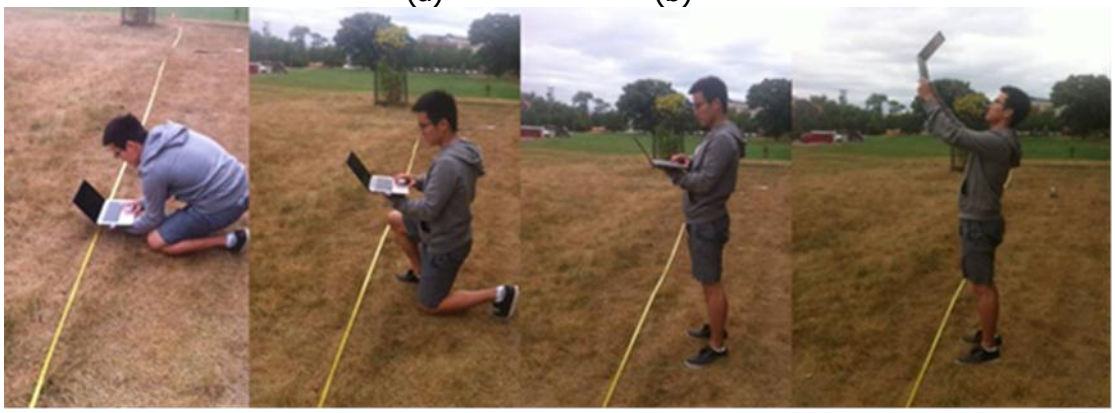

(c)

Figure 13: Success rate test: (a) wireless MEMS system inside concrete buried underground, (b) measuring horizontal distance, (c) four positions to measure vertical distance

The temperature and RH measurements acquired by the wireless sensor system during the success rate test are presented in Figures 14 and 15. The implemented wireless communication system was able to transmit temperature and RH measurement when the receiver was positioned approximately 46m away from transmission end with an almost 100% success rate. Furthermore, it was also found that the success rate increased as the vertical distance decreased.

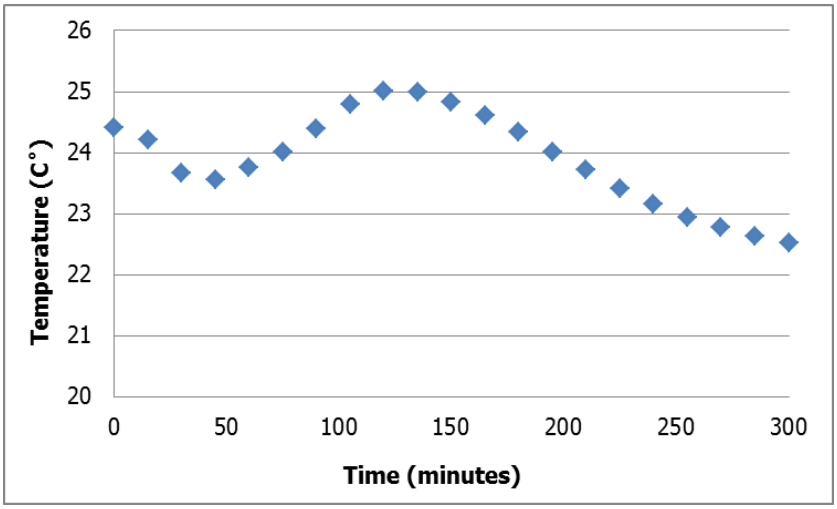

Figure 14: Temperature measurement

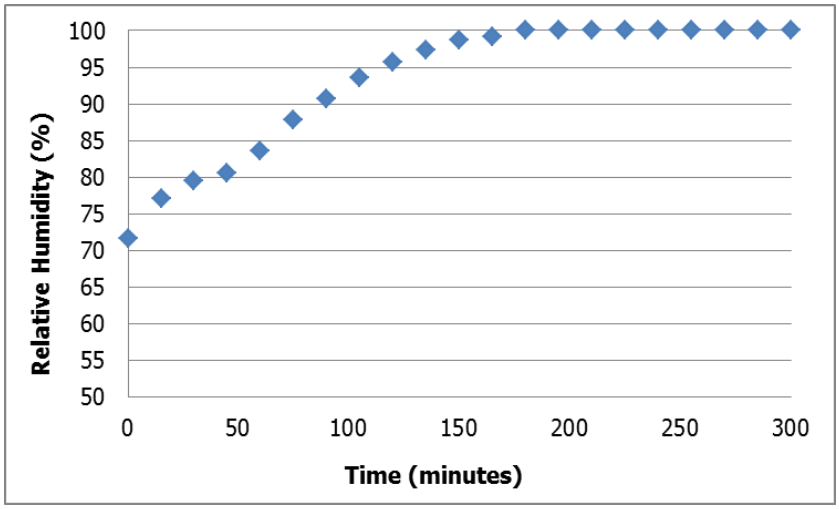

Figure 15: Relative humidity measurement

5. SUMMARY

The objective of this study is to investigate the feasibility of developing wireless based MEMS for concrete pavement structural health monitoring. The system requirements in the development of wireless MEMS system were identified from field experiences from US-30 highway wired MEMS system installation and monitoring. In the development, a wireless communication system was integrated with off-the-shelf MEMS sensors that were originally designed to be wired. The wireless MEMS system developed was capable of providing reliable temperature and RH measurement data over more than approximately 46m (150 ft.) from the receiver when it was embedded inside concrete. However, the entire system was still energy consuming under current limited energy source. At a reasonable data sampling rate, it can just work for few days with twelve 1.5AA batteries. Also, the lifetime of batteries could easily be impaired by the harsh environmental factors like high temperature during concrete hydration. Both extremes of temperature and humidity magnitudes can reduce the

lifetime and capacitance of the batteries. Furthermore, future research should focus on improving the memory capacity and making the whole system smaller.

Some recommendations to resolve the aforementioned issues are:

- A power management circuit called Texas Instruments Debuts TPL5000 power timer can be used to control power output of battery, which can extend the current working time to approximately several years in ideal conditions.
- A micro-SD card or QuadRam Shield can be added on the microcontroller to tremendously increase the memory size.
- A smaller microcontroller called Arduino Fio with XBee plug as shown in Figure 16 can be used to replace the original microcontroller to reduce the overall system size.

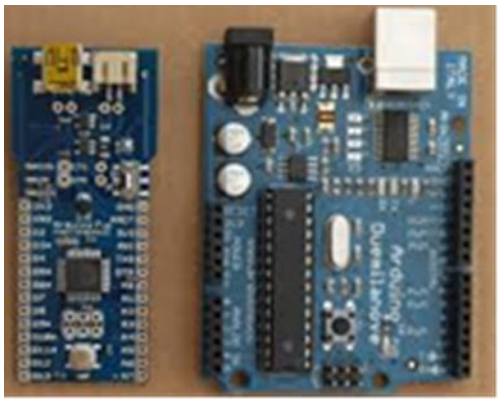

Figure 16: Comparison between Arduino Fio (left) and Arduino Uno (right)

6. REFERENCE

Al-Khatib, Z., Yu, J. M., Al-Khakani, H. G., and Kombarji, S. 2009. *A Wireless Multivariable Control Scheme for A Quadrotor Hovering Robotic Platform Using IEEE® 802.15.4*. Concordia University, Canada

ARDUINO. 2014. Products
http://arduino.cc/en/Main/Products#.UxTTlfm9l8E (Accessed in March 29, 2014)

Atmel. 2014. Atmel AVR 8-bit and 32-bit Microcontrollers
http://www.atmel.com/products/microcontrollers/avr/ (Accessed in March 29, 2014)

Barroca, N., Borges, L. M., Velez, F. J., Monteriro, F., Gorski, M., and Castro-Gomes, J. 2013. *Wireless Sensor Networks for Temperature and Humidity Monitoring within Concrete Structures*. Construction and Building Materials Vol.40, pp. 1156–1166.

Bennett, R., Hayes-Gill, B., Crowe, J. A., Armitage, R., Rodgers, D., and Hendroff, A. 1999. *Wireless Monitoring of Highways*. Smart Systems for Bridges, Structures, and Highways, Newport Beach, CA, March 1–2, Proceedings of the SPIE, Vol.3671, pp. 173–182.

Buenfeld, N., Davis, R., Karmini, A., and Gilbertson, A. 2008. *Intelligent Monitoring of Concrete Structures*. CIRIA, pp. 150, UK.

Cepero, E. D. 2013. *Structural Health Monitoring Inside Concrete and Grout Using the Wireless Identification and Sensing Platform (WISP)*. Dissertation, Florida International University, FL.

Ceylan, H., Gopalakrishnan, K., Taylor, P., Shrotriya, P., Kim, S., Prokudin, M., Wang, S. Y., Buss, A. F., and Zhang J. K. 2011. *A Feasibility Study on Embedded Micro-Electromechanical Sensors and Systems (MEMS) for Monitoring Highway Structures*. Iowa Highway Research Board Publication No. IHRB Project TR-575, Iowa State University, Ames, IA.

Cho, S., Yun, C. B., Lynch, J. P., Zimmerman, A. T., Spencer Jr, B. F., and Nagayama, T. 2008. *Smart Wireless Sensor Technology for Structural Health Monitoring of Civil Structures*. International Journal of Steel Structures, 8(4), pp. 267-275.

Choi, S. and Won, M. 2008. *Literature Review of Curing in Portland Cement Concrete Pavement*. FHWA Publication No. FHWA/TX-09/0-5106-2, pp. 21-30, Center for Transportation Research, the University of Texas at Austin.

DIgI. 2014. ZigBee Wireless Standards
https://www.digi.com/technology/rf-articles/wireless-zigbee (Accessed in March 25, 2014)

Every, E. V., Faridazar, F., and Deyhim, A. 2009. *Embedded sensors for life-time monitoring of concrete*. 4th International Conference on Structural Health Monitoring on Intelligent Infrastructure (SHMII-4), 22-24 July 2009, Zurich, Switzerland.

IDENTEC SOLUTIONS. 2008. *Technology rises with New York skyline*. Press Release. March 2008.
http://www.wakeinc.com/PDF/FreedomTowerRelease.pdf (Accessed in March 27, 2014)

Jackson, T., Mansfield, K., Saafi, M., Colman, T., and Romine, P. 2008. *Measuring Soil Temperature and Moisture Using Wireless MEMS Sensors*. Cement and Concrete Research 35, pp. 2158-2164.

Kim, S. K., Pakzad, S., Culler, D., Demmel, J., Fenves, G., Glaser, S., and Turon, M. 2007. *Health Monitoring of Civil Infrastructures Using Wireless Sensor Networks*. IPSN'07, pp254-263, Cambridge, Massachusetts, USA.

Lajnef, N., Chatti, K., Chakrabartty, S., Rhimi, M., and Sarkar, P. 2013. *Smart Pavement Monitoring System*. FHWA Publication No. FHWA-HRT-12-072, Michigan State University, MI.

Lajnef, N., Rhimi, M., Chatti, K., Mhamdi, L., and Faridazar, F. 2011. *Toward an Integrated Smart Sensing System and Data Interpretation Techniques for Pavement Fatigue Monitoring*. Computer-Aided Civil and Infrastructure Engineering, 26(7), pp. 513-523.

Lee, J. S., Su, Y. W., and Shen, C. C. 2007. *A comparative study of wireless protocols: Bluetooth, UWB, ZigBee, and Wi-Fi*. Industrial Electronics Society (IECON), 33rd Annual Conference of the IEEE, Nov. 5-8, Taipei, Taiwan.

Lewis, F. L. 2004. *Wireless Sensor Networks*. Smart Environments: Technologies, Protocols, and Applications, pp11-46.

Loh, K. J., Zimmerman, A. T., and Lynch, J. P., 2007. *Wireless Monitoring Techniques for Structural Health Monitoring*. In proceeding of the International Symposium of Applied Electromagnetics & Mechanics, Lansing, MI, September 9-12.

Lynch, J. P. 2002. *Decentralization of Wireless Monitoring and Control Technologies for Smart Civil Structures*. Technical Report No.140, John A. Blume Earthquake Engineering Center. Stanford, CA: Stanford University.

Lynch, J. P., 2007. *An Overview of Wireless Structural Health Monitoring for Civil Structures*. Phil. Trans. R. Soc. A 365, pp. 345-372.

Lynch, J. P., and Loh, K. J. 2006. *A Summary Review of Wireless Sensors and Sensor Networks for Structural Health Monitoring*. The Shock and Vibration Digest, Vol.38, No.2, pp. 91–128.

Lynch, J. P., Sundararajan, A., Law, K. H., Kiremidjian, A. S., and Carryer, E. 2003. *Power-efficient Wireless Structural Monitoring with Local Data Processing*. In proceedings of the International Conference on Structural Health Monitoring and Intelligent Infrastructure, Tokyo, Japan, November 13–15, Vol.1, pp. 331–338.

Maser, K., Egri, R., Lichtenstein, A., and Chase, S. 1996. *Field Evaluation of a Wireless Global Bridge Evaluation and Monitoring System*. In proceedings of the 11th Conference on Engineering Mechanics, Fort Lauderdale, FL, May 19–22, Vol.2, pp. 955–958.

Mccarter, W. and Vennesland, O. 2004. *Sensor Systems for Use in Reinforced Concrete Structures*. Construction and Building Materials, 18(6), pp. 351–358.

Norris, A., Saafi, M., and Romine, P. 2006. *Temperature and Moisture Monitoring in Concrete Structures Using Embedded Nanotechnology/microelectromechanical Systems (MEMS) Sensors*. Construction and Building Materials. 22(2), pp. 111-120.

Park, S., Ahmad, S., Yun, C. B., and Roh, Y. 2006. *Multiple Crack Detection of Concrete Structures Using Impedance-based Structural Health Monitoring Techniques*. Experimental Mechanics. 46, pp. 609–618.

Saafi, M., and Romine, P. 2005. *Preliminary Evaluation of MEMS Devices for Early Age Concrete Property Monitoring*. Cement and Concrete Research 35, pp. 2158-2164.

Sensirion, Inc. 2014. Datasheet SHT7X Humidity and Temperature Sensor. http://www.sensirion.com/en/technology/humidity/ (Accessed in March 24, 2014)

Shen, K. Y. 2013. *Wireless System for Sensors on US-30*, Creative Component, Iowa State University, Ames, IA.

SILICON LABS. Silicon Laboratories, Inc. *The Evolution of Wireless Sensor Networks* http://www.silabs.com/Support%20Documents/TechnicalDocs/evolution-of-wireless-sensor-networks.pdf (Accessed in March 25, 2014)

Sparkfun Electronics. CoolTerm (Windows, Mac, Linux) https://learn.sparkfun.com/tutorials/terminal-basics/coolterm-windows-mac-linux (Accessed in March 20, 2014)

Read more: CoolTerm - Free download and software reviews - CNET Download.com http://download.cnet.com/CoolTerm/3000-2383_4-10915882.html#ixzz2ueTEGqCd

Texas Instruments. 2013. ZigBee Wireless Networking Overview. http://www.ti.com/lit/sg/slyb134d/slyb134d.pdf (Accessed in December 5, 2013)

Texas Instruments. 2014. TPL5000 Datasheet http://pdf1.alldatasheet.com/datasheet-pdf/view/530828/TI/TPL5000.html (Accessed in March 22, 2014)

Wang, X. T. 2013. *Study of Sensor Network Applications in Building Construction*. Thesis, Kungliga Tekniska Högskolan Royal Institute of Technology, Sweden.

Wong, K. 2004. *Instrumentation and Health Monitoring of Cable-supported Bridges*. Struct. Control Health Monit. 11, pp. 91-124.

Ye, D., Zollinger, D., Choi, S., and Won, M. 2006. *Literature Review of Curing in Portland Cement Concrete Pavement*. FHWA Publication No. FHWA/TX06/0-5106-1, pp. 8-13, Center for Transportation Research, the University of Texas at Austin.

SMART AIRPORT PAVEMENT INSTRUMENTATION AND HEALTH MONITORING

By:
Shuo Yang, Graduate Student
24 Town Engineering Building
Department of Civil, Construction and Environmental Engineering
Iowa State University, Ames, IA 50011-3232
Phone: +1-515-294-4698, E-mail:

Halil Ceylan, Ph.D., Associate Professor
Director, Program for Sustainable Pavement Engineering and Research (PROSPER)
406 Town Engineering Building
Department of Civil, Construction and Environmental Engineering
Iowa State University, Ames, IA 50011-3232
Phone: +1-515-294-8051, E-mail: hceylan@iastate.edu

Kasthurirangan Gopalakrishnan, Ph.D., Senior Research Scientist
354 Town Engineering Building
Department of Civil, Construction and Environmental Engineering
Iowa State University, Ames, IA 50011-3232
Phone: +1-515-294-3044, E-mail: rangan@iastate.edu

Sunghwan Kim, Ph.D., P.E., Research Assistant Professor
24 Town Engineering Building
Department of Civil, Construction and Environmental Engineering
Iowa State University, Ames, IA 50011-3232
Phone: +1-515-294-4698, E-mail: sunghwan@iastate.edu

PRESENTED FOR THE
2014 FAA WORLDWIDE AIRPORT TECHNOLOGY TRANSFER CONFERENCE
Galloway, New Jersey, USA

August 2014

ABSTRACT

Realistic characterization of pavement layer properties and responses under in-situ field conditions is critical for accurate airport pavement life predictions, planning pavement management activities as well as for calibration and validation of mechanistic-based pavement response prediction models. The recent advancements in Micro-Electro-Mechanical Sensor (MEMS)/Nano-Electro-Mechanical Sensor (NEMS) technologies and wireless sensor networks combined with efficient energy scavenging paradigms provide opportunities for long-term, continuous, real-time response measurement and health monitoring of transportation infrastructure systems.

This paper presents a summary review of some recent studies that have focused on the development of advanced smart sensing and monitoring systems for highway pavement system with potential applications for long-term airport pavement health monitoring. Some examples of these potential applications include: the use of wireless Radio-Frequency Identification (RFID) tags for determining thermal gradients in pavement layers; self-powered MEMS/NEMS multifunction sensor system capable of real-time, remote monitoring of localized strain, temperature and moisture content in airport pavement that will eventually prevent catastrophic failures such as blow-ups on runways during heat waves.

INTRODUCTION

Airfield pavements are designed and constructed to provide adequate support for the various loads imposed by both aircrafts and environmental (climate) conditions such as temperature or moisture variations. In general, airfield pavements are fundamentally different from highway pavement in terms of the applied load properties. Typically, airfield pavement deals with higher load magnitude and tire pressure from airplanes, but fewer load repetitions compared to highway pavement. Although both airfield and highway pavements are prone to have deterioration from traffic and environment loads, airfield pavement usually predominately shows the environmental load related distresses rather than traffic load related ones [1].

For airport concrete pavement, one of the most common environmental related distresses is blowup [2], which is the disintegration of pavement due to axial compression force generated by slab expansion due to pavement temperature and moisture changes. It usually occurs at transverse joints or cracks in hot weather if their widths are not wide enough for concrete expansion. If pressure from concrete expansion in insufficient width cannot be relieved in time, it results in a localized upward movement of slab edges or shattering in the vicinity of the joint [3, 4, 5, and 6].

Blowup in the airport runway is very dangerous for aircraft operations and it needs immediate attention. Figure 1 presents a case of airport runway pavement blowup failure at Ankeny Regional Airport in Iowa in summer, 2011, which was reported in Central Region Airport Certification Bulletin [7]. Excessive hot weather and the associated heat wave reportedly caused the pavement blowup and buckling. As shown in Figure 2, a Raytheon Premier One jet hit the blowup spot during taking off and damaged its landing gear.

Figure 1. Blowup in Ankeny Regional Airport Runway (Photo courtesy of Snyder & Associates, Inc./Polk County Aviation Authority)

Figure 2. Damaged Aircraft in Ankeny Regional Airport Runway [7]

The other airport concrete pavement distress types caused by environmental (climate) loads in association with traffic loads include corner break, longitudinal, transverse, and diagonal cracks. These distresses can be aggravated by curling stresses induced by different thermal gradients between top and bottom parts of concrete slab.

Airport pavement distresses, when deemed detrimental to aircraft operations, can also lead to runway closure. For instance, a number of international flights in Tribhuvan International Airport in Kathmandu, Nepal were delayed, diverted and cancelled due to airport flexible pavement distress during August 2013 [8]. Figure 3 presents rutting and potholes occurring in the asphalt overlay of the runway. During the summer season of 2013, the asphalt overlay surface temperature went over 60 ˚C leading to rutting under repeated heavy aircraft loads. In the coming monsoon rain after summer season, water was accumulated on the rutting surface and then infiltrated inside the pavement through cracks. Potholes were developed from water in the underlying structure and aircraft wheel loads. As a consequence, this runway had to be closed. The impact of this event not only delivered a negative message to other countries but also caused a huge loss on their tourism business.

Figure 3. Airport Pavement Rutting (Left) and Potholes (Right) [8]

In addition to pavement distresses, the Foreign Object Debris (FOD) referred as a foreign substance or debris is considered to cause aircraft damage during its operation on airport runway [9]. Common FOD include aircraft parts, ground vehicle parts, stone, wild animals, garbage, and so on. Pavement deterioration including raveling and weathering, blowup, various cracks, corner break, popouts, and patching have significant potential to produce FOD as well [10, 11].

Pavement distresses and FOD are dangerous for aircraft operations. Once they occur on airport runways without any attention, the aircraft can be damaged during takeoff or landing and consequently the passengers inside the aircraft may be injured or lose their lives. The runway needs to be closed for repairing distresses removal of FOD. A closed runway signifies economic losses resulting from flight delays, cancellations, etc.

Pavement deterioration, as a major airport safety concern, can be controlled through in-situ pavement response and performance monitoring. In addition, realistic pavement responses from in-situ field conditions are critical for accurate airport pavement life predictions, management, calibration and validation of mechanistic-based pavement response prediction models. Real-time and continuous health monitoring and management of airport pavement systems have the potential to enable sustainable, smoother, and also safer airport infrastructure systems. This paper aims to review the state-of-the-art in smart airport pavement instrumentation and proposes a conceptual model of a smart airport pavement health monitoring system which includes MEMS-based sensors, a FOD detector, an intelligent data mapping model, as well as pavement distress and FOD warning systems.

HEALTH MONITORING OF AIRPORT PAVEMENT SYSTEMs

Needs of Airport Pavement Health Monitoring

Pavement deteriorations caused by aircraft loading, temperature, and moisture variations can be one of the major concerns in the safety of airport operations. Other pavement related safety concerns include the skid resistance (friction), FOD on pavement surface and the infiltration of water into the pavement sub-structure. Pavement health monitoring could be an effective solution to prevent the aircraft accidents and damages caused by poor pavement

performance and FOD. Pavement health monitoring is an extension of the structural health monitoring (SHM) concept which employs advanced technology to allow the assessment of the structural reliability and detection of structural changes in civil infrastructure, mainly of buildings and bridges.

In recent years, with advancement in sensor and wireless technologies, SHM demonstrates that it can be applied for pavement functional and structural assessments by monitoring pavement responses and environmental conditions (temperature, moisture, etc.) in real-time. An early warning of incipient problems enabling the in-time scheduling and planning of maintenance can be provided before the appearance of remarkable structural changes to minimize unnecessary costs.

In the end, the continuously measured data can be utilized to improve distress prediction models, which can help engineers prolong the structure service life to minimize life cycle costs and the current existing defects can be corrected as well. Hence, SHM employing smart sensor system is an effective way to improve the pavement safety and to reduce maintenance cost for airfield pavement.

How to Conduct Health Monitoring of Airport Pavement Systems?

Health monitoring of airport pavement system requires smart sensing technology which can provide long term, continuous and real time monitoring of pavement conditions. In order to achieve these goals, embedded sensor interfaced with advanced wireless sensor networks is a cost-effective solution.

MEMS Sensors

The recent advancement in Micro-Electromechanical Systems (MEMS)/ Nano-Electromechanical Systems (NEMS) technologies represent an emerging solution in health monitoring for transportation infrastructure system. MEMS/NMES sensor is generally comprised of miniaturized mechanical sensing element fabricated with silicon chip. The techniques of microfabrication enable different complex electromechanical systems to be integrated in the miniaturized mechanical sensing element. Therefore, the typical dimension of MEMS devices can vary from one micron to several millimeters [12]. In addition to small size, MEMS/NEMS sensor also has high performance with relatively low energy consumption. As a result, MEMS sensors have much potential in providing cost-effective health monitoring solutions to help engineers identify pavement deterioration before the distress is noticeable to the aircrafts.

Radio-Frequency Identification (RFID) tag is a MEMS-based sensor using the radio-frequency spectrum for digital data transmission. It can be an active or passive sensing device capable of both data receiving and storing. Various RFID tag types are available for different applications.

For pavement temperature monitoring purpose, some of the commercial RFID tags available include GT-301 by GENTAG, Inc, RFID chips by RF SAW, Inc, PaveTag RFID by Minds, Inc, i-Q32T tag by WAKE, Inc., etc. Among these, the i-Q32T RFID tag has the capability to detect the inside temperature of concrete and to communicate the information to the portable Pro [13]. The i-Q32T, as shown in Figure 4, contains an internal MEMS sensor for temperature monitoring that measures and logs the temperature in definable intervals. The collected data could be imported into the portable Pro, shown in Figure 5, wirelessly for maturity calculation and saving data for posterity. The use of two-way RF communication between the buried tag and a portable Pro enables the portable Pro to read and write data.

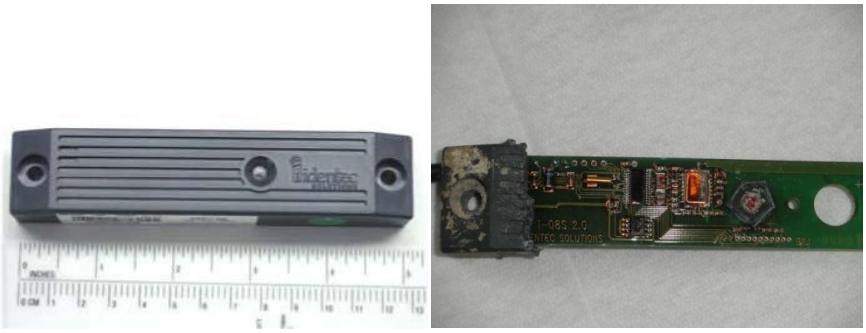

Figure 4. i-Q32T Wireless RFID Transponder (Photo courtesy of WAKE, Inc.)

Figure 5. HardTrack Portable Pro (Photo courtesy of WAKE, Inc.)

A MEMS based multifunction sensor system is currently being developed at Iowa State University (ISU) to design an integrated sensor system capable of measuring different properties such as temperature, moisture, and strain simultaneously. MEMS based multifunction sensor system can reduce installation cost and installation time which will otherwise be incurred by installation of large number of traditional single-function sensors to measure each of the properties. Moreover, if it could be integrated with a wireless transmission system, the MEMS based multifunction sensor system will not just save time and money but also improve the convenience and workability of health monitoring.

However, a truly integrated miniature multifunction sensor to detect these factors at same time is not commercially available because the device dimension and unit cost may be relatively large due to fabrication and assembling. Furthermore, it may also be more complex to implement a wireless transmission system for this kind of multifunction sensor compared to single-function sensor. Additionally, the energy consumption may be large because of measuring several parameters at the same time. One possible solution is to design an energy harvesting system by using piezoelectric materials, which can generate electric power subject to traffic loads, thunder vibrations, etc.

Wireless Networks

Traditional wired sensors generally cost more money than wireless sensors for health monitoring in civil infrastructures due to longer installation time. Furthermore, the damage and corrosion of wires in civil infrastructures is difficult to repair or replace as well. Wireless

sensor technologies based health monitoring has been investigated in civil infrastructures mainly focusing on building and bridges structures.

Typical, wireless technologies available for sensor systems include Bluetooth, cellular telephony, Wi-Fi, Zigbee, and radio frequency. These technologies have different data rate, range, power consumption, ease of implementation, cost, and so on. The use of different wireless technologies also leads to the use of different wireless network topologies including star, peer-to-peer, and two-tier network [14]. Hence, the choice of the appropriate wireless technologies and networks depends on the specific environment. A robust hardware architecture and packaging for wireless sensor is also required to make wireless sensor system functional under the high alkali environment from concrete hydration and repeated vehicle loads. In addition, the limited power sources of on-site conditions can affect the working life of the wireless sensors in concrete structure. Moreover, the effective distance range of sensors in concrete should be considered as well. Typically, the longer the distance, the more power consumption there will be. It is critical to select a balance point between these factors.

Electro-optical (EO) Sensing

A FOD detection system can help airport management to detect FOD which can pose a serious threat to the safety of airport operations. An Electro-optical (EO) sensing system has been proposed as a potential solution that can detect FOD by converting light ray into electronic signal. In 2009, Stratech Systems, Ltd., developed an electro-optical sensing system called as iFerret to evaluate runway condition of Chicago O'Hare International Airport (ORD). The performance of this electro-optical sensors system was assessed and reported by various studies [11, 15, and 16]. This iFerret is an optical video based sensors system consisting of high-quality image capture system. The high resolution video sensors with zoom capabilities in the passive sensing system were mounted in several towers to ensure it to sweep a large scan area continuously. Furthermore, the video sensor can scan the pavement surface almost up to 1,100-ft by using ambient lighting conditions [15]. All the sensors in the system interfaced with image-processing software are networked to the central console located in the air traffic control tower. The iFerret system detects the FOD by interpreting the data collected by the electro-optical sensors and then sends an alert to the operator if an FOD is detected. The location and video image of the FOD will be also sent to the operator to confirm. As a consequence, hazard assessment and clear-up work can be processed.

Figure 6. iFerret Electro-optical Sensor at Chicago O'Hare International Airport (Source : iFerret™, http://www.stratechsystems.com/iv_iferret.asp)

HEALTH MONITORING OF PAVEMENTS: EXAMPLES

Runway Instrumentation at Denver International Airport

In the 1990s, the runway construction at Denver International Airport (DIA) included a comprehensive instrumentation of strain gages, Thermocouples, and Time Domain Reflectometrs (TDR). A total of 460 sensors were instrumented in the sixteen slabs in the runway to monitor the pavement response generated from aircraft wheel and environment loading. Among the installed sensors, dynamic sensors measured strain, vertical displacement, airplane speed and acceleration when an airplane pass triggered the sensors. A data acquisition system (DAS) was placed in-situ for data collection and downloading to an ORACLE7 database managed by FAA technical center to analyze aircraft and pavement data. Furthermore, the performance of this system was also assessed later by Dong [17], Lee [18], Rufino [19], etc.

Optical Fiber Sensors in Kai-Shek International Airport

In 2002, Chou and Chen [20, 21] conducted a study at Chiang Kai-Shek (CKS) International Airport in Taiwan to monitor pavement joint movements and thermal stresses at one taxiway. In this study, several different types of dynamic and static strain gages were installed in concrete pavements. Dynamic strain gages in this study include H-bar strain gages, dowel bar strain gages, and gear position gauges. For static strain gages, optical fiber sensors and thermal sensors were installed. The Smartec SOFO optical fiber sensors measured concrete joint movements (expansion and contraction). The optical fiber sensors were tied to the rebar racks before concrete paving and they started recording data after concrete paving with a 20 minute interval. A DAS was connected to optical fiber for data transmission.

(a) (b)

Figure 7. (a) SOFO Optical Fiber Sensor, (b) DAS System [21],

Piezoelectric Strain Sensor for Smart Asphalt Pavement Monitoring

Lajnef et al. [22] investigated a wireless piezoelectric strain sensor system to estimate fatigue damage for asphalt pavements in 2013. A wireless integrated circuit sensor was interfaced with a piezoelectric transducer for relatively low energy consumption. The piezoelectric transducer had an array of ultra-low power floating gate (FG) computational circuits to supply sensor operating power from vehicle movements. The sensor could measure strain change and store the data on-board for periodical transmission trough RF. A central database was required to receive the uploaded data from sensors. A RF reader mounted on a moving vehicle could be used to read and download the data from the sensor as well.

Figure 8. Prototype Installation of Self-powered Strain Sensor [22]

Wireless MEMS System for Concrete Moisture Monitoring

Figure 9 compares the wired MEMS scheme for in-situ concrete moisture monitoring with a wireless MEMS scheme in a recently completed study conducted by the authors and collaborators from the electrical engineering department at ISU. In the working scheme of wired MEMS scheme, the sensor should be connected to the data reader and the computer through cables to continuously monitor the concrete properties and download the data. As a consequence, both the data reader and the computer require electrical supply for operations. However, the wireless system does not require any external cables which can save installation time and reduce the risk of malfunction of sensors.

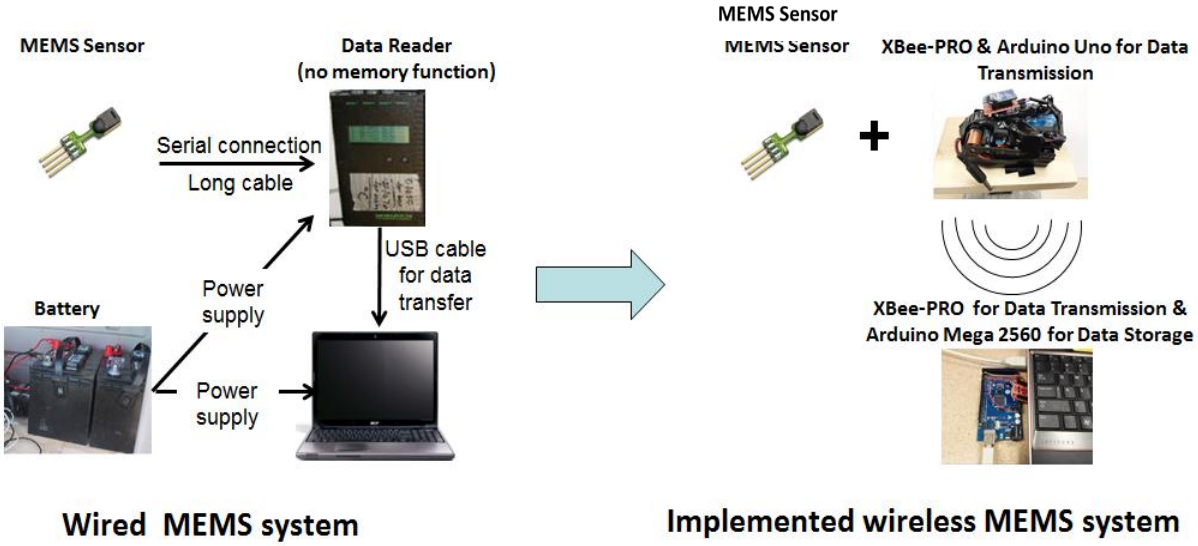

Figure 9. Comparison between Wired MEMS based Moisture Sensor System and Wireless MEMS based Moisture Sensor System

A health monitoring and management system for airport pavements could provide in-situ pavement conditions and responses to prevent multi-faceted safety concerns including pavement deteriorations and FODs from aircraft operations.

Figure 9 illustrates a conceptual design of airport health monitoring system. In this figure, the embedded smart MEMS sensor subsystem is a wireless multifunction MEMS which can measure strain, temperature, and moisture simultaneously. The robust packaging subsystem should be implemented to protect the embedded smart MEMS sensors during installation and operation under harsh climatic and traffic conditions. The smart MEMS sensor subsystem can be integrated with EO based distress and FOD detectors to monitor actual pavement surface condition. A reliable data acquisition subsystem mounted on a moving vehicle or control tower can be used to collect, store, and transfer data from MEMS sensors and EO based detectors. The intelligent data mapping model subsystem employing sensing data fusion and geo-spatial analysis approach can be utilized in data mapping of entire section from collected data from sensor installed in specific locations. Realistic characterization of pavement layer properties and responses through intelligent data mapping model subsystem can be utilized for early warning of critical distress initiation, accurate airport pavement life predictions, planning pavement management activities as well as for calibration and validation of mechanistic-based pavement response prediction models.

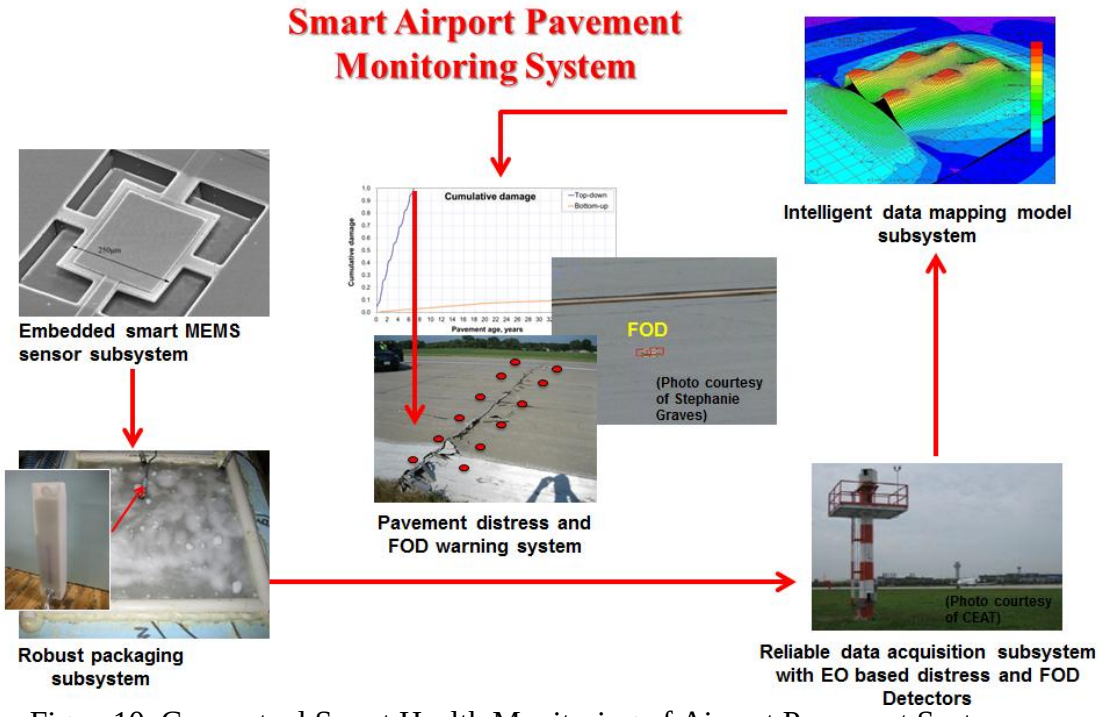

Figure10. Conceptual Smart Health Monitoring of Airport Pavement Systems

SUMMARY

The recent advancements in Micro-Electro-Mechanical Sensor (MEMS)/Nano-Electro-Mechanical Sensor (NEMS) technologies and wireless sensor networks combined with efficient energy scavenging paradigms provide opportunities for long-term, continuous, real-time response measurement and health monitoring of airport pavement systems. MEMS/NEMS represent an innovative solution in airport pavement condition monitoring that can be used to wirelessly detect and monitor structural health (damage initiation and growth) as well as functional health in airport pavement structures. Static or dynamic sensors, such as strain gages or pressure cells, have also been used in new or existing airport pavements, but are mostly restricted to experimental studies on a short-term basis. The required properties for health monitoring of airport pavement systems include multifunction sensing capacity, wireless communications, lower energy consumption for operation, robust packaging, reliable data acquisition, intelligent data mapping, and early warning of critical distress initiation. Such health monitoring of airport pavement systems is crucial for:

- Maintaining the structural and functional performance for safe aircraft operations
- Providing optimal timing of maintenance/rehabilitation activities and efficient allocation of scanty resources
- Understanding complex pavement system behavior to achieve sustainable airport pavement systems

ACKNOWLEDGEMENTS

This paper was prepared from a study conducted at Iowa State University (ISU) with partial support from Iowa Department of Transportation (Iowa DOT). The contents of this paper reflect the views of the authors who are responsible for the facts and accuracy of the data presented within. The contents do not necessarily reflect the official views and policies of the FAA or Iowa DOT. This paper does not constitute a standard, specification, or regulation. The presentation of this information is in the interest of invoking comments by the technical community on the results and conclusions of the research.

REFERENCES

1. Federal Aviation Administration, U.S. Department of Transportation, "Development of Standards for Nonprimary Airports," Advisory Circular AC 150/5100-13B, 2011.
2. Lary, Jo., "Airport Pavement Maintenance and Management," Airfield Safety, Sign Systems and Maintenance Management Workshop, Pavement Consultants Inc., April 2009.
3. Applied Pavement Technology, Inc., "Creston Municipal Airport Pavement Management Report," Iowa Department of Transportation, Office of Aviation, December 2011.
4. Applied Pavement Technology, Inc., "Washington Airport Pavement Management System- Pavement Management Manual," Washington State Department of Transportation Aviation, Arlington, WA.
5. Federal Aviation Administration, U.S. Department of Transportation, "Guidelines and Procedures for Maintenance of Airport Pavements," Advisory Circular AC 150/5380-6B, 2007.
6. Garg, Navneet., Guo, Edward., and McQueen, Roy., "Operational Life of Airport Pavements," Technical Report DOT/FAA/AR-04/46, U.S. Department of Transportation, Federal Aviation Administration, Office of Aviation Research, Washington, DC, December 2004.
7. Mullen, Mike., "Special Inspections of Paved Areas During Excessive Heat Periods," Central Region Airport Certification Bulletin, Federal Aviation Administration, Central Region, Airports Division, Kansas City, MO, July 2011.
8. Nepal, Shailesh., " TIA Runway Overlay Project Failure: A Case Study from Nepal," *PM World Journal*, Vol. 3, Issue. 5, 2014.
9. Ang, Li., "Research and Design of an Airfield Runway FOD Detection System Based on WSN," *International Journal of Distributed Sensor Networks*, Hindawi Publishing Corporation, 2013.
10. Federal Aviation Administration, U.S. Department of Transportation, "Airport Foreign Object Debris (FOD) Detection Equipment," Advisory Circular AC 150/5220-24, 2009.
11. Graves, Stephanie W., "Electro-optical Sensor Evaluation of Airfield Pavement," Thesis, University of Illinois at Urbana-Champaign, Urbana, Illinois, 2012
12. MNX, *What is MEMS Technology*. https://www.mems-exchange.org/MEMS/what-is.html. 2014.
13. Ceylan, Halil., Gopalakrishnan, Kasthurirangan., Taylor, Peter., Shrotriya, Pranav., Kim, Sunghwan., Prokudin, Max., Wang, Shiyun., Buss, Ashley F., and Zhang Jiake., "A Feasibility Study on Embedded Micro-Electromechanical Sensors and Systems (MEMS) for Monitoring Highway Structures," Technical Report IHRB Project TR-575, National Concrete Pavement Technology Center, Ames, IA, June 2011.
14. Lynch, Jerome P., and Loh, Kenneth J., "A Summary Review of Wireless Sensors and Sensor Networks for Structural Health Monitoring," *The Shock and Vibration Digest*, Vol. 38, No. 2, pp. 91–128, 2006.
15. Herricks, Edwin E., Lazar, Peter., Woodworth, Elizabeth., and Patterson, James., "Performance Assessment of An Electro-optical-based Foreign Object Debris Detection System," Technical Report DOT/FAA/AR-11/13, U.S. Department of Transportation, Federal Aviation Administration, William J. Hughes Technical Center, Aviation Research Division, Atlantic City International Airport, New Jersey, March 2012.

16. Lazar, Peter., and Herricks, Edwin E., "Procedures for FOD Detection System Performance Assessments: Electro-optical FOD Detection System," FAA Worldwide Airport Technology Transfer Conference, Atlantic City, New Jersey, USA, April 2010.
17. Dong, Mingyao., and Hayhoe, Gordon F., "Denver International Airport Sensor Processing and Database," Technical Report DOT/FAA/AR-00/17, U.S. Department of Transportation, Federal Aviation Administration, Office of Aviation Research, Washington, DC, March 2000.
18. Lee, Xiaogong., Hovan, Michel., King, Ryan., Dong, Mingyao., and Hayhoe, Gordon F., "Runway Instrumentation at Denver International Airport Development of Database," *Aircraft/pavement technology: in the midst of change*, pp. 348, 1997.
19. Rufino, Dulce., Roesler, Jeffery., and Barenberg, Ernest., "Mechanistic Analysis of Pavement Responses from Denver International Airport," FAA Center of Excellence (COE) for Airport Technology Report No.26, Department of Civil and Environmental Engineering, University of Illinois at Urbana-Champaign, January 2004.
20. Chou, Chia-pei., Cheng, Hsiang-Jen., and Lin, Shyh-tai., "Analysis of Concrete Joint Movements and Seasonal Thermal Stresses at the Chiang Kai-Shek International Airport," FAA Worldwide Airport Technology Transfer Conference, Atlantic City, New Jersey, USA, April 2004.
21. Wang, Chung-Yue., Wang, Hao-Lin., and Chen, Ming-Hung., "Structural Health Monitoring Activities of Applying Optical Fiber Sensors in Taiwan," International Workshop on Structural Health Monitoring and Damage Assessment, National Chung Hsing University, Taichung, Taiwan, ROC, December 14-15, 2006.
22. Lajnef, Nizar., Chatti, Karim., Chakrabartty, Shantanu., Rhimi, Mohamed., and Sarkar, Pikul., "Smart Pavement Monitoring System," Technical Report FHWA-HRT-12-072, U.S. Department of Transportation, Federal Highway Administration, Research, Development, and Technology Turner-Fairbank Highway Research Center, McLean, VA, May, 2013.

APPENDIX B: TEMPERATURE, MOISTURE AND STRAIN PROFILES FROM US-30 HIGHWAY

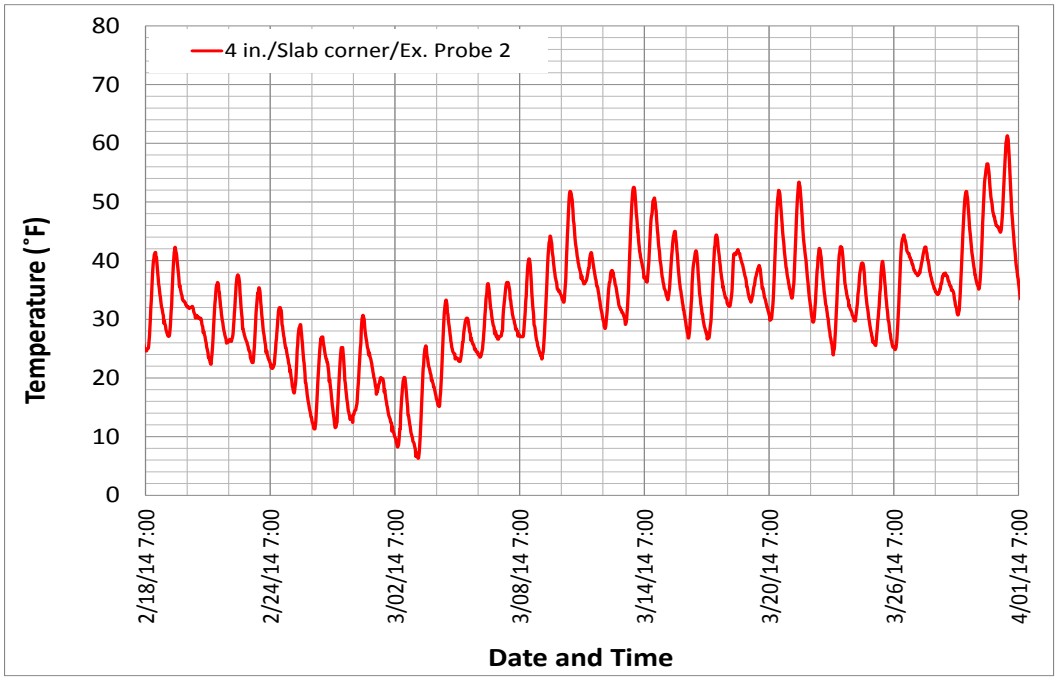

Figure B-1. RFID extended probe measurement in spring 2014.

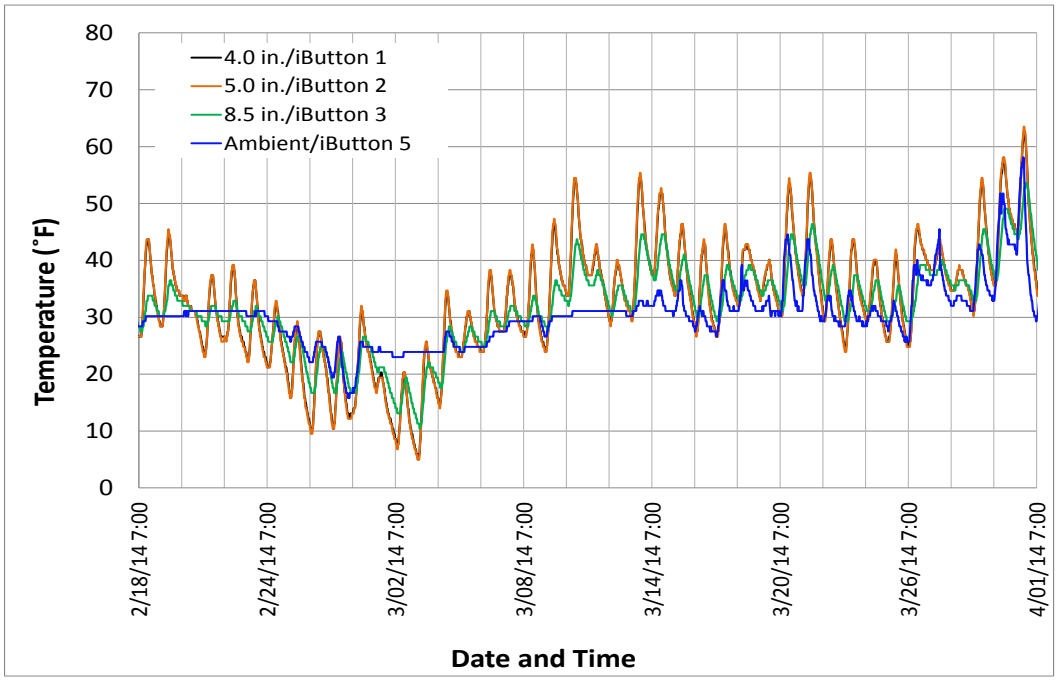

Figure B-2. iButton measurement in spring 2014.

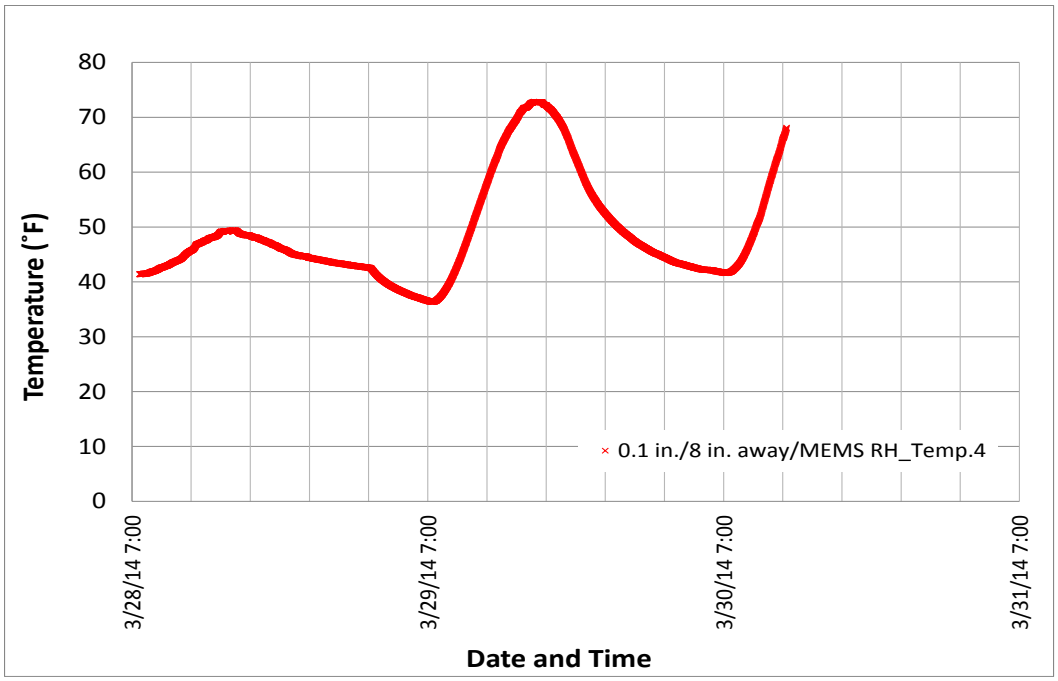

Figure B-3. MEMS digital humidity sensor temperature measurement in spring 2014.

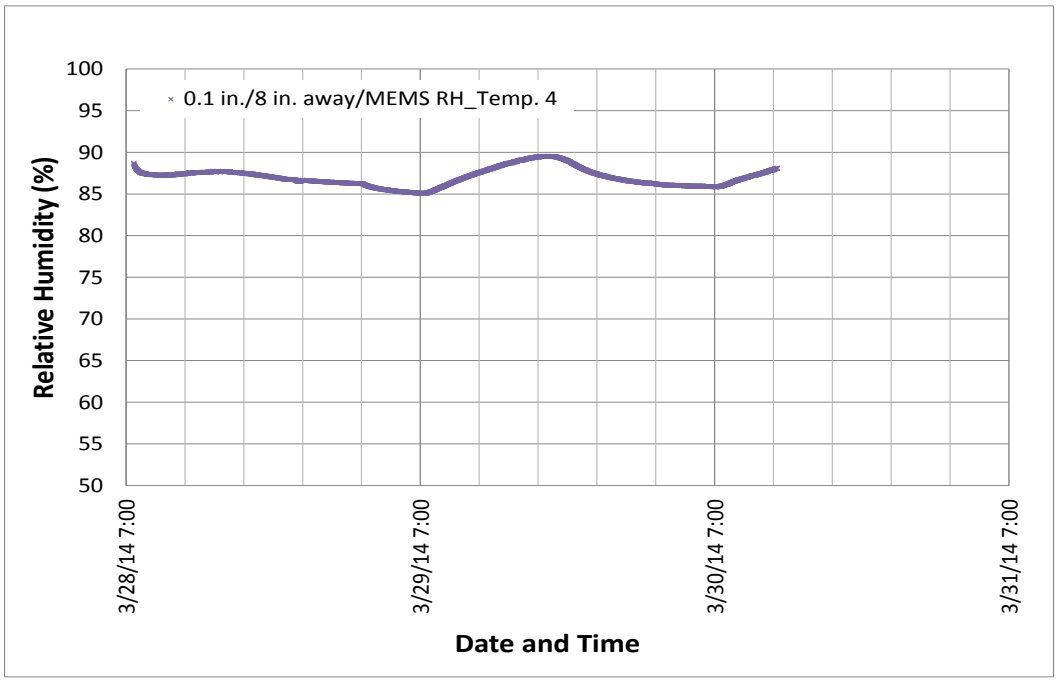

Figure B-4. MEMS digital humidity sensor RH measurement in spring 2014.

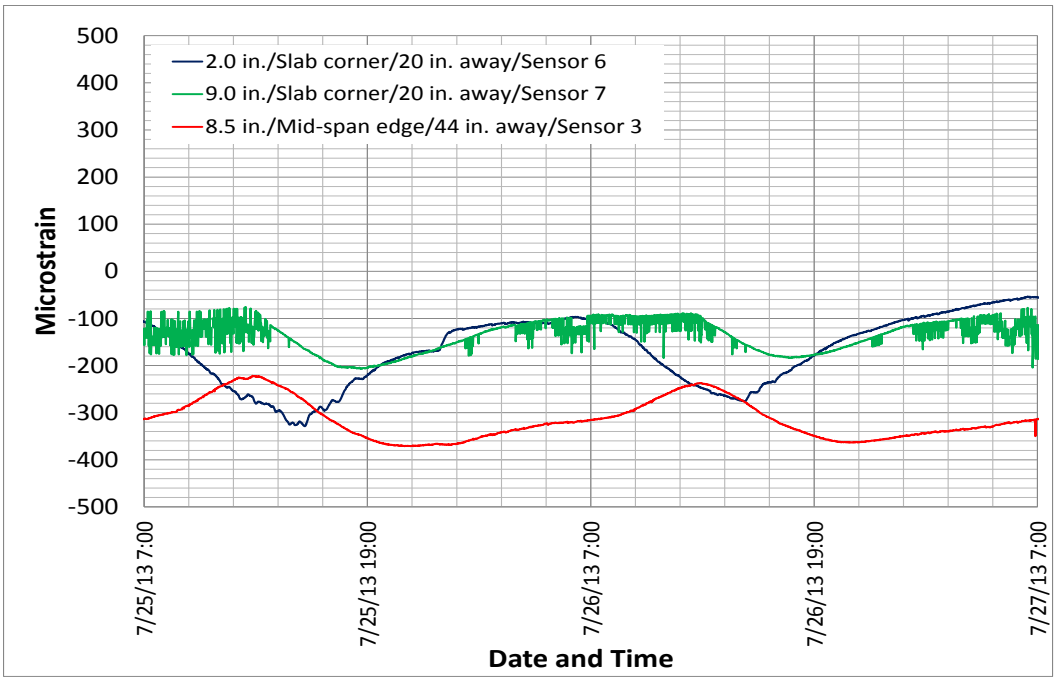

Figure B-5. Strain measurement in summer 2013.

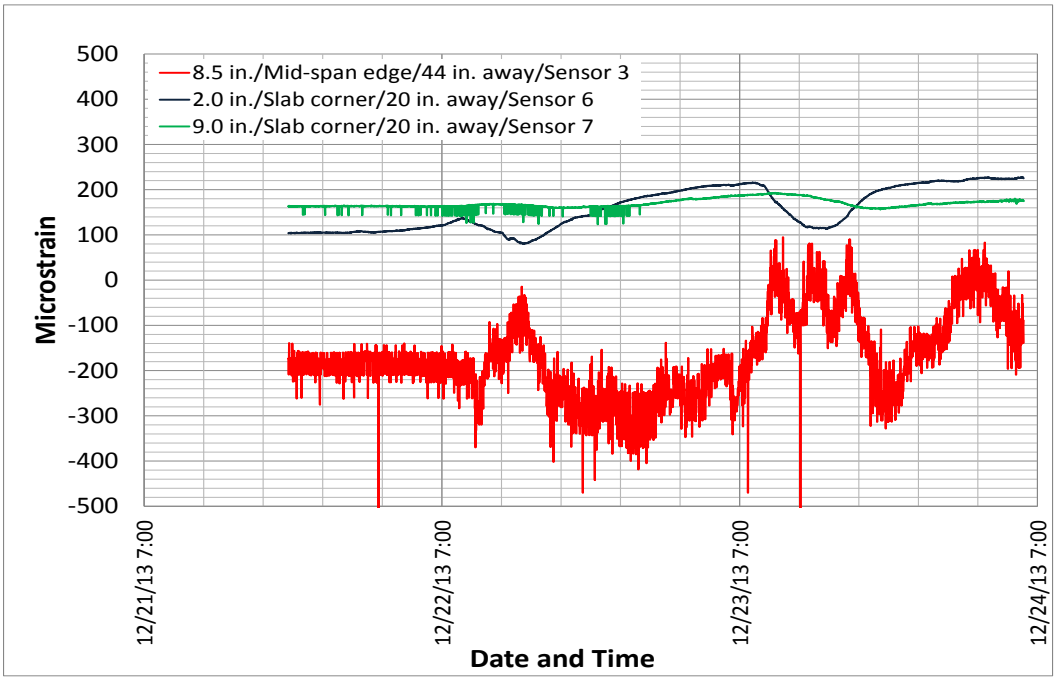

Figure B-5. Strain measurement in winter 2013.

APPENDIX C: SET TIME TESTING (ASTM C403)

This appendix displays the set time test in accordance with ASTM C403.

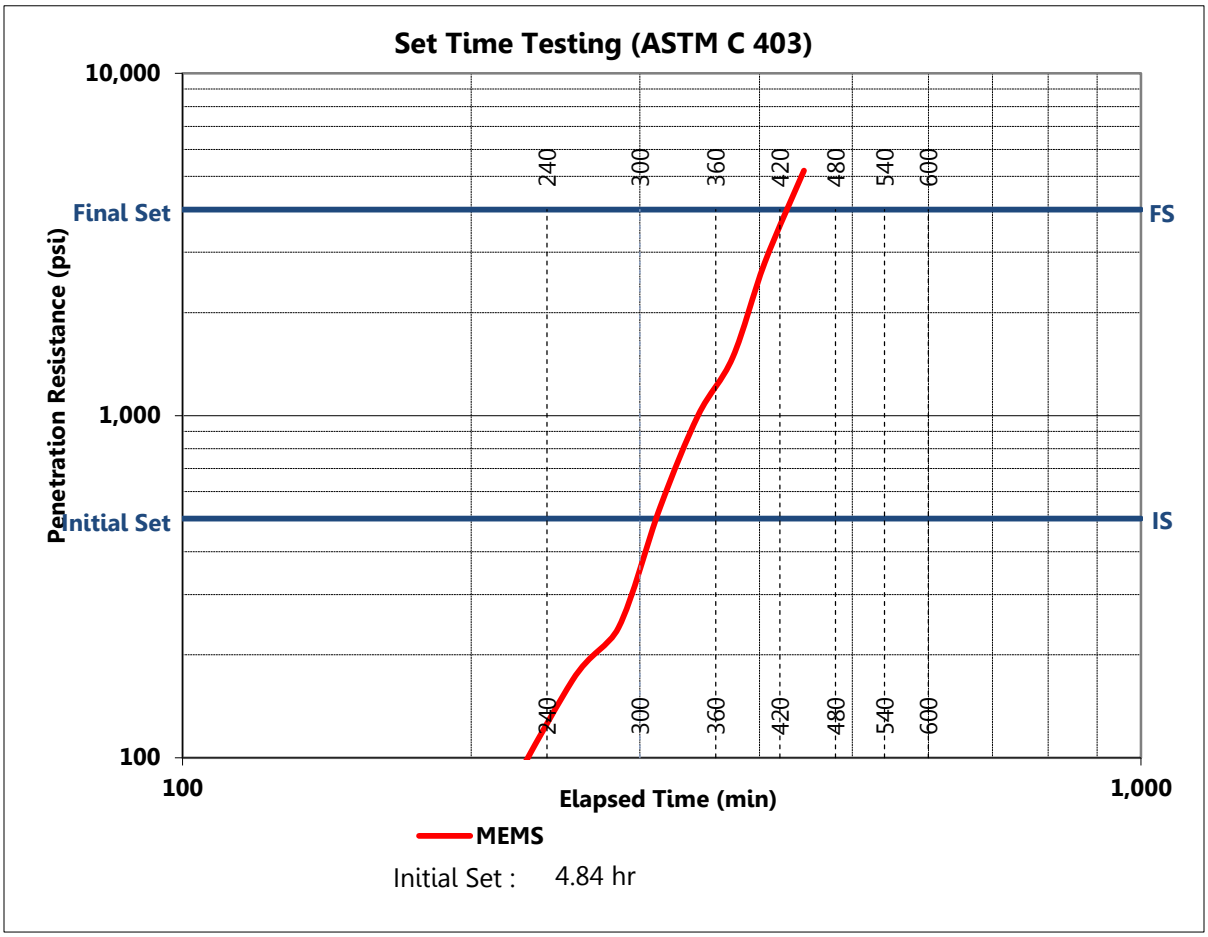

Figure C-1. Set time test (ASTM C403)

APPENDIX D: SUCCESSFUL RATE TEST RESULTS

This appendix displays the results from successful rate test and temperature and moisture data obtained from the test.

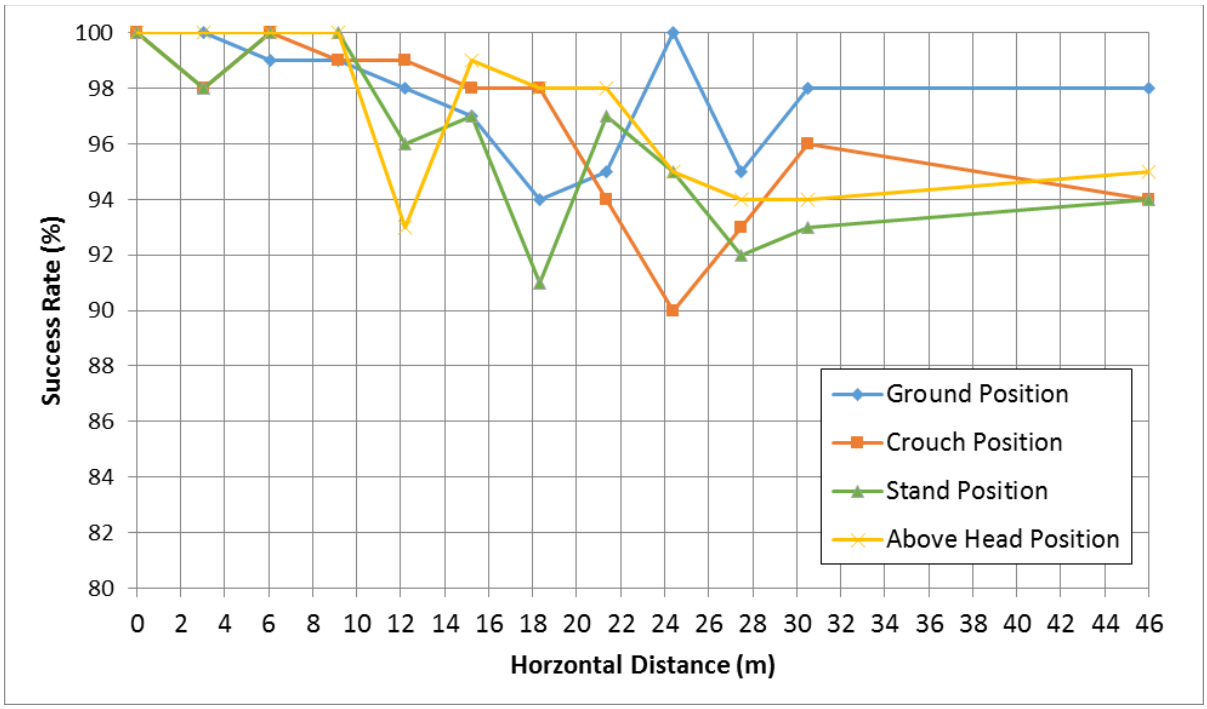

Figure D-1. Success rate test results.

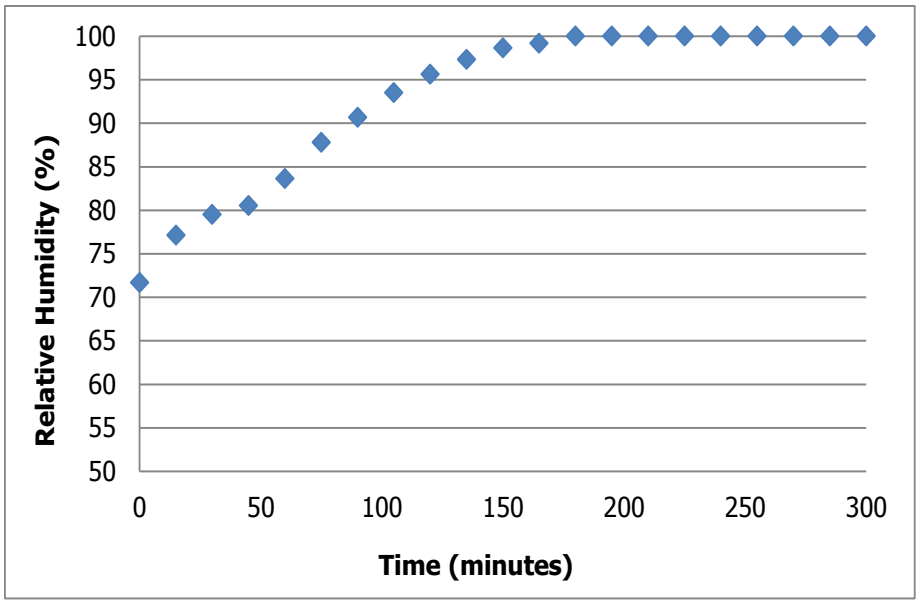

Figure D-2. RH measurement from success rate test.

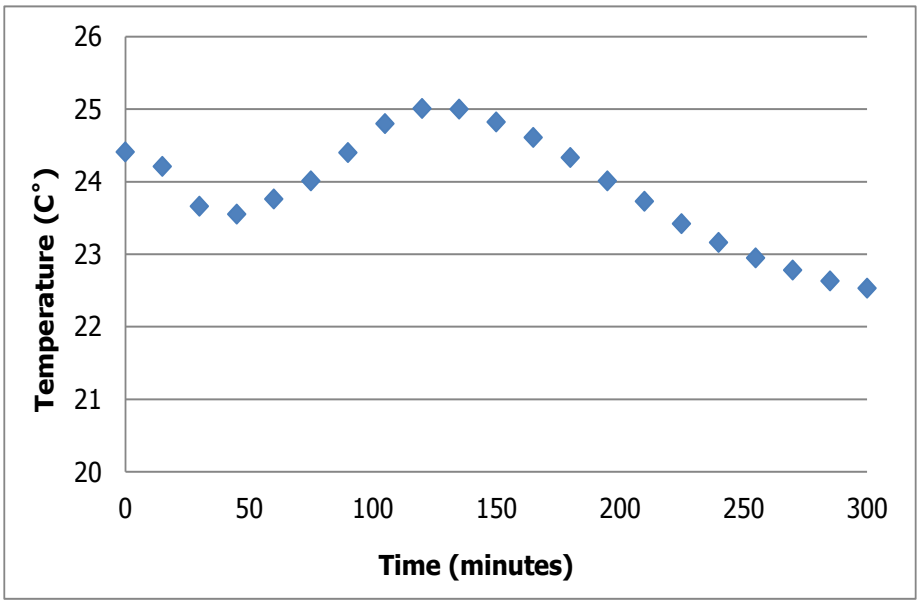

Figure D-3. Temperature measurement from success rate test.